THESIS

I. THE STRUCTURE OF OCTACHLOROCYCLOBUTANE, C_4Cl_8

II. FURTHER STUDY OF THE STRUCTURE OF C_8F_{12}

THOMAS BARRON OWEN

1950

I THE STRUCTURE OF OCTACHLOROCYCLOBUTANE, C_4Cl_8

II FURTHER STUDY OF THE STRUCTURE OF C_8F_{12}

A Thesis

Presented to the Faculty of the Graduate School of

Cornell University for the Degree of

Doctor of Philosophy

By

Thomas Barron Owen

June, 1950

BIOGRAPHICAL SKETCH

The author was born on March 19, 1920 in Seattle, Washington. He attended the Seattle public schools and was graduated from Broadway High School in 1936. In June, 1940 he received the degree of Bachelor of Science in Chemical Engineering, cum laude. While employed by the Union Oil Company of California, he was called to active duty in the United States Navy in December of that year. After five years overseas service he returned to this country with the permanent rank of Lieutenant Commander, United States Navy. He studied electronic engineering for one year at the United States Naval Postgraduate School, Annapolis, Maryland and then entered Cornell University in 1947.

He was married to Rosemary Stolz in December, 1944 and has two children, Catherine Adams and Thomas Jr. of ages four and two respectively.

ACKNOWLEDGMENTS

The author wishes to express his appreciation to Dr. T. J. Killian of the Office of Naval Research who first recommended to the Navy Department that a group of officers be trained to recognize and to appreciate the problems of fundamental research.

He is particularly grateful to Professors J. L. Hoard, P. Morrison, and E. R. Van Artsdalen for their inspiration and guidance during his tour of duty at Cornell University.

In future assignments it is felt that the experience he has gained here will serve to increase the mutual respect and understanding of the scientist and the naval officer.

TABLE OF CONTENTS

PART I

THE STRUCTURE OF OCTACHLOROCYCLOBUTANE, C_4Cl_8

INTRODUCTION

During the past few years Professor W. T. Miller and his students have been engaged in the preparation and study of a variety of fluoro- and chlorocarbons. One of the most interesting of these is the saturated dimer of hexafluorobutadiene, C_8F_{12},[16] the structure of which is to be discussed in part II of this thesis. X-ray studies of this compound thus far have been predicated on a molecular model possessing a center of symmetry which, if it were to exist, would greatly simplify the structure problem. Since C_8F_{12} is thought to contain three fused cyclobutane rings it would be desirable to know whether or not a simple cyclobutane structure has a plane or puckered ring. If puckering of the ring were confirmed, it would be reasonable to assume that the molecule of C_8F_{12} has no center of symmetry.

In reviewing the literature it is found that spectroscopic studies of cyclobutane and of its fluorinated analogue C_4F_8 have been interpreted as indicating the carbon ring to be planar. Dunitz[8] in the X-ray study of one form of tetraphenyl cyclobutane found the structure to have a planar ring also. He states however that an isomer of this compound may have a fourfold alternating axis of symmetry (S_4). However Livingston[14]

INTRODUCTION

During the past few years Professor W. T. Miller and his students have been engaged in the preparation and study of a variety of fluoro- and chlorocarbons. One of the most interesting of these is the saturated dimer of hexafluorobutadiene, C_8F_{12},[11] the structure of which is to be discussed in part II of this thesis. Prior studies of this compound thus far have been predicated on a molecular model possessing a center of symmetry which, if it were to exist, would greatly simplify the structure problem. Since C_8F_{12} is thought to contain three fused cyclobutane rings it would be desirable to know whether or not a simple cyclobutane structure has a plane or puckered ring. If puckering of the ring were confirmed, it would be reasonable to assume that the molecule of C_8F_{12} has no center of symmetry.

In reviewing the literature it is found that spectroscopic studies of cyclobutane and of its fluorinated analogue C_4F_8 have been interpreted as indicating the carbon ring to be planar. Dunitz[5] in the X-ray study of one form of (tetraphenyl) cyclobutane found the structure to have a planar ring also. He states however that an isomer of this compound may have a fourfold alternating axis of symmetry (S_4). However Livingston[13]

in a private communication to this Department has stated that preliminary evidence from the electron diffraction investigation of $C_4 F_8$ indicates a puckered ring with unusually long carbon - carbon distances.

Recently Mr. Fred McLafferty working under Professor Miller's direction has prepared octochlorocyclobutane, $C_4 F_8$, thus making it available for X-ray studies. This presented an excellent opportunity to establish the configuration of the four-membered carbon ring so as to obtain ideas of the probable structure of $C_8 F_{12}$.

Part I of this dissertation concerns itself with the investigation of the structure of $C_4 Cl_8$.

EXPERIMENTAL PROCEDURE

Preparation and Mounting of Samples.

As remarked above, the compound was prepared by Mr. Fred McLafferty. Essentially the synthesis consists of chlorinating butadiene to give a chlorobutene which in the presence of $Al\ Cl_3$ at 100° C. gives several products, one of which is C_4Cl_8. The material is separated and purified by recrystallization from methyl alcohol.

A portion of the sample was dissolved in benzene in a small test tube and allowed to crystallize slowly overnight. Clear flat needle-like crystals were obtained which when examined microscopically between crossed Nicol prisms showed continuous extinction parallel to the needle axis irrespective of any angular rotation about this axis. Nevertheless, it later appeared that the needle axis was not the unique symmetry axis of the monoclinic crystal.

A needle approximately 0.3 mm. in diameter was mounted vertically on the goniometer head such that the needle axis coincided with the rotation axis. Since the compound has an appreciable vapor pressure it was necessary to dip the crystal in a solution of Canada balsam in xylene to form a protective coating which

would prevent sublimation. Prior to photography coarse adjustments for alignment were made on a one circle goniometer.

Photographic Recording of Diffraction Data.

Oscillation photographs were taken and the method of Hendershot[12] was employed to align the crystal for use on the Weissenberg instrument. The oscillation pictures indicated a spacing of 6.3 Å. along the needle axis which was tentatively designated as the c axis.

The zero and four higher layer equi-inclination Weissenberg photographs of this crystal were obtained using Cu Kα radiation. The observed symmetry of the X-ray diffraction effects was C_{2h} - 2/m with the monoclinic axis lying in a plane normal to the needle axis. Only (0k0) reflections for k odd were missing. The following space groups satisfy these conditions: C_2^2 - $P2_1$ or C_{2h}^2 - $P2_1/m$. The latter has a center of symmetry, whereas the former does not.

To obtain sufficient data for structure analysis it is necessary to observe reflections for rotation about at least one other axis. Since the unit cell is monoclinic, the unique axis which lies in the cross section of the needle-like crystals could be located. Sections perpendicular to the needle axis were cut out

using a sharp razor blade. The approximate orientation of the monoclinic axis was known from a comparison of the symmetry of the reflections obtained on the original oscillation photographs with the crystal position. Again oscillation pictures were used for alignment and the zero and six upper layer equi-inclination Weissenberg photographs were obtained for rotation about the monoclinic axis, $\underline{b}$. The triple film technique was used throughout.

Lattice Constants.

The lattice constants were determined from the two zero layer Weissenberg photographs (i.e. around $\underline{b}$ and $\underline{c}$) upon which reflections from NaCl had been superimposed. The monoclinic angle was determined by the method of angular lag as described by Buerger[5] and by direct measurement on the zero layer $\underline{b}$-axis film. Final values are:

$$\underline{a} = 8.00 \text{ Å}.$$
$$\underline{b} = 10.64$$
$$\underline{c} = 6.28$$
$$\beta = 107^\circ\text{-}45'$$

Molecules per Unit Cell.

Although no pycnometric density has been measured for this compound, it was reasonable to assume it roughly

as 2 gm./cc. The volume of the unit cell is 509.5 $\mathring{A}^3$.
Thus from the formula

$$= 1.660 \; nM/V$$

where n = number of molecules per unit cell

M = molecular weight

V = volume of unit cell in $\mathring{A}^3$.

we get, for n=2, an X-ray density of 2.16 gm./cc.

Measurement of Intensities.

The reflections were indexed and the value of sin θ for each spot was determined graphically from construction of the reciprocal lattice. The method is described by Bunn.(6) Relative intensities for each film of each layer photograph were estimated by visual comparison with a calibrated intensity scale having spots of a size comparable to those appearing on the films and with the following range of intensities:

2:3:5:6:9:11:13:15:19:22:26:30:35:40:42:43:50:57:64:76:79:82:88:100:118:130:139:145:147.

The value of 2 indicated a spot that was just visible whereas that of 147 indicated near saturation. The use of the triple film technique permitted a good estimation of intensities over a wide range. The values obtained were corrected for the Lorentz and Polarization factor and the Tunell(19) factor where applicable to obtain relative $|F_{hk\ell}|^2$ values.

The zero layer Weissenberg photograph about c was taken as the standard film and by careful cross-calibration all relative $|F_{hk\ell}|^2$ were reduced to the common level. The factors by which the observations from the respective films were multiplied to reach the common level are listed below:

c_1	1.18	b_0	4.15
c_2	1.23	b_1	1.52
c_3	1.82	b_2	1.54
c_4	2.86	b_3	1.25
		b_4	0.95
		b_5	1.43
		b_6	1.43

where the letter denotes the axis of rotation and the subscript the layer line.

The effects of absorption were small enough to be neglected.

All summations described here were calculated using Beevers and Lipson[2] strips.

Patterson Projection, $P(X,Y)$.

Since hk0 data were first available the Patterson projection, $P(X,Y)$ on the (001) plane was made.

For the diffraction symmetry for this crystal

$$|F_{hk0}|^2 = |F_{\bar{h}k0}|^2 = |F_{h\bar{k}0}|^2 = |F_{\bar{h}\bar{k}0}|^2;$$

and it can be shown that

$$P(X,Y) = 4 \sum_{h=1}^{\infty} \sum_{k=1}^{\infty} |F_{hk0}|^2 \cos 2\pi hX \cos 2\pi kY$$
$$+ 2 \sum_{h=1}^{\infty} |F_{h00}|^2 \cos 2\pi hX$$
$$+ 2 \sum_{k=1}^{\infty} |F_{0k0}|^2 \cos 2\pi kY + |F_{000}|^2.$$

This projection was used to determine with which of the two space groups, $P2_1$ or $P2_1/m$, the data were consistent. If the former is correct, $P(X,Y)$ should have peaks at (2x, 1/2) for each pair of equivalent atoms in the cell as well as peaks due to vectors between non-equivalent atoms.

If the space group $P2_1/m$ is correct, atoms lying in the planes of symmetry occupy positions:

(e) $x, 1/4, z; \bar{x} 3/4 \bar{z}$. For atoms in fourfold positions there are the following positions:

(f)$x,y,z;\bar{x},\bar{y},\bar{z};x,1/2-y,z;\bar{x},y+1/2,\bar{z}$. Vectors between equivalent atoms occupying twofold positions will give rise to peaks at $(2x,1/2)$ whereas those between equivalent atoms occupying fourfold positions will give rise to peaks at:

$\overline{2x},\overline{2y};0,1/2-2y;\overline{2x},1/2;2x,1/2;0,2y+1/2;\overline{2x},2y;$

$2x,2y;0,2y-1/2;2x,-1/2;\overline{2x},-1/2;0,-2y-1/2;2x,\overline{2y}.$

The projection is shown in Figure 1. Only one-fourth the plane is shown since the other quarters are related to the first by two mutually perpendicular mirror planes as can be seen from a consideration of the Patterson function.

If the centrosymmetrical group be correct and if one considers the orientation of a model of the molecule with respect to the symmetry plane, he should be able to predict the positions of compatible peaks in the Patterson. If the ring lay in the plane one would expect a strong Cl-Cl peak at X=0, Y=0.3 but such an orientation would give no peak at X=0, Y=0.5. If no atoms lay in the symmetry plane the molecule would have to be oriented such that the symmetry plane bisected the parallel legs of the carbon ring. Again one would expect a strong Cl-Cl peak along X=0 but not at X=0, Y=1/2. The last possibility is that the diagonal of the carbon ring could lie in the symmetry plane.

$(x,y,z;\bar{x},\bar{y},z;\bar{x},1/2+y,\bar{z};x,1/2-y,\bar{z})$, vectors between equivalent atoms occupying twofold positions will give rise to peaks at $(2x,1/2)$ whereas those between equivalent atoms occupying fourfold positions will give rise to peaks at:

$$\overline{2x},\overline{2y};0,1/2-2y;\overline{2x},1/2;2x,1/2;0,2y+1/2;\overline{2x},2y;$$

$$2x,2y;0,2y-1/2;2x,+1/2;\overline{2x},-1/2;0,-2y-1/2;2x,\overline{2y}.$$

The projection is shown in Figure 1. Only one-fourth the plane is shown since the other quarters are related to the first by two mutually perpendicular mirror planes as can be seen from a consideration of the Patterson function.

If the centrosymmetrical group be correct and if one considers the orientation of a model of the molecule with respect to the symmetry plane, he should be able to predict the positions of important peaks in the Patterson. If the ring lay in the plane one would expect a strong Cl–Cl peak at X=0, Y=0.5 but such an orientation would give no peak at X=0, Y=0.5. If no atoms lay in the symmetry plane the molecule would have to be oriented such that the symmetry plane bisected the parallel legs of the carbon ring. Again one would expect a strong Cl–Cl peak along X=0 but not at X=0, Y=1/2. The last possibility is that the diagonal of the carbon ring could lie in the symmetry plane.

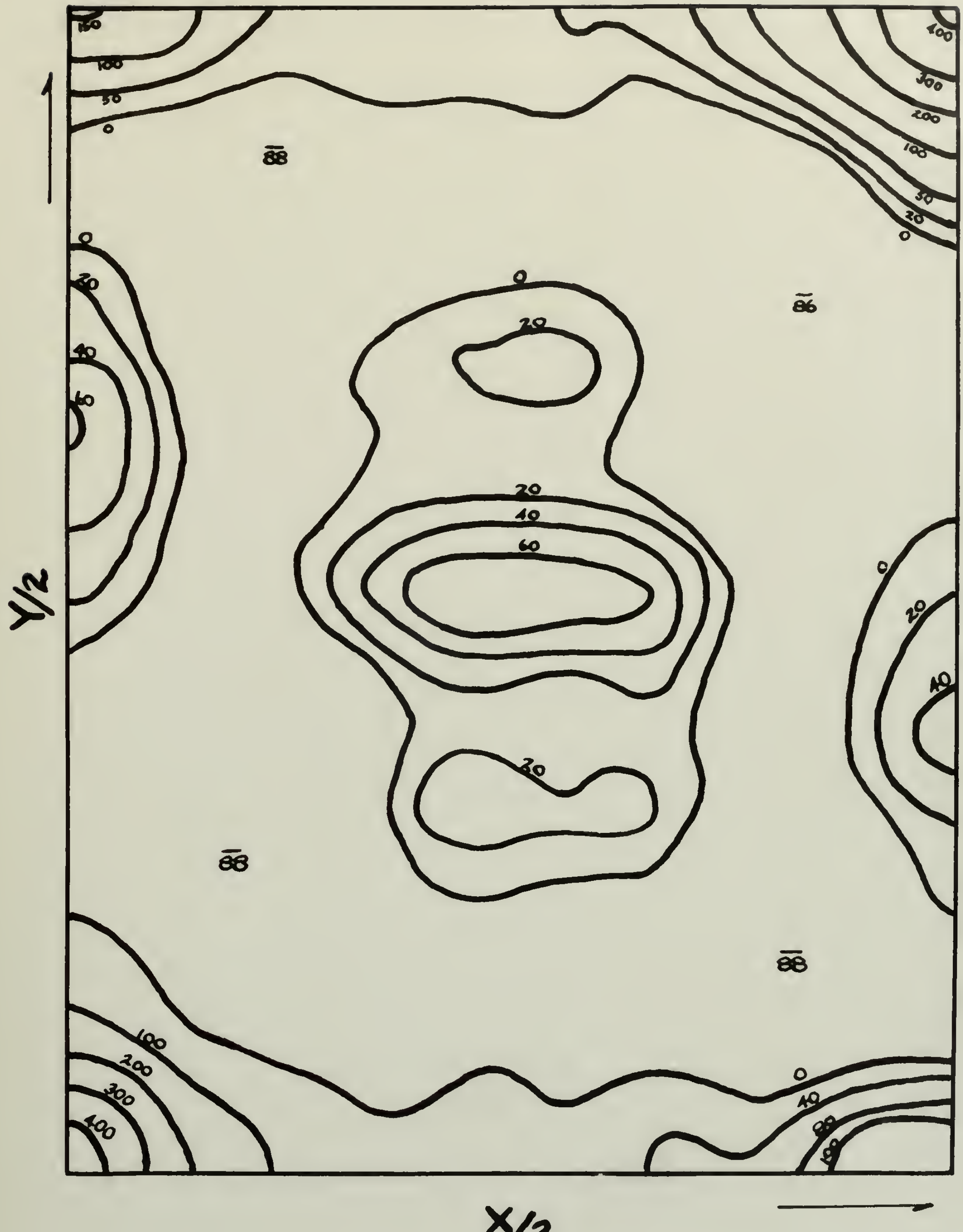

PATTERSON PROJECTION

P(XY)

Figure 1

If a scaled molecular model is so oriented and allowed to pucker it can be seen that the last configuration would give rise to two different Cl-Cl separations parallel to the unique axis. The shorter Cl-Cl vector would cause a peak at X=0 somewhere between Y=1/4 and Y=1/2. The longer vector would show up at X=0 and near Y=1/2. Such maxima do appear in the projection so this orientation of the molecule is consistent thus far. The peak at X=1/2, Y=0.19 if caused by a set of equivalent fourfold atoms would also mean a peak at X=0 y=0.31 (i.e. 2x=1/2, 2y=0.19 corresponds to 0,0.50-0.19 or 0,0.31) if one considers the list above. Also, if the peak at X=1/2, Y=1/2 included a vector due to the other set of fourfold chlorines one would expect a peak at X=0, Y=1/2 which indeed is obtained. The chosen position of the molecule thus fits in with the interpretation of the Patterson and all peaks can be explained. The projection is then consistent with the space group, $P2_1/m$.

It was possible to assign x and y parameters to the chlorine atoms of the molecule and by assuming normal C-C bond lengths to assign parameters to the carbons as well. These were:

	x	y		x	y		x	y
C_1	+0.125	1/4	Cl_1	+0.235	+0.092	Cl_6	+0.045	1/4
C_2	+0.250	+0.156	Cl_4	+0.255	+0.255	Cl_7	-0.075	1/4
C_3	+0.375	1/4	Cl_5	+0.465	1/4	Cl_8	+0.565	1/4

It might be well to describe the configuration of the molecule as postulated. In the symmetry plane the four chlorines form an isosceles trapezoid. The perpendicular bisector of the bases of this quadrilateral lies almost along the trace of the plane x=1/4 in the symmetry plane. The four chlorine atoms out of the plane also form a trapezoid the plane of which is almost coincident with x=1/4. Figure 2 is a sketch of the molecule and will serve to clarify the above. The puckering of the ring can be seen.

Amplitude Calculations.

For the space group $P2_1/m$ it can be shown that the contribution to the reflection amplitude $F_{hk\ell}$ from two like atoms occupying twofold positions is

$$A = 2fa \cos 2\pi(hx + \ell z) \cos \frac{\pi k}{2} \text{ for k even}$$
$$= -2fa \sin 2\pi(hx + \ell z) \sin \frac{\pi k}{2} \text{ for k odd}$$

where fa is the atomic scattering power of the atom. The contribution from four like atoms occupying fourfold positions is

$$A = 4fa \cos 2\pi(hx + \ell z) \cos 2\pi ky \text{ for k even}$$

and $A = -4fa \sin 2\pi(hx + \ell z) \sin 2\pi ky$ for k odd.

From these relations the following relations can be deduced:

$$F_{hk\ell} = F_{\overline{hk\ell}} \text{ for all k}$$
$$F_{hk\ell} = F_{h\bar{k}\ell} \text{ for k even}$$
$$F_{hk\ell} = -F_{h\bar{k}\ell} \text{ for k odd.}$$

It might be well to describe the configuration of the molecule as postulated. In the symmetry plane the four chlorines form an isosceles trapezoid. The perpendicular bisector of the bases of this quadrilateral lies almost along the trace of the plane $x=1/4$ in the symmetry plane. The four chlorine atoms out of the plane also form a trapezoid the plane of which is almost coincident with $x=1/4$. Figure 3 is a sketch of the molecule and will serve to clarify the above. The puckering of the ring may be seen.

Amplitude Calculations.

For the space group $P2_1/c$ it can be shown that the contribution to the reflection amplitude F_{hkl} from two like atoms occupying twofold positions is

$$A = 2f_a \cos 2\pi(hx + lz) \cos \frac{\pi k}{2} \text{ for } k \text{ even}$$

$$= -2f_a \sin 2\pi(hx + lz) \sin \frac{\pi k}{2} \text{ for } k \text{ odd}$$

where f_a is the atomic scattering power of the atom. The contribution from four like atoms occupying fourfold positions is

$$A = 4f_a \cos 2\pi(hx + lz) \cos 2\pi ky \text{ for } k \text{ even}$$

$$\text{and } A = -4f_a \sin 2\pi(hx + lz) \sin 2\pi ky \text{ for } k \text{ odd.}$$

From these relations the following relations can be deduced:

$$F_{hkl} = F_{\bar{h}\bar{k}\bar{l}} \text{ for all } k$$

$$F_{hkl} = F_{h\bar{k}l} \text{ for } k \text{ even}$$

$$F_{hkl} = -F_{h\bar{k}l} \text{ for } k \text{ odd.}$$

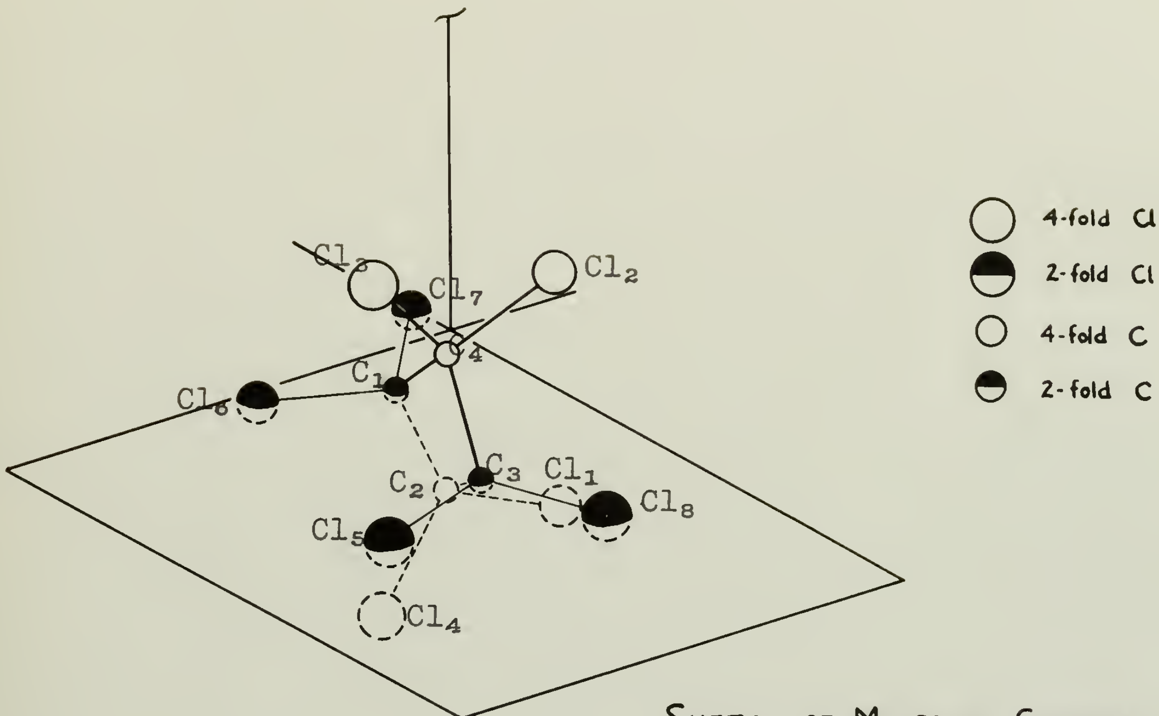

SKETCH OF MOLECULE CENTERED IN PLANE $Y = \frac{1}{4}$

Figure 2

Fourier Projection, $\rho(x,y)$.

Using the trial parameters obtained from the interpretation of the Patterson, the phases for (hk0) data were calculated in order to make the Fourier projection, $\rho(x,y)$, on (001). It can be shown that

$$K\,\rho(x,y) = 4 \sum_{h=1}^{\infty} \sum_{\substack{k=2n \\ n \geq 1}}^{\infty} F_{hk0} \cos 2\pi hx \cos 2\pi ky$$

$$+ 2 \sum_{h=1}^{\infty} F_{h00} \cos 2\pi hx + 2 \sum_{\substack{k=2n \\ n \geq 1}} F_{0k0} \cos 2\pi ky$$

$$- 4 \sum_{h=1}^{\infty} \sum_{\substack{k=2n+1 \\ n \geq 0}}^{\infty} F_{hk0} \sin 2\pi hx \sin 2\pi ky$$

(neglecting constant additive terms).

The projection is shown in Figure 3. The positions of maxima were not too well resolved, but sufficiently so to confirm the postulated model. Chlorine peaks superimpose to some extent but are clear enough to obtain parameters. Carbon peaks are lost in those of the chlorines so carbon positions must be assigned from consideration of known C-C and C-Cl bond lengths. Atomic coordinates now became:

	x	y		x	y		x	y
C_1	+0.100	1/4	Cl_1	+0.238	+0.095	Cl_6	+0.038	1/4
C_2	+0.234	+0.159	Cl_4	+0.245	+0.020	Cl_7	-0.080	1/4
C_3	+0.383	1/4	Cl_5	+0.470	1/4	Cl_8	+0.568	1/4

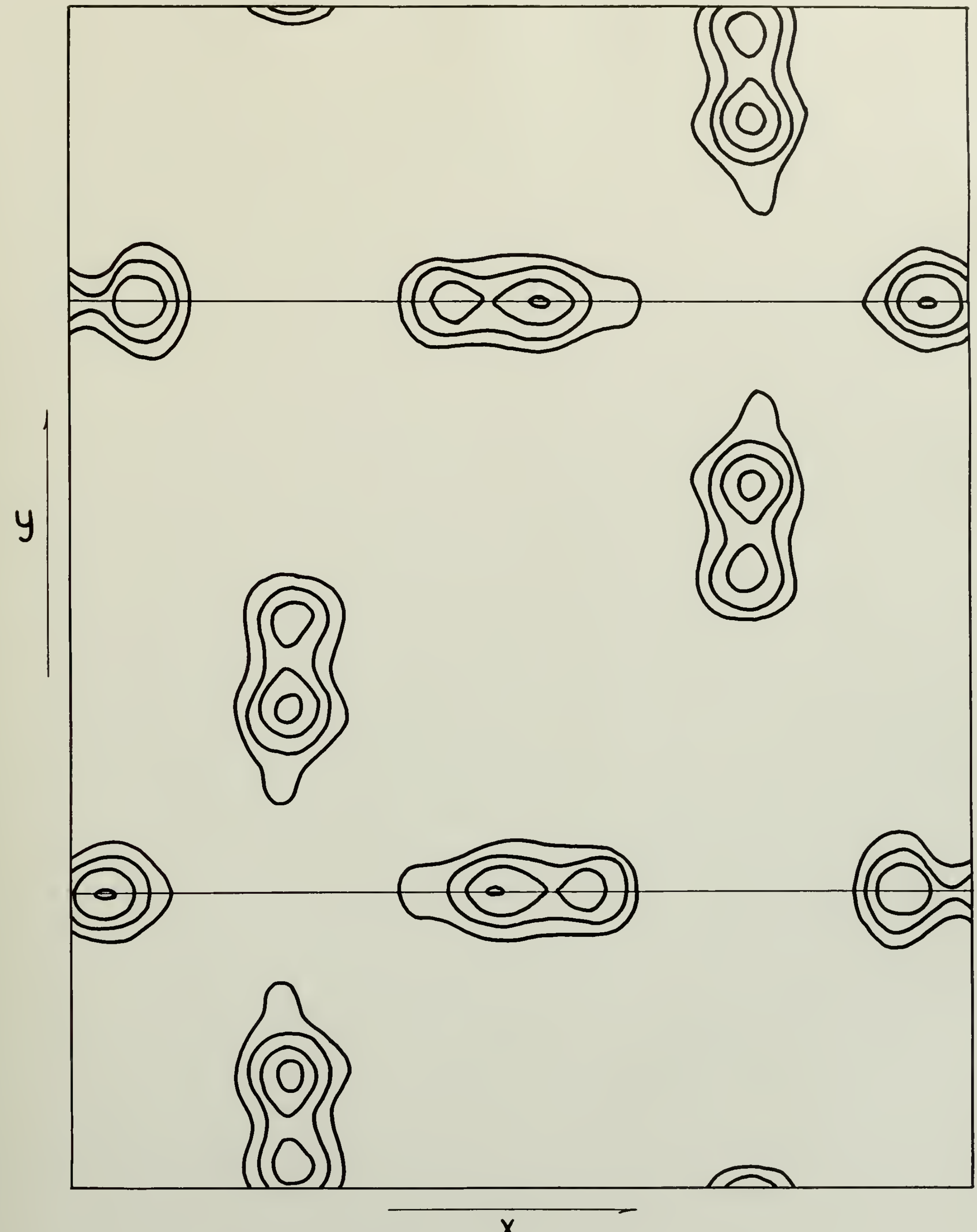

FOURIER PROJECTION $\rho(x,y)$

Figure 3

Orientation Along z.

At this stage, x and y coordinates were fairly well determined. The next problem was to determine positions along z. In effect there are two strings of molecules, one centered at x=1/4,y=1/4 and the other at x=3/4,y=3/4 but the orientation along z of the one string with respect to the other was not yet fixed. Then too there is the question as to the orientation of the trapezoid of the chlorines in the symmetry plane. The projection does not reveal whether the long or short base is most advanced along z.

In an attempt to resolve these ambiguities, reflection amplitudes $F_{(00\ell)}$ were calculated for motion of the molecule along z with a chosen orientation of the trapezoid. Since no agreement of the calculated amplitudes with those observed was obtained, the obvious step would have been to reverse the molecule and again compare amplitudes.

Patterson Sections P(0,Y,0) and P(X,1/2,Z).

A better idea presented itself however. If one calculates the Patterson section P(X,1/2,Z) he obtains peaks resulting from vectors whose Y separation is 1/2. For atoms related to each other by the screw axis, peaks should appear in the section at 2x,1/2,2z. Since x parameters are known, one would then be able to determine

Orientation Along z.

At this stage, x and y coordinates were fairly well determined. The next problem was to determine positions along z. In effect there are two strings of molecules, one centered at $x=1/4, y=1/4$ and the other at $x=3/4, y=3/4$ but the orientation along z of the one string with respect to the other was not yet fixed. Then too there is the question as to the orientation of the trapezoid of the chlorines in the symmetry plane. The projection does not reveal whether the long or short base is most advanced along z.

In an attempt to resolve these ambiguities, reflection amplitudes $F_{(00\ell)}$ were calculated for motion of the molecule along z with a chosen orientation of the trapezoid. Since no agreement of the calculated amplitudes with those observed was obtained, the obvious step would have been to reverse the molecule and again compare amplitudes.

Patterson Sections $P(0,Y,0)$ and $P(X,1/2,Z)$.

A better idea presented itself however. If one calculates the Patterson section $P(X,1/2,Z)$ he obtains peaks resulting from vectors whose Y separation is 1/2. For atoms related to each other by the screw axis, peaks should appear in the section at $2x,1/2,2z$. Since x parameters are known, one would then be able to determine

z coordinates from peaks that are sufficiently resolved. There will of course be peaks indicating vectors between non-equivalent atoms lying in the symmetry planes.

The sections were made using relative $|F_{hk\ell}|^2$ values divided by an arbitrary temperature factor $e^{-3\left(\frac{\sin\theta}{\lambda}\right)^2}$ to sharpen up the peaks and to improve resolution. At the same time it was decided to compute the Patterson line section P(0,Y,0) which will give peaks corresponding to vectors which are parallel to the unique axis. For the molecule under discussion accurate separations of fourfold chlorine atoms should be observed as indeed they were.

The line section may be expressed as:

$$P(0,Y,0) = |F_{000}|^2 + 2\,B_0 + 4\sum_{k=1}^{\infty} B_k \cos 2\pi kY$$

$$\text{where } B_0 = 1/2\sum_{h=1}^{\infty} |F_{h00}|^2 + 1/2\sum_{h=-\infty}^{\infty}\sum_{\ell=1}^{\infty} |F_{h0\ell}|^2$$

$$B_k = 1/2\,|F_{0k0}|^2 + \sum_{h=1}^{\infty} |F_{hk0}|^2 + \sum_{h=-\infty}^{\infty}\sum_{\ell=1} |F_{hk\ell}|^2$$

Figure 4 shows P(0,Y,0) for C_4Cl_8. It was only necessary to evaluate the function from Y=0 to Y=1/2 since the latter point is a center of symmetry.

The peak at Y=0 arises from null vectors for each of the atoms in the unit cell. The peak at Y=0.325 must be

due to the shorter fourfold Cl-Cl spacing in the molecule. Thus if

$$1/2 - 2y = 0.325$$

then $$y = 0.088.$$

The peak at Y=1/2 is associated with overlapping peaks resulting from the longer fourfold Cl-Cl spacing. If the single peak is resolved into the proper component peaks as shown by the dotted curves in the figure then

$$1/2 - 2y = 0.466$$

and $$y = 0.017.$$

The small hump at Y = 0.207 may be a spurious peak resulting from the "sharpening up" process or may actually correspond to the expected fourfold carbon separation of 2.2 Å. If

$$1/2 - 2y = 0.206$$

then $$y = 0.147$$

At any rate, good y parameters may now be assigned to the fourfold chlorines atoms.

Returning to the section P(X,1/2,Z) it can be shown:

$$P(X,1/2,Z) = |F_{000}|^2 + 2B_{00} + 4\sum_{h=1}^{\infty} B_{h0} \cos 2\pi hX$$

$$+ 4\sum_{h=0}^{\infty}\sum_{\ell=1}^{\infty} B^{1}_{h\ell} \cos 2\pi hX \cos 2\pi \ell Z$$

$$- 4\sum_{h=0}^{\infty}\sum_{\ell=1}^{\infty} B^{11}_{h\ell} \sin 2\pi hX \sin 2\pi \ell Z$$

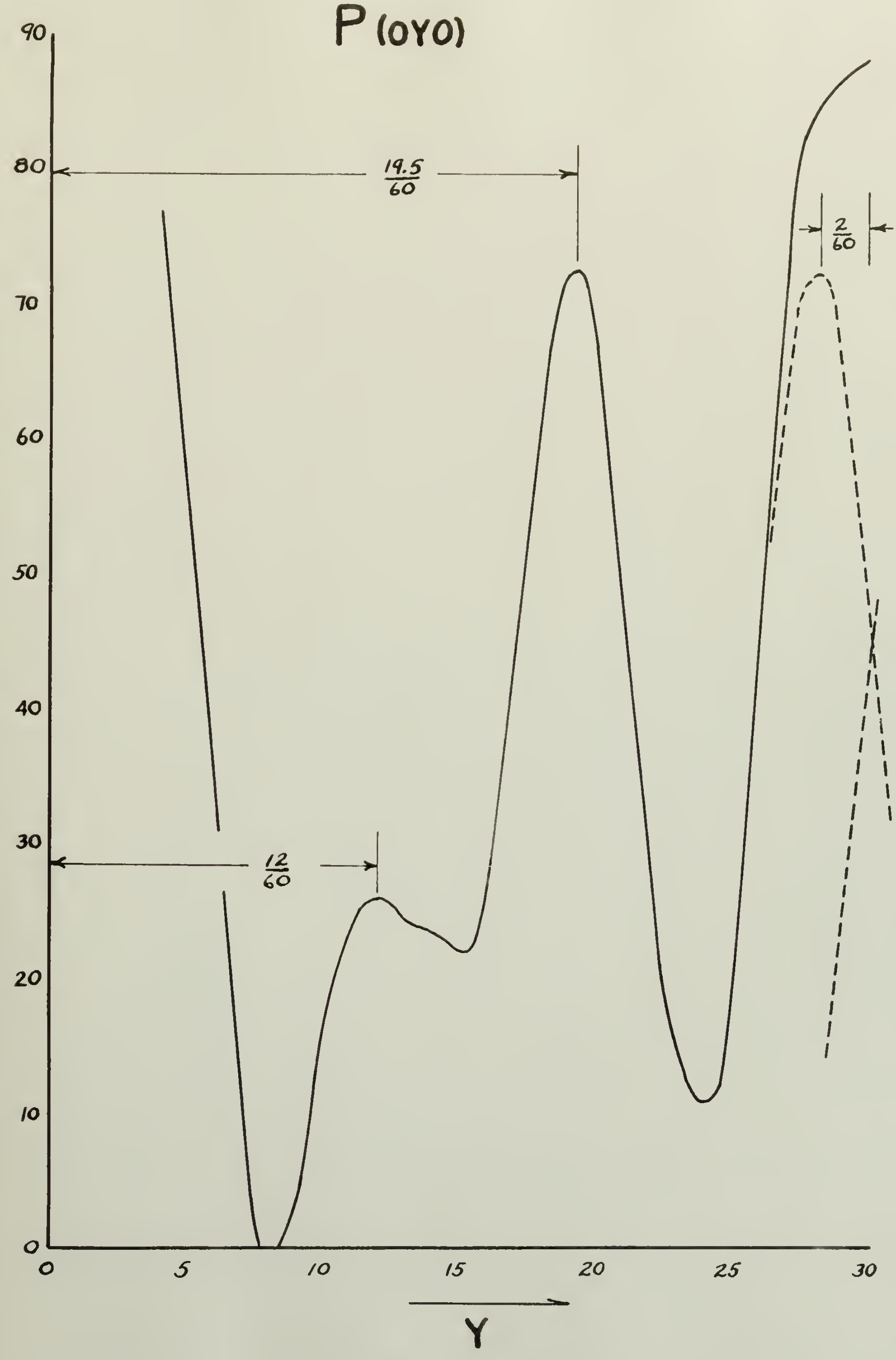

Figure 4

where $$B_{00} = 1/2 \sum_{k=2}^{\infty} |F_{0k0}|^2$$

$$B_{h0} = 1/2|F_{h00}|^2 + \sum_{k=1}^{\infty} (-1)^k |F_{hk0}|^2$$

$$B^{1}_{h\ell} = B_{h\ell} + B_{\bar{h}\ell}$$

$$B^{11}_{h\ell} = B_{h\ell} - B_{\bar{h}\ell}$$

and $$B_{h\ell} = 1/2 |F_{h0\ell}|^2 + \sum_{k=1}^{\infty} (-1)^k |F_{hk\ell}|^2.$$

The section is shown in Figure 5. It is apparent that peaks indicative of vectors of $X = 2x = 1/2$, of which there will be many arising from the fourfold atoms, all run together so cannot be clearly resolved. However by considering the x parameters of the twofold chlorines (i.e. those in the symmetry plane) it was possible to pick the proper orientation of the trapezoid they form and to obtain their proper z coordinates. It was established that the short base of this trapezoid was most advanced in the +z direction and the proper orientation is as shown in Figure 2. Parameter values available now are listed. Small changes in x parameters have occurred as a result of including all the data in the summation.

where $g_{00} = 1/2 \sum_{k=1}^{\infty} |F_{0k0}|^2$

$$g_{h0} = 1/2|F_{h00}|^2 + \sum_{k=1}^{\infty} (-1)^k |F_{hk0}|^2$$

$$g^{I}_{h\ell} = g_{h\ell} + \bar{g}_{h\ell}$$

$$g^{II}_{h\ell} = g_{h\ell} - \bar{g}_{h\ell}$$

and $$g_{h\ell} = 1/2 |F_{h0\ell}|^2 + \sum_{k=1}^{\infty} (-1)^k |F_{hk\ell}|^2.$$

The section is shown in Figure 5. It is apparent that peaks indicative of vectors at X = 2x = 1/2, of which there will be many arising from the fourfold atoms, all run together so cannot be clearly resolved. However by considering the x parameters of the twofold chlorines (i.e. those in the symmetry plane) it was possible to pick the proper orientation of the trapezoid they form and to obtain their proper z coordinates. It was established that the short base of this trapezoid was most advanced in the +z direction and the proper orientation is as shown in Figure 2. Parameter values available now are listed. Small changes in x parameters have occurred as a result of including all the data in the summation.

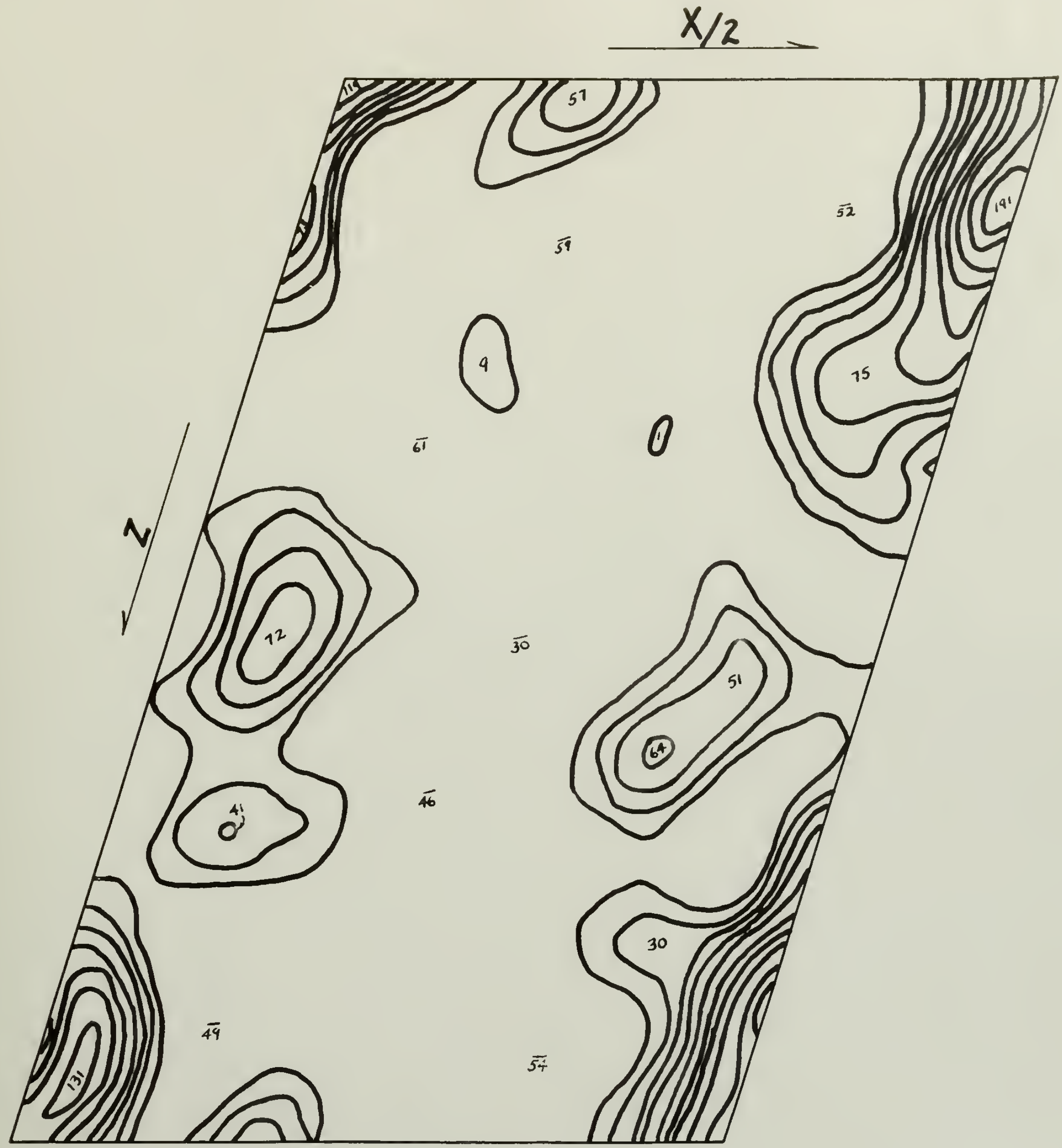

PATTERSON SECTION

$P(x\frac{1}{2}z)$

Figure 5

	x	y	z
C_1	+0.108	1/4	+0.238
C_2	+0.250	+0.147	+0.230
C_3	+0.392	1/4	+0.362
Cl_1	+0.245	+0.088	-0.035
Cl_4	+0.238	+0.017	+0.425
Cl_5	+0.470	1/4	+0.655
Cl_6	+0.038	1/4	+0.488
Cl_7	-0.078	1/4	-0.017
Cl_8	+0.568	1/4	+0.225

Fourier Projection $\rho(x,z)$.

In order to obtain better x and z coordinates the phases of the $h0\ell$ reflections were calculated and the Fourier projection $\rho(x,z)$ on (010) evaluated. Here

$$K\rho(x,z) = F_{000} + \sum_{h=0}^{\infty}\sum_{\ell=1}^{\infty}(F_{h0\ell} + F_{\bar{h}0\ell})\cos 2\pi hx \cos 2\pi\ell z$$
$$+ \sum_{h=1}^{\infty} F_{h00}\cos 2\pi hx$$
$$- \sum_{h=1}^{\infty}\sum_{\ell=1}^{\infty}(F_{h0\ell} - F_{\bar{h}0\ell})\sin 2\pi hx \sin 2\pi\ell z.$$

There was some superposition of peaks corresponding to twofold chlorines in this projection and carbon maxima were rather fuzzy. The fourfold chlorines were well defined. Atomic coordinates were obtained, phases were redetermined,

and the Fourier function re-evaluated until no sign changes occurred. Figure 6 shows the projection of matter in the unit cell along the unique axis. The overlap of the twofold chlorines is evident. Atomic coordinates are now:

	x	y	z
C_1	+0.100	1/4	+0.233
C_2	+0.238	+0.147	+0.262
C_3	+0.378	1/4	+0.338
Cl_1	+0.244	+0.088	-0.008
Cl_4	+0.238	+0.017	+0.423
Cl_5	+0.467	1/4	+0.636
Cl_6	+0.012	1/4	+0.458
Cl_7	-0.092	1/4	-0.003
Cl_8	+0.572	1/4	+0.255

It may be well to note that coordinates given by the projections $\rho(x,y)$ and $\rho(x,z)$ cannot be considered as final. The X-ray photographs of the crystals show several reflections of considerable amplitude at high values of $(\sin \theta)/\lambda$ indicating that the Fourier series will be slow in converging. To obtain the best set of positions all the data must be used and even then there may be errors due to non-convergence. This point will be discussed later.

and the Fourier function re-evaluated until no sign changes occurred. Figure 4 shows the projection of matter in the unit cell along the unique axis. The overlap of the twofold chlorines is evident. Atomic coordinates are now:

	x	y	z
C_1	+0.190	1/4	+0.233
O_2	+0.238	+0.147	+0.062
O_3	+0.378	1/4	+0.028
Cl_1	+0.244	+0.088	-0.008
Cl_2	+0.220	+0.017	+0.433
Cl_3	+0.467	1/4	+0.505
Cl_4	+0.012	3/4	+0.439
Cl_5	-0.092	1/4	-0.003
Cl_6	+0.372	1/4	+0.258

It may be well to note that coordinates given by the projections $\rho(x,y)$ and $\rho(x,z)$ cannot be considered as final. The x-ray photographs of the crystals show several reflections of considerable amplitude at high values of $(\sin\theta)/\lambda$ indicating that the Fourier series will be slow in converging. To obtain the best set of positions all the data must be used and even then there may be errors due to non-convergence. This point will be discussed later.

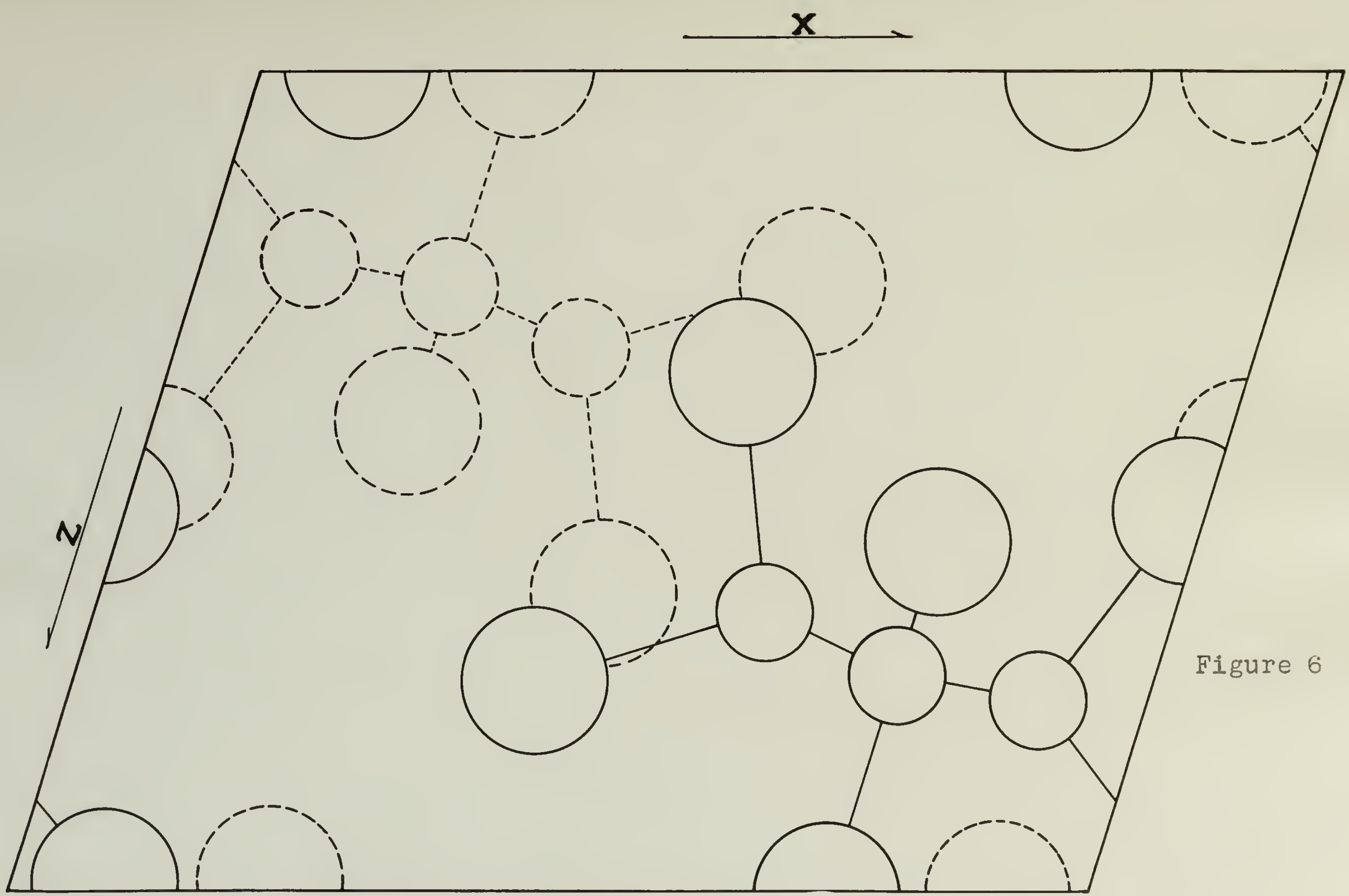

Figure 6

PROJECTION OF UNIT CELL ALONG UNIQE AXIS

Fourier Sections $\rho(x,1/4,z)$ and $\rho(1/4,y,z)$.

It is particularly fortunate that half of the atoms of the molecule lie in the symmetry plane y = 1/4 and even moreso that the other half lie almost exactly in the plane x = 1/4. Thus by taking sections through the unit cell at y = 1/4 and at x = 1/4 good parameter values should be obtained. This is particularly true since all reflections are used in the syntheses.

The Fourier section $\rho(x,1/4,z)$ may be evaluated as:

$$
\begin{aligned}
K\rho(x,1/4,z) = & \; 4 \sum_{h=1}^{\infty} \sum_{\ell=1}^{\infty} A^{1} \cos 2\pi hx \cos 2\pi \ell z \\
& -4 \sum_{h=1}^{\infty} \sum_{\ell=1}^{\infty} A^{11} \sin 2\pi hx \sin 2\pi \ell z \\
& +4 \sum_{\ell=1}^{\infty} A^{111} \cos 2\pi \ell z + 4 \sum_{h=1}^{\infty} A^{1111} \cos 2\pi hx \\
& -4 \sum_{h=1}^{\infty} \sum_{\ell=1}^{\infty} B^{1} \cos 2\pi hx \sin 2\pi \ell z \\
& -4 \sum_{h=1}^{\infty} \sum_{\ell=1}^{\infty} B^{11} \sin 2\pi hx \cos 2\pi \ell z \\
& -4 \sum_{h=1}^{\infty} B^{111} \sin 2\pi hx - 4 \sum_{\ell=1}^{\infty} B^{1111} \sin 2\pi \ell z \, .
\end{aligned}
$$

(constant additive terms are neglected) where:

$$A^{1} = 1/2 \, (F_{h0\ell} + F_{\bar{h}0\ell}) + \sum_{\substack{k=2n \\ n \geq 1}}^{\infty} (F_{hk\ell} + F_{\bar{h}k\ell})(-1)^{k/2} \, .$$

Fourier sections $\rho(x,1/4,z)$ and $\rho(1/4,y,z)$.

It is particularly fortunate that half of the atoms of the molecule lie in the symmetry plane y = 1/4 and even moreso that the other half lie almost exactly in the plane x = 1/4. Thus by taking sections through the unit cell at y = 1/4 and at x = 1/4 good parameter values should be obtained. This is particularly true since all reflections are used in the synthesis.

The Fourier section $\rho(x,1/4,z)$ may be evaluated as:

$$K\rho(x,1/4,z) = \sum_{h=1}^{\infty}\sum_{\ell=1}^{\infty} A^{I}\cos 2\pi hx \cos 2\pi \ell z$$

$$+ \sum_{h=1}^{\infty}\sum_{\ell=1}^{\infty} A^{II}\sin 2\pi hx \sin 2\pi \ell z$$

$$+ \sum_{\ell=1}^{\infty} A^{III}\cos 2\pi \ell z + 4\sum_{h=1}^{\infty} A^{IIII}\cos 2\pi hx$$

$$+ \sum_{h=1}^{\infty}\sum_{\ell=1}^{\infty} B^{I}\cos 2\pi hx \sin 2\pi \ell z$$

$$+ \sum_{h=1}^{\infty}\sum_{\ell=1}^{\infty} B^{II}\sin 2\pi hx \cos 2\pi \ell z$$

$$+ \sum_{h=1}^{\infty} B^{III}\sin 2\pi hx + \sum_{\ell=1}^{\infty} B^{IIII}\sin 2\pi \ell z \,,$$

(constant additive terms are neglected) where:

$$A^{I} = 1/2\,(F_{h0\ell} + F_{\bar{h}0\ell}) + \sum_{\substack{n=2n \\ n\geq 1}}^{\infty} (F_{hn\ell} + F_{\bar{h}n\ell})(-1)^{n/2} \,.$$

$$A^{11} = 1/2\,(F_{h0\ell} - F_{\bar{h}0\ell}) + \sum_{\substack{k=2n \\ n \geq 1}}^{\infty} (F_{hk\ell} - F_{\bar{h}k\ell})(-1)^{k/2} ,$$

$$A^{111} = 1/2\,F_{00\ell} + \sum_{\substack{k=2n \\ n \geq 1}}^{\infty} F_{0k\ell}\,(-1)^{k/2} ,$$

$$A^{1111} = 1/2\,F_{h00} + \sum_{\substack{k=2n \\ n \geq 1}}^{\infty} F_{hk0}\,(-1)^{k/2} ,$$

$$B^{1} = \sum_{\substack{k=2n+1 \\ n \geq 0}}^{\infty} (F_{hk\ell} + F_{\bar{h}k\ell})(\sin \frac{\pi k}{2}) ,$$

$$B^{11} = \sum_{\substack{k=2n+1 \\ n \geq 0}}^{\infty} (F_{hk\ell} - F_{\bar{h}k\ell})(\sin \frac{\pi k}{2}) ,$$

$$B^{111} = \sum_{\substack{k=2n+1 \\ n \geq 0}}^{\infty} F_{hk0}\,(\sin \frac{\pi k}{2}) ,$$

$$B^{1111} = \sum_{\substack{k=2n+1 \\ n \geq 0}}^{\infty} F_{0k\ell}\,(\sin \frac{\pi k}{2}) .$$

The section in the plane $x = 1/4$ may be evaluated as (neglecting constant additive terms):

$$K\rho(1/4,y,z) = 4 \sum_{\substack{k=2n \\ n \geq 0}}^{\infty} \sum_{\ell=1}^{\infty} \left[\sum_{\substack{h=2n \\ n \geq 1}}^{\infty} (F_{hk\ell} + F_{\bar{h}k\ell}) \cos \frac{\pi h}{2} + F_{0k\ell} \right] \cos 2\pi ky \cos 2\pi \ell z$$

$$+ 4 \sum_{\substack{k=2n \\ n \geq 0}}^{\infty} \left[\sum_{\substack{h=2n \\ n \geq 0}}^{\infty} F_{hk0} \cos \frac{\pi h}{2} + 1/2\,F_{0k0} \right] \cos 2\pi ky$$

$$+ 4 \sum_{\ell=1}^{\infty} \left[\sum_{\substack{h=2n \\ n \geq 1}}^{\infty} \left(\frac{F_{h0\ell} + F_{\bar{h}0\ell}}{2}\right) \cos \frac{\pi h}{2} + 1/2\ F_{00\ell} \right] \cos 2\pi \ell z$$

$$-4 \sum_{\substack{k=2n+1 \\ n \geq 0}}^{\infty} \sum_{\ell=1}^{\infty} \left[F_{0k\ell} + \sum_{\substack{h=2n \\ n \geq 1}}^{\infty} (F_{hk\ell} + F_{\bar{h}k\ell}) \cos \frac{\pi h}{2} \right] \sin 2\pi ky \sin 2\pi \ell z$$

$$-4 \sum_{\substack{k=2n \\ n \geq 0}}^{\infty} \sum_{\ell=1}^{\infty} \left[\sum_{\substack{h=2n+1 \\ n \geq 0}}^{\infty} (F_{hk\ell} - F_{\bar{h}k\ell}) \sin \frac{\pi h}{2} \right.$$

$$\left. + \sum_{\substack{h=2n+1 \\ n \geq 0}}^{\infty} \left(\frac{F_{h0\ell} - F_{\bar{h}0\ell}}{2}\right) \sin \frac{\pi h}{2} \right] \cos 2\pi ky \sin 2\pi \ell z$$

$$-4 \sum_{\substack{k=2n+1 \\ n \geq 0}}^{\infty} \sum_{\ell=1}^{\infty} \left[\sum_{\substack{h=2n+1 \\ n \geq 0}}^{\infty} (F_{hk\ell} - F_{\bar{h}k\ell}) \sin \frac{\pi h}{2} \right.$$

$$\left. + \sum_{\substack{h=2n+1 \\ n \geq 0}}^{\infty} F_{hk0} \left(\sin \frac{\pi h}{2}\right) \right] \sin 2\pi ky \cos 2\pi \ell z.$$

The two Fourier functions were evaluated and appropriate parameters obtained. Phases were recalculated and the final sections are shown in Figures 7 and 8. Contours commence at 25 and are drawn at intervals of 25 units of arbitrary relative electron density. It is readily seen that the carbon positions as given by the weak carbon peaks will not be very accurate. The contours for all atoms were redrawn on large coordinate paper and final atomic coordinates obtained in this study are:

$$- \sum_{l=1}^{\infty} \left[\sum_{\substack{h=2n \\ n \geq 1}}^{\infty} \frac{(F_{h0l} + F_{\bar{h}0l})}{2} \cos \frac{\pi h}{2} + 1/2\, F_{00l} \right] \cos 2\pi l z$$

$$- \sum_{\substack{k=2m+1 \\ m \geq 0}}^{\infty} \sum_{l=1}^{\infty} \left[F_{0kl} + \sum_{\substack{h=2n \\ n \geq 1}}^{\infty} (F_{hkl} + F_{\bar{h}kl}) \cos \frac{\pi h}{2} \right] \sin 2\pi k y \sin 2\pi l z$$

$$- \sum_{\substack{h=2n \\ n \geq 0}}^{\infty} \sum_{l=1}^{\infty} \left[\sum_{\substack{k=2m+1 \\ m \geq 0}}^{\infty} (F_{hkl} + F_{\bar{h}kl}) \sin \frac{\pi h}{2} \right]$$

$$+ \sum_{\substack{h=2n+1 \\ n \geq 0}}^{\infty} \left[\frac{(F_{h0l} - F_{\bar{h}0l})}{2} \sin \frac{\pi h}{2} \right] \cos 2\pi k y \sin 2\pi l z$$

$$- \sum_{\substack{k=2m+1 \\ m \geq 0}}^{\infty} \sum_{l=1}^{\infty} \left[\sum_{\substack{h=2n+1 \\ n \geq 0}}^{\infty} (F_{hkl} - F_{\bar{h}kl}) \sin \frac{\pi h}{2} \right]$$

$$+ \sum_{\substack{h=2n+1 \\ n \geq 0}}^{\infty} F_{hk0} \left[\sin \frac{\pi h}{2} \right] \sin 2\pi k y \cos 2\pi l z.$$

The two Fourier functions were evaluated and appropriate parameters obtained. Phases were recalculated and the final sections are shown in Figures 7 and 8. Contours commence at 20 and are drawn at intervals of 10 units of arbitrary relative electron density. It is readily seen that the carbon positions as given by the main carbon peaks will not be very accurate. The contours for all atoms were redrawn on large coordinate paper and final atomic coordinates obtained in this study are:

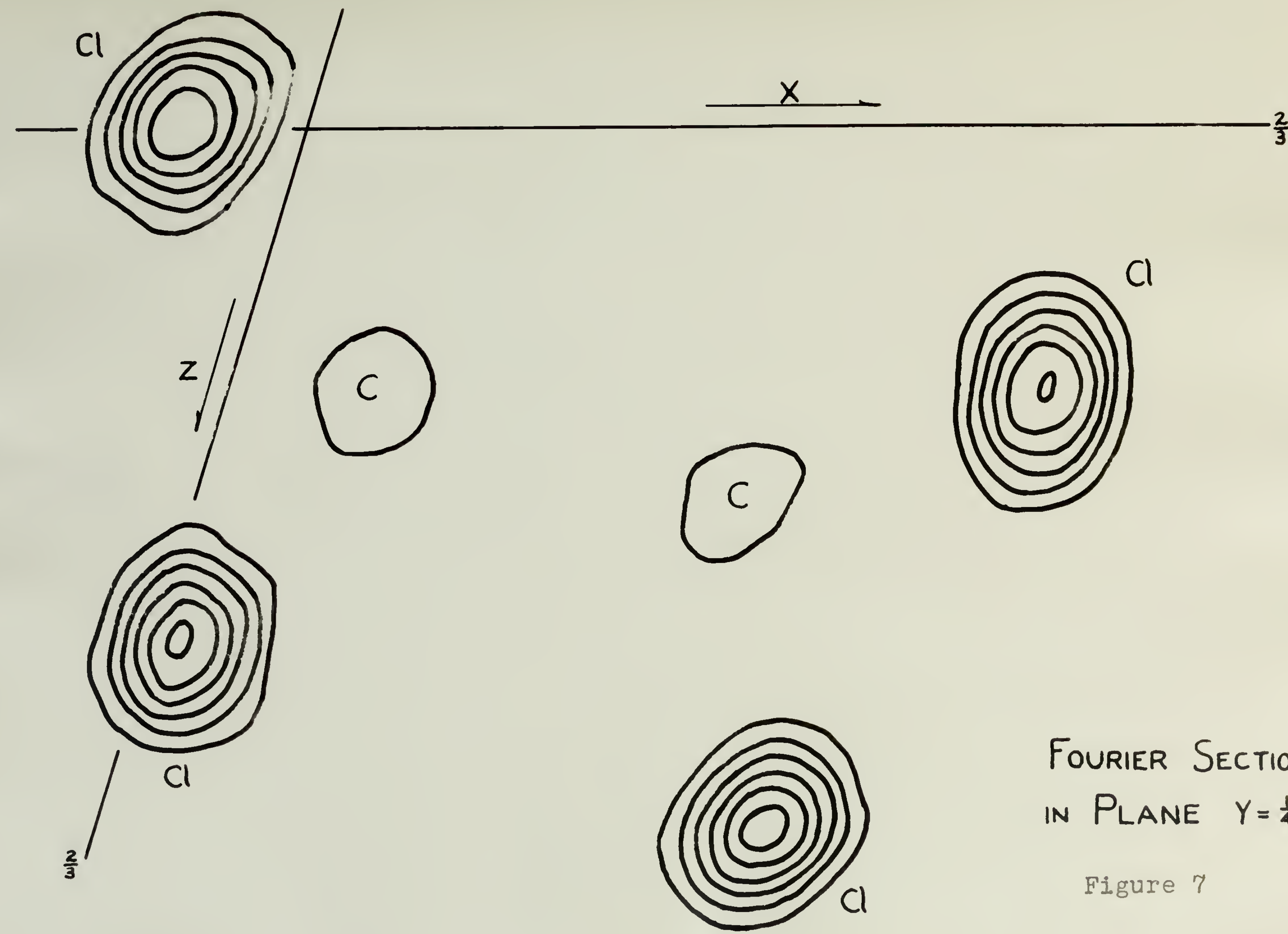

FOURIER SECTION IN PLANE $Y = \frac{1}{4}$

Figure 7

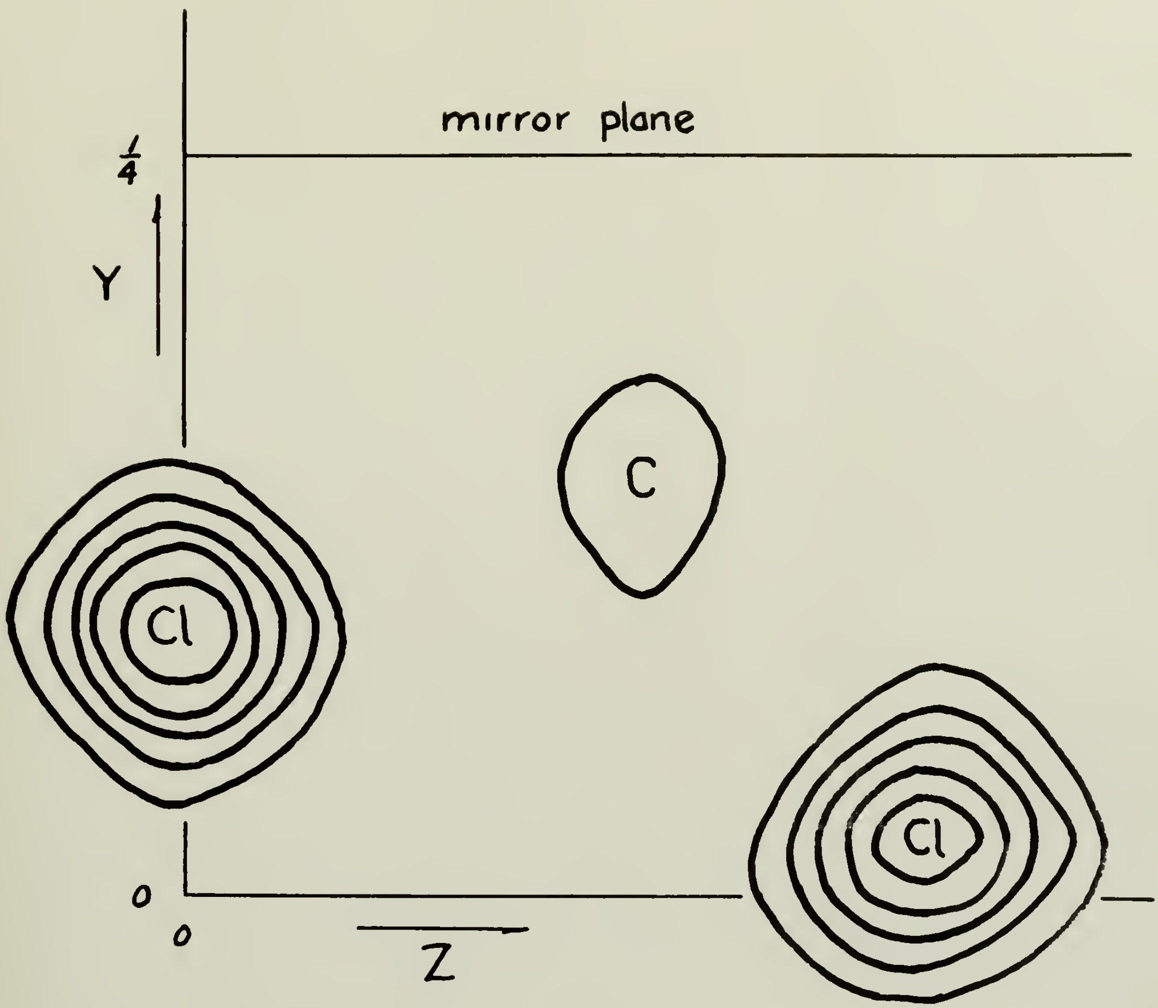

FOURIER SECTION IN PLANE $X = \frac{1}{4}$

Figure 8

	x	y	z
C_1	+0.100	1/4	+0.246
C_2	+0.242	+0.146	+0.264
C_3	+0.378	1/4	+0.334
Cl_1	+0.243	+0.091	-0.005
Cl_4	+0.237	+0.019	+0.425
Cl_5	+0.462	1/4	+0.638
Cl_6	+0.022	1/4	+0.465
Cl_7	-0.084	1/4	-0.006
Cl_8	+0.564	1/4	+0.242

COMPARISON OF CALCULATED AND OBSERVED AMPLITUDES

In order to compare calculated and observed amplitudes as a check on the validity of parameters obtained, the effects of thermal motion of the atoms must be considered. While not completely satisfactory an isotropic temperature factor of the form $e^{-B\left(\frac{\sin\theta}{\lambda}\right)^2}$ (where B must be determined) may be used to multiply the amplitudes calculated on the assumption the atoms are at rest in order that a comparison may be made. This is the usual practice in X-ray work. In addition to temperature factor determination it must be remembered that observed amplitudes are on a relative basis. Thus a factor must be determined which will correct them to an absolute scale. Mathematically then:

$$K\,|F_{obs.}| = |F_{calc}|\,e^{-B\left(\frac{\sin\theta}{\lambda}\right)^2}.$$

This may be rewritten in logarithmic form as

$$\ln\frac{|F_{calc.}|}{|F_{obs.}|} = \ln K + B\left(\frac{\sin\theta}{\lambda}\right)^2$$

which is of the form y=mx+b, an equation of a straight line where b=lnK and m=B. The method of least squares was used to determine best values of the slope and intercept of the straight line. It was found that

$$K = 2.87$$

$$B = 2.97\ \text{Å}^2.$$

when the 592 forms were used in the calculation.

Table I lists $\left(\frac{F_{calc.}}{2}\right) e^{-3\left(\frac{\sin \theta}{\lambda}\right)^2}$ and 2.87 $F_{obs.}$

for each reflection;

TABLE I

	$\frac{F_{hk\ell}}{2}$	
$hk\ell$	Calc.	Obs.
020	-29.0	35.0
040	+47.6	53.9
060	-34.1	37.6
080	+30.4	31.5
0,10,0	- 9.8	4.9
0,12,0	+16.7	18.3
100	+ 4.2	4.6
110	-25.5	28.4
120	+ 2.8	3.4
130	-36.6	32.7
140	+ 0.5	0
150	- 8.3	11.5
160	+ 0.5	0
170	- 1.1	0
180	+ 0.4	0
190	- 0.3	0
1,10,0	+ 0.5	0
1,11,0	- 6.2	6.6
1,12,0	+ 0.2	0
1,13,0	- 6.6	9.5
200	-18.6	18.7
210	+ 2.2	2.3
220	-68.2	57.5
230	- 6.8	8.6
240	+27.9	32.1
250	+ 1.4	0
260	-20.2	24.1
270	- 8.8	0
280	+ 9.8	8.6
290	+ 0.5	0
2,10,0	-18.2	20.7
2,11,0	- 1.9	0
2,12,0	+ 3.0	0
2,13,0	- 0.2	0

	$\frac{F_{hk\ell}}{2}$	
$hk\ell$	Calc.	Obs.
300	- 9.5	11.5
310	+21.6	25.0
320	- 4.2	4.0
330	+20.6	24.1
340	- 2.5	0
350	+11.9	12.3
360	- 0.2	0
370	- 3.1	0
380	- 1.9	0
390	+ 3.3	0
3,10,0	- 0.7	0
3,11,0	+ 3.2	2.9
3,12,0	- 0.9	0
3,13,0	+ 7.1	6.0
400	+38.1	45.6
410	+ 3.1	3.7
420	+16.3	18.1
430	+ 4.0	4.6
440	+ 2.6	5.2
450	+ 2.5	0
460	- 2.5	0
470	- 0.3	0
480	+ 6.0	7.2
490	+ 1.8	0
4,10,0	+ 4.3	4.6
4,11,0	+ 1.3	0
4,12,0	+ 4.5	4.3
500	+ 8.2	9.5
510	-10.7	10.6
520	+ 6.2	4.9
530	-15.8	16.3
540	+ 1.4	0
550	- 5.7	5.5
560	+ 1.4	0

when the 992 forms were used in the calculation.

Table 7 lists $\left(\frac{F_{calc.}}{2}\right) e^{-B\left(\frac{\sin\theta}{\lambda}\right)^2}$ and 2.67 $F_{obs.}$ for each reflection:

TABLE 7

	$\frac{F_{hk\ell}}{2}$			$\frac{F_{hk\ell}}{2}$	
hkℓ	Calc.	Obs.	hkℓ	Calc.	Obs.
020	-29.0	25.0	300	- 9.5	11.8
040	+47.6	53.9	310	+21.6	20.0
060	-34.1	37.6	320	- 4.2	4.0
080	+30.4	31.3	330	+20.6	24.1
0,10,0	- 9.8	4.6	340	- 2.5	0
0,12,0	+14.7	18.2	350	+11.9	12.3
			360	- 0.2	0
100	+ 4.2	4.6	370	- 0.1	0
110	-25.5	28.6	380	- 1.9	0
120	+ 2.9	3.4	390	+ 3.3	0
130	-30.6	32.7	3,10,0	- 0.7	0
140	+ 0.3	0	3,11,0	+ 3.2	2.9
150	- 5.3	11.8	3,12,0	- 0.9	0
160	+ 0.9	0	3,13,0	+ 7.1	6.0
170	- 1.1	0			
180	+ 0.4	0	400	+33.1	43.6
190	- 3.3	0	410	+ 3.1	3.7
1,10,0	+ 0.5	0	420	+10.0	10.1
1,11,0	- 6.2	6.9	430	+ 4.0	4.6
1,12,0	+ 0.2	0	440	+ 2.6	5.2
1,13,0	- 0.6	9.5	450	+ 2.5	0
			460	+ 2.5	0
200	-18.6	18.7	470	- 5.3	0
210	+ 2.1	2.3	480	+ 5.0	7.2
220	-62.2	57.5	490	+ 1.6	0
230	- 4.8	5.6	4,10,0	+ 4.3	4.6
240	+17.9	22.1	4,11,0	+ 1.3	0
250	+ 1.4	0	4,12,0	+ 4.8	4.3
260	-29.2	24.1			
270	- 8.8	0	500	+ 8.3	9.5
280	+ 9.8	8.6	510	-10.7	10.6
290	+ 0.5	0	520	+ 6.3	4.9
2,10,0	-18.9	20.7	530	-13.8	16.3
2,11,0	- 1.9	0	540	+ 1.4	0
2,12,0	+ 3.9	0	550	- 3.7	9.8
2,13,0	+ 0.2	0	560	+ 1.4	0

TABLE I (Continued)

hkℓ	Calc.	Obs.
570	+ 0.4	0
580	+ 1.4	0
590	- 0.7	0
5,10,0	+ 1.5	0
5,11,0	- 3.3	0
600	-26.7	31.0
610	- 7.0	6.0
620	- 6.3	4.6
630	- 1.9	0
640	- 4.7	6.3
650	- 4.2	4.0
660	+ 5.1	4.6
670	+ 1.7	0
680	- 6.1	7.2
690	- 2.4	0
6,10,0	- 1.5	0
6,11,0	+ 0.8	0
700	- 4.9	2.9
710	- 0.3	0
720	- 7.4	6.0
730	+15.5	13.2
740	+ 0.8	0
750	- 2.0	0
760	- 2.8	4.6
770	+ 4.2	0
780	- 0.1	0
790	- 2.9	0
800	+ 9.4	7.2
810	+ 0.4	0
820	+ 9.4	9.5
830	+ 5.0	5.5
840	- 3.0	4.0
850	+ 0.4	0
860	+ 1.4	0
870	+ 1.0	0
880	+0	0
900	+ 9.9	10.9
910	-10.8	13.8
920	- 0.7	3.4
930	+ 1.7	4.6
940	+ 4.8	5.7

hkℓ	Calc.	Obs.
950	- 7.8	8.0
001	- 7.9	10.0
011	-22.9	22.4
021	- 2.1	1.6
031	+ 5.4	6.6
041	-35.0	35.6
051	- 6.8	5.2
061	-18.3	18.1
071	- 0.6	0
081	-10.5	10.6
091	- 9.8	8.3
0,10,1	+ 6.4	0
0,11,1	+ 0.7	0
0,12,1	+ 1.8	0
0,13,1	- 3.0	0
101	-10.9	6.6
111	- 1.0	2.3
121	-19.5	21.2
131	-23.2	25.0
141	+ 2.0	2.3
151	+ 9.9	7.8
161	-14.3	14.4
171	+11.9	11.2
181	- 3.6	0
191	+17.8	16.1
1,10,1	- 2.5	2.9
1,11,1	+ 2.4	0
1,12,1	+ 2.1	0
1,13,1	+ 1.4	0
$\bar{1}01$	+28.0	32.8
$\bar{1}11$	- 2.5	0
$\bar{1}21$	+ 2.6	2.9
$\bar{1}31$	+26.6	26.2
$\bar{1}41$	+ 3.8	6.9
$\bar{1}51$	-11.8	9.2
$\bar{1}61$	+ 3.7	4.0
$\bar{1}71$	-12.3	11.5
$\bar{1}81$	+ 5.5	4.6
$\bar{1}91$	-19.8	16.6
$\bar{1}$,10,1	- 1.7	0
$\bar{1}$,11,1	- 2.5	0
$\bar{1}$,12,1	+ 0.9	0

TABLE I (Continued)

hkℓ	Calc.	Obs.
$\bar{1}$,13,1	- 2.1	0
201	-29.2	30.8
211	+ 8.7	8.9
221	+29.5	34.7
231	- 0.2	0
241	+ 4.5	5.5
251	+ 3.6	0
261	+33.8	30.1
271	+ 3.9	0
281	- 5.0	0
291	+ 8.5	6.6
2,10,1	+ 4.0	0
2,11,1	+ 1.5	0
2,12,1	- 8.7	4.6
2,13,1	+ 1.9	0
$\bar{2}$01	+ 2.3	0
$\bar{2}$11	- 4.4	4.0
$\bar{2}$21	+ 9.5	9.2
$\bar{2}$31	+15.7	16.4
$\bar{2}$41	+28.2	30.4
$\bar{2}$51	- 8.3	7.5
$\bar{2}$61	+21.8	20.6
$\bar{2}$71	+ 8.0	7.8
$\bar{2}$81	+ 7.9	8.3
$\bar{2}$91	- 0.3	3.7
$\bar{2}$,10,1	- 4.4	0
$\bar{2}$,11,1	+ 3.9	0
$\bar{2}$,12,1	- 3.0	0
$\bar{2}$,13,1	- 1.2	0
301	+16.7	15.8
311	+20.4	25.6
321	+ 5.5	4.9
331	+ 0.5	0
341	+ 9.7	9.8
351	+ 6.7	6.9
361	+ 6.5	8.0
371	-19.7	17.8
381	+ 6.6	5.7
391	- 6.1	6.6
3,10,1	- 2.0	0
3,11,1	- 7.2	8.9
3,12,1	+ 0.5	0

hkℓ	Calc.	Obs.
$\bar{3}$01	-27.6	33.0
$\bar{3}$11	-33.2	31.6
$\bar{3}$21	+ 9.9	8.9
$\bar{3}$31	+10.4	9.2
$\bar{3}$41	-10.7	10.8
$\bar{3}$51	-13.8	12.9
$\bar{3}$61	+ 6.4	4.6
$\bar{3}$71	+29.2	24.4
$\bar{3}$81	- 9.4	5.7
$\bar{3}$91	+ 4.6	0
$\bar{3}$,10,1	+ 5.4	0
$\bar{3}$,11,1	+11.5	9.8
$\bar{3}$,12,1	- 2.7	0
$\bar{3}$,13,1	- 4.4	0
401	-20.2	28.1
411	+ 7.9	10.6
421	+20.2	25.5
431	-11.0	11.8
441	-35.2	40.2
451	+ 6.3	8.9
461	+ 3.1	4.0
471	-12.3	11.2
481	-17.8	14.4
491	- 2.1	0
4,10,1	+12.1	8.9
4,11,1	- 6.0	5.2
4,12,1	- 3.9	0
$\bar{4}$01	+ 1.5	0
$\bar{4}$11	- 5.4	5.7
$\bar{4}$21	-10.8	11.5
$\bar{4}$31	- 3.8	4.0
$\bar{4}$41	-18.5	16.6
$\bar{4}$51	+ 0.6	0
$\bar{4}$61	-20.0	18.7
$\bar{4}$71	+ 0.2	0
$\bar{4}$81	- 5.0	4.0
$\bar{4}$91	- 1.9	0
$\bar{4}$,10,1	+ 2.3	0
$\bar{4}$,11,1	+ 0.1	0
$\bar{4}$,12,1	+ 3.5	0

TABLE I (Continued)

$hk\ell$	Calc.	Obs.
501	- 8.3	9.5
511	- 1.5	0
521	- 6.8	4.6
531	-11.5	12.3
541	- 6.0	6.6
551	+ 4.4	5.2
561	- 8.2	8.0
571	+ 6.2	0
581	- 3.7	0
591	+ 9.1	7.5
5,10,1	+ 0.5	0
5,11,1	+ 1.0	0
$\bar{5}$01	-14.4	19.2
$\bar{5}$11	-11.8	15.5
$\bar{5}$21	+21.1	27.0
$\bar{5}$31	+22.8	23.0
$\bar{5}$41	-20.0	20.6
$\bar{5}$51	-14.9	14.1
$\bar{5}$61	+14.6	14.6
$\bar{5}$71	- 2.6	0
$\bar{5}$81	-10.0	6.6
$\bar{5}$91	-18.2	14.6
$\bar{5}$,10,1	+ 8.0	0
$\bar{5}$,11,1	+ 1.4	0
$\bar{5}$,12,1	- 5.3	0
601	-19.8	24.6
611	+ 5.4	5.2
621	+16.5	22.6
631	- 3.2	5.5
641	- 4.0	6.3
651	+ 4.7	4.6
661	+19.8	19.2
671	+ 2.1	0
681	- 6.4	7.2
691	+ 7.7	7.5
6,10,1	+ 4.5	4.0
$\bar{6}$01	+ 0.1	0
$\bar{6}$11	+ 7.3	7.7
$\bar{6}$21	+ 6.6	5.5
$\bar{6}$31	- 0.7	4.0
$\bar{6}$41	+12.9	11.2
$\bar{6}$51	+ 2.0	0

$hk\ell$	Calc.	Obs.
$\bar{6}$61	+14.2	11.8
$\bar{6}$71	- 7.2	0
$\bar{6}$81	+ 4.0	0
$\bar{6}$91	+ 2.1	0
$\bar{6}$,10,1	- 2.0	0
$\bar{6}$,11,1	- 1.9	0
701	+ 5.0	0
711	+ 3.2	0
721	+ 4.9	0
731	+ 5.6	0
741	+ 4.4	4.3
751	- 0.8	0
761	+ 6.2	6.3
771	- 4.8	0
781	+ 2.6	0
791	- 4.4	0
$\bar{7}$01	-15.0	21.5
$\bar{7}$11	-10.1	11.8
$\bar{7}$21	+11.2	11.2
$\bar{7}$31	+ 2.1	0
$\bar{7}$41	- 6.4	8.6
$\bar{7}$51	- 4.3	5.7
$\bar{7}$61	+ 9.5	9.8
$\bar{7}$71	+12.6	9.8
$\bar{7}$81	- 6.6	7.8
$\bar{7}$91	+ 3.1	2.6
$\bar{7}$,10,1	+ 5.0	0
801	- 0.6	0
811	- 1.2	0
821	+ 1.6	4.6
831	+ 0.5	3.4
841	- 8.6	8.6
851	- 1.6	0
861	- 1.7	2.9
871	- 2.8	0
$\bar{8}$01	- 1.8	0
$\bar{8}$11	+ 1.0	0
$\bar{8}$21	- 2.7	0
$\bar{8}$31	- 5.2	5.2
$\bar{8}$41	- 8.8	6.9
$\bar{8}$51	+ 3.6	3.4

TABLE I (Continued)

hkℓ	Calc.	Obs.	hkℓ	Calc.	Obs.
$\bar{8}61$	- 7.7	5.2	192	+11.7	8.3
$\bar{8}71$	- 0.5	0	1,10,2	- 6.2	0
$\bar{8}81$	- 3.5	3.1	1,11,2	- 7.8	6.3
			1,12,2	+ 7.0	5.5
901	- 4.1	0	1,13,2	- 2.9	3.4
911	- 2.3	0			
921	- 1.6	0	$\bar{1}02$	+12.5	16.1
931	- 3.0	0	$\bar{1}12$	+20.9	21.0
941	- 4.0	0	$\bar{1}22$	-44.5	44.8
			$\bar{1}32$	+10.3	13.8
$\bar{9}01$	+ 0.5	0	$\bar{1}42$	+12.0	12.1
$\bar{9}11$	- 1.2	0	$\bar{1}52$	+21.6	18.1
$\bar{9}21$	- 0.3	0	$\bar{1}62$	-25.7	21.0
$\bar{9}31$	+ 5.1	4.0	$\bar{1}72$	-10.1	7.5
$\bar{9}41$	- 3.9	5.4	$\bar{1}82$	+ 9.0	0
$\bar{9}51$	- 3.0	0	$\bar{1}92$	- 0.2	0
$\bar{9}61$	- 0.6	0	$\bar{1}$,10,2	-11.5	10.6
			$\bar{1}$,11,2	+ 1.1	0
$\overline{10}$,0,1	+ 2.2	0	$\bar{1}$,12,2	+ 6.1	0
$\overline{10}$,1,1	+ 1.5	0	$\bar{1}$,13,2	+ 9.1	7.5
$\overline{10}$,2,1	+ 1.0	0			
			202	-14.6	13.5
002	+32.6	38.4	212	+ 5.4	4.9
012	+ 0.1	0	222	-19.5	21.8
022	+18.1	21.2	232	-14.3	15.5
032	+ 9.4	10.1	242	+ 5.5	4.0
042	+ 4.0	5.2	252	- 1.0	0
052	+ 4.7	2.9	262	+ 4.9	4.9
062	-11.6	11.8	272	-10.2	3.4
072	+ 8.0	5.2	282	+ 3.0	0
082	+ 2.3	0	292	- 1.1	0
092	+ 4.2	3.4	2,10,2	- 9.4	7.8
0,10,2	+ 7.5	7.2	2,11,2	- 6.9	4.6
0,11,2	+ 5.4	5.7	2,12,2	- 2.6	0
0,12,2	+ 5.4	4.3			
0,13,2	+ 2.8	4.0	$\bar{2}02$	-28.2	33.0
			$\bar{2}12$	-22.0	22.4
102	+46.0	46.5	$\bar{2}22$	-24.9	28.4
112	+ 8.1	9.8	$\bar{2}32$	+12.6	11.8
122	- 8.2	9.2	$\bar{2}42$	- 1.3	0
132	-32.2	31.8	$\bar{2}52$	-18.4	12.9
142	+32.7	31.0	$\bar{2}62$	+ 6.2	5.2
152	+ 0.4	0	$\bar{2}72$	+ 3.9	2.3
162	- 9.5	7.2	$\bar{2}82$	- 0.2	0
172	- 4.1	0	$\bar{2}92$	-12.9	9.5
182	+16.5	15.2	$\bar{2}$,10,2	- 9.8	8.6

TABLE I (Continued

hkℓ	Calc.	Obs.	hkℓ	Calc.	Obs.
$\bar{2}$,11,2	+ 1.4	0	$\bar{4}$02	+22.2	26.1
$\bar{2}$,12,2	- 4.0	3.7	$\bar{4}$12	-13.4	14.6
$\bar{2}$,13,2	- 6.0	5.2	$\bar{4}$22	+21.8	19.5
			$\bar{4}$32	+14.2	14.1
302	- 9.1	7.5	$\bar{4}$42	+ 0.9	3.1
312	+21.1	20.1	$\bar{4}$52	- 7.8	9.8
322	-19.9	22.4	$\bar{4}$62	- 3.2	4.9
332	- 1.3	0	$\bar{4}$72	+13.0	10.0
342	- 3.2	0	$\bar{4}$82	0	0
352	+19.4	16.1	$\bar{4}$92	- 1.4	0
362	- 9.4	7.5	$\bar{4}$,10,2	+ 8.8	8.3
372	-14.0	7.8	$\bar{4}$,11,2	+ 7.0	5.7
382	- 0.3	0	$\bar{4}$,12,2	+ 3.2	3.7
392	- 2.0	0			
3,10,2	- 5.3	4.0	502	+ 6.0	0
3,11,2	- 3.0	0	512	- 3.9	4.9
3,12,2	+ 0.6	0	522	+15.6	16.9
			532	- 7.7	8.6
$\bar{3}$02	+27.0	36.0	542	+ 1.3	0
$\bar{3}$12	+ 2.8	4.6	552	- 4.9	0
$\bar{3}$22	- 3.5	5.2	562	+ 7.1	6.9
$\bar{3}$32	-28.8	29.3	572	+ 4.1	0
$\bar{3}$42	+20.8	21.0	582	- 0.4	0
$\bar{3}$52	- 4.3	6.0	592	+ 4.1	0
$\bar{3}$62	- 2.4	4.0	5,10,2	+ 5.0	5.2
$\bar{3}$72	- 3.6	0			
$\bar{3}$82	+10.7	10.9	$\bar{5}$02	- 3.8	2.3
$\bar{3}$92	+ 7.8	5.7	$\bar{5}$12	+17.6	18.4
$\bar{3}$,10,2	- 4.2	0	$\bar{5}$22	- 7.6	8.6
$\bar{3}$,11,2	- 7.6	7.2	$\bar{5}$32	+ 3.9	3.7
$\bar{3}$,12,2	+ 3.7	0	$\bar{5}$42	- 3.9	0
$\bar{3}$,13,2	- 4.8	0	$\bar{5}$52	+18.3	20.1
			$\bar{5}$62	- 6.8	8.9
402	+20.2	20.4	$\bar{5}$72	- 8.2	6.9
412	+10.3	8.3	$\bar{5}$82	- 1.4	0
422	+ 0.3	0	$\bar{5}$92	+ 2.8	0
432	- 1.5	0	$\bar{5}$,10,2	- 0.8	0
442	+ 5.0	5.7	$\bar{5}$,11,2	+ 0.4	0
452	+12.5	8.6	$\bar{5}$,12,2	+ 0.8	0
462	-13.1	10.4			
472	- 1.3	0	602	+ 1.3	6.0
482	+ 3.7	0	612	- 2.3	0
492	+ 7.1	0	622	-11.6	12.6
4,10,2	+ 1.7	0	632	- 4.0	2.9
4,11,2	+ 1.0	0	642	+ 9.2	5.7

TABLE I (Continued)

hkℓ	Calc.	Obs.
652	- 4.8	5.2
662	- 0.3	0
672	- 2.0	0
682	+ 5.6	5.5
692	- 2.2	0
$\bar{6}02$	-22.8	21.8
$\bar{6}12$	+ 2.2	0
$\bar{6}22$	- 8.9	9.2
$\bar{6}32$	- 2.0	4.3
$\bar{6}42$	- 7.5	6.6
$\bar{6}52$	+ 0.7	0
$\bar{6}62$	+ 6.6	5.2
$\bar{6}72$	- 4.9	4.0
$\bar{6}82$	- 4.2	0
692	- 2.2	0
6,10,2	- 4.1	4.9
6,11,2	- 2.3	0
702	-13.2	14.3
712	- 3.2	4.6
722	- 1.2	0
732	+ 9.1	7.8
742	- 8.3	8.0
752	- 1.8	0
762	+ 2.6	3.7
772	+ 0.7	0
$\bar{7}02$	+ 0.1	0
$\bar{7}12$	+ 3.0	5.7
$\bar{7}22$	+ 3.9	4.6
$\bar{7}32$	-16.1	16.1
$\bar{7}42$	+ 1.5	0
$\bar{7}52$	- 1.4	0
$\bar{7}62$	+ 5.1	5.7
$\bar{7}72$	- 4.0	4.6
$\bar{7}82$	+ 0.4	0
$\bar{7}92$	+ 4.7	5.4
$\bar{7}$,10,2	+ 0.2	0
802	+ 8.2	8.3
812	- 1.9	0
822	- 3.5	4.6
832	+ 5.9	6.6
842	+ 2.8	4.3
852	- 0.3	0
$\bar{8}02$	+ 9.7	9.5
$\bar{8}12$	+ 9.7	11.8
$\bar{8}22$	+11.0	8.6
$\bar{8}32$	-10.3	10.6
$\bar{8}42$	+ 0.7	0
$\bar{8}52$	+ 8.0	8.6
$\bar{8}62$	- 0.5	0
$\bar{8}72$	- 4.6	5.2
882	- 0.1	0
$\bar{9}02$	- 1.2	0
$\bar{9}12$	+ 4.1	0
$\bar{9}22$	+ 0.7	0
$\bar{9}32$	+ 4.3	0
$\bar{9}42$	- 2.4	0
$\bar{9}52$	+ 5.7	4.3
$\bar{9}62$	- 1.3	0
$\overline{10}$,3,2	- 6.4	0
$\overline{10}$,1,2	+ 7.5	0
$\overline{10}$,2,2	- 5.8	0
$\overline{10}$,3,2	- 5.8	0
003	+25.4	31.6
013	+11.9	13.2
023	- 5.4	4.6
033	-10.9	9.5
043	- 2.2	2.0
053	- 2.1	0
063	-18.5	16.4
073	-13.1	10.6
083	+ 3.5	0
093	- 1.1	0
0,10,3	+ 1.0	0
0,11,3	- 8.1	7.8
0,12,3	+ 5.8	7.5
103	-18.0	18.4
113	-19.7	18.7
123	- 5.8	5.2
133	- 2.7	3.4
143	-21.7	24.1
153	-11.4	7.2
163	- 1.7	0
173	+14.1	8.9

TABLE I (Continued)

$hk\ell$	Calc.	Obs.
183	- 8.0	0
193	+ 1.1	0
1,10,3	+ 0.4	0
1,11,3	+ 3.8	0
1,12,3	- 2.4	0
$\bar{1}03$	+ 7.0	0
$\bar{1}13$	- 5.6	6.0
$\bar{1}23$	+19.8	24.4
$\bar{1}33$	+28.8	26.4
$\bar{1}43$	+11.6	11.8
$\bar{1}53$	-10.6	7.5
$\bar{1}63$	+ 9.8	10.3
$\bar{1}73$	+ 0.5	0
$\bar{1}83$	+ 1.4	0
$\bar{1}93$	-14.3	11.8
$\bar{1}$,10,3	+ 4.9	4.6
$\bar{1}$,11,3	+ 0.2	0
$\bar{1}$,12,3	- 0.6	0
203	- 7.3	4.6
213	+13.7	14.9
223	-11.8	12.3
233	-13.4	16.1
243	+11.7	12.0
253	+19.5	17.8
263	+ 4.1	0
273	- 2.6	0
283	+ 4.3	0
293	+12.0	8.3
2,10,3	- 6.6	0
2,11,3	- 0.5	0
2,12,3	- 1.2	0
$\bar{2}03$	-13.2	20.4
$\bar{2}13$	-11.5	12.0
$\bar{2}23$	- 1.9	0
$\bar{2}33$	+12.2	10.1
$\bar{2}43$	+12.7	10.1
$\bar{2}53$	+ 2.2	0
$\bar{2}63$	+12.5	10.1
$\bar{2}73$	+12.4	9.8
$\bar{2}83$	+ 2.2	0
$\bar{2}93$	+ 0.3	0
$\bar{2}$,10,3	- 4.2	0
$\bar{2}$,11,3	+ 7.9	7.2
$\bar{2}$,12,3	- 3.3	4.3

$hk\ell$	Calc.	Obs.
303	- 4.7	7.5
313	+ 1.8	0
323	+20.7	22.1
333	+15.7	12.1
343	+ 2.3	4.6
353	+ 2.2	0
363	+14.6	12.3
373	- 1.4	0
383	- 3.0	0
393	- 6.0	0
3,10,3	+ 6.1	0
3,11,3	+ 2.0	0
$\bar{3}03$	-14.8	14.9
$\bar{3}13$	-23.2	21.2
$\bar{3}23$	-11.5	10.3
$\bar{3}33$	+ 0.8	0
$\bar{3}43$	-15.5	15.2
$\bar{3}53$	-11.1	7.8
$\bar{3}63$	- 3.2	3.7
$\bar{3}73$	+18.4	16.4
$\bar{3}83$	- 4.8	0
$\bar{3}93$	+ 1.6	0
$\bar{3}$,10,3	- 2.2	0
$\bar{3}$,11,3	+ 6.2	6.0
$\bar{3}$,12,3	- 1.6	0
403	+ 8.0	4.6
413	+ 8.8	13.2
423	+ 8.4	7.8
433	- 6.4	6.9
443	- 5.9	5.2
453	+ 0.3	0
463	- 3.4	0
473	- 9.9	8.0
483	- 1.8	0
493	- 0.6	0
4,10,3	+ 4.8	2.9
$\bar{4}03$	+ 0.5	0
$\bar{4}13$	-17.5	15.2
$\bar{4}23$	+ 7.6	8.6
$\bar{4}33$	+12.8	11.4
$\bar{4}43$	-19.5	16.6
$\bar{4}53$	-21.4	17.5
$\bar{4}63$	+ 6.2	0
$\bar{4}73$	+ 6.5	0

TABLE I (Continued)

hkℓ	Calc.	Obs.
$\bar{4}83$	- 6.9	6.9
$\bar{4}93$	-11.5	7.8
$\bar{4},10,3$	+ 6.4	6.3
$\bar{4},11,3$	+ 1.5	0
$\bar{4},12,3$	+ 0.6	0
503	-13.1	11.4
513	- 5.6	0
523	+ 3.0	0
533	- 5.7	0
543	-17.0	16.6
553	- 4.2	0
563	+ 2.2	0
573	+ 3.6	0
583	- 7.3	0
593	+ 2.6	0
$\bar{5}03$	+ 4.6	5.2
$\bar{5}13$	+ 4.5	4.3
$\bar{5}23$	+15.2	12.4
$\bar{5}33$	+13.2	12.6
$\bar{5}43$	+ 5.1	6.3
$\bar{5}53$	- 4.3	0
$\bar{5}63$	+ 6.4	0
$\bar{5}73$	- 5.7	0
$\bar{5}83$	- 0.2	0
$\bar{5}93$	- 9.1	10.4
$\bar{5},10,3$	+ 4.8	0
$\bar{5},11,3$	- 0.5	0
603	-13.0	11.2
613	- 2.5	0
623	+ 1.0	0
633	+ 0.2	0
643	- 3.6	6.6
653	+ 2.4	0
663	+ 7.1	7.2
673	+ 4.5	0
683	- 3.3	0
$\bar{6}03$	- 9.2	12.4
$\bar{6}13$	-12.6	14.9
$\bar{6}23$	+ 5.8	6.0
$\bar{6}33$	+15.6	14.6
$\bar{6}43$	+ 7.0	4.9
$\bar{6}53$	- 4.6	3.2
$\bar{6}63$	+12.5	11.8
$\bar{6}73$	+11.2	10.1
$\bar{6}83$	- 0.1	0
$\bar{6}93$	- 4.6	0
$\bar{6},10,3$	- 0.5	0
703	- 3.2	0
713	+ 1.8	3.7
723	+ 7.7	6.9
733	+ 4.8	2.9
743	+ 1.3	2.3
753	+ 1.8	0
763	+ 6.4	0
$\bar{7}03$	-10.4	10.6
$\bar{7}13$	+ 0.4	0
$\bar{7}23$	- 3.3	6.0
$\bar{7}33$	-10.3	9.2
$\bar{7}43$	- 8.7	8.3
$\bar{7}53$	+ 5.0	3.7
$\bar{7}63$	+ 1.5	0
$\bar{7}73$	+ 3.5	0
$\bar{7}83$	- 3.7	0
$\bar{7}93$	+ 7.8	6.0
803	+ 1.1	0
813	- 0.3	0
$\bar{8}03$	+ 4.3	5.7
$\bar{8}13$	- 6.8	10.3
$\bar{8}23$	- 3.6	0
$\bar{8}33$	+ 3.4	6.3
$\bar{8}43$	- 6.1	0
$\bar{8}53$	- 8.8	10.9
$\bar{8}63$	- 8.0	7.2
$\bar{8}73$	+ 2.8	5.7
$\bar{8}83$	- 0.7	0
$\bar{9}03$	+ 3.1	0
$\bar{9}13$	+ 8.2	9.5
$\bar{9}23$	+ 4.6	5.5
$\bar{9}33$	- 1.9	0
$\bar{9}43$	+ 1.9	0
$\bar{9}53$	+ 3.5	4.6
$\bar{9}63$	+ 0.8	0

TABLE I (Continued)

hkℓ	Calc.	Obs.	hkℓ	Calc.	Obs.
$\overline{10}$,0,3	+ 1.9	0	224	- 4.3	4.9
$\overline{10}$,1,3	- 2.7	0	234	- 7.0	7.8
$\overline{10}$,2,3	- 1.2	0	244	+16.4	14.4
$\overline{10}$,3,3	+ 4.5	0	254	- 2.5	0
			264	+ 4.2	5.2
004	+21.6	28.7	274	- 4.3	0
014	+11.3	10.3	284	+ 4.8	0
024	-10.2	8.3	294	- 1.7	0
034	- 3.3	0	2,10,4	- 4.1	0
044	- 3.3	5.5			
054	+12.7	9.5	$\bar{2}$04	- 8.8	13.8
064	-16.8	15.5	$\bar{2}$14	+11.8	11.2
074	- 1.1	0	$\bar{2}$24	- 6.8	6.6
084	+ 4.4	0	$\bar{2}$34	-16.4	16.4
094	+ 7.9	6.6	$\bar{2}$44	+15.2	14.6
0,10,4	- 1.8	0	$\bar{2}$54	+ 4.5	5.7
0,11,4	+ 0.7	0	$\bar{2}$64	+ 5.4	4.9
			$\bar{2}$74	-13.8	11.2
104	+21.6	32.7	$\bar{2}$84	+ 3.3	0
114	+ 1.7	0	$\bar{2}$94	+ 1.5	0
124	+ 1.3	0	$\bar{2}$,10,4	- 4.6	0
134	-17.8	18.7	$\bar{2}$,11,4	- 8.5	11.8
144	+14.9	15.5			
154	+ 9.1	5.7	304	- 5.8	0
164	- 2.5	4.9	314	+16.5	16.1
174	+ 1.9	0	324	-11.1	13.8
184	+ 8.1	0	334	- 3.2	0
194	+ 9.9	0	344	- 0.9	0
1,10,4	- 1.6	0	354	+ 6.7	6.3
1,11,4	- 0.5	0	364	- 5.2	6.0
			374	- 13.2	8.9
$\bar{1}$04	- 1.7	0	384	+ 0.1	0
$\bar{1}$14	+ 6.5	7.2	394	+ 2.2	0
$\bar{1}$24	-23.3	23.5	3,10,4	- 3.4	0
$\bar{1}$34	+13.8	14.9			
$\bar{1}$44	+ 0.6	0	$\bar{3}$04	+15.4	19.8
$\bar{1}$54	- 2.8	0	$\bar{3}$14	-20.7	18.4
$\bar{1}$64	-13.5	11.5	$\bar{3}$24	+ 8.5	6.9
$\bar{1}$74	- 6.2	0	$\bar{3}$34	- 1.1	3.4
$\bar{1}$84	+ 2.5	0	$\bar{3}$44	+12.9	10.6
$\bar{1}$94	- 6.4	5.5	$\bar{3}$54	- 9.1	8.6
$\bar{1}$,10,4	- 6.7	11.2	$\bar{3}$64	+ 3.9	0
$\bar{1}$,11,4	- 0.9	0	$\bar{3}$74	+13.8	10.6
			$\bar{3}$84	+ 5.5	5.7
204	- 1.2	0	$\bar{3}$94	- 1.0	0
214	- 0	0	$\bar{3}$,10,4	+ 0.7	0
			3,11,4	+ 4.7	0

TABLE I (Continued)

hkℓ	Calc.	Obs.
404	+ 2.0	0
414	+ 0.7	0
424	- 0.1	0
434	+ 5.2	5.2
444	-10.6	8.9
454	+ 1.7	0
464	- 5.1	0
474	+ 2.5	0
484	- 2.5	0
494	+ 1.0	0
$\bar{4}04$	+ 8.7	13.5
$\bar{4}14$	+13.5	14.9
$\bar{4}24$	+ 8.1	4.9
$\bar{4}34$	- 9.3	9.8
$\bar{4}44$	-12.8	10.0
$\bar{4}54$	+15.9	12.4
$\bar{4}64$	- 3.3	0
$\bar{4}74$	- 2.8	0
$\bar{4}84$	- 2.9	0
$\bar{4}94$	+10.7	13.5
$\bar{4}$,10,4	+ 4.8	0
$\bar{4}$,11,4	- 0.7	0
504	+ 8.6	0
514	+ 2.3	0
524	+ 2.4	0
534	- 9.8	8.0
544	+ 3.8	0
554	+ 6.6	5.5
564	- 0.6	0
574	+ 0.9	0
$\bar{5}04$	-12.2	11.5
$\bar{5}14$	- 0.3	0
$\bar{5}24$	- 6.4	6.3
$\bar{5}34$	+17.5	14.6
$\bar{5}44$	-12.2	8.0
$\bar{5}54$	- 5.4	0
$\bar{5}64$	- 3.1	0
$\bar{5}74$	+ 0.1	0
$\bar{5}84$	- 5.1	0
$\bar{5}94$	- 6.8	0
$\bar{5}$,10,4	+ 0.1	0

hkℓ	Calc.	Obs.
604	- 5.4	5.7
614	- 4.6	4.6
624	+ 5.3	5.2
634	+ 0.2	0
644	+ 2.9	2.9
654	- 4.1	0
$\bar{6}04$	-19.8	21.5
$\bar{6}14$	+ 9.6	10.6
$\bar{6}24$	+ 3.4	0
$\bar{6}34$	-10.0	10.0
$\bar{6}44$	- 1.2	0
$\bar{6}54$	+ 3.2	0
$\bar{6}64$	+10.2	8.0
$\bar{6}74$	-10.7	10.3
$\bar{6}84$	- 4.6	0
$\bar{6}94$	+ 8.0	0
6,10,4	+ 0.8	0
704	- 1.1	0
714	+ 4.0	0
$\bar{7}04$	+ 2.7	0
$\bar{7}14$	- 4.1	4.6
$\bar{7}24$	+ 9.1	6.3
$\bar{7}34$	- 9.0	8.0
$\bar{7}44$	+ 4.5	5.2
$\bar{7}54$	- 0.1	0
$\bar{7}64$	+ 6.4	0
$\bar{7}74$	+ 2.1	0
$\bar{7}84$	+ 0.7	0
$\bar{7}94$	+ 2.4	0
$\bar{8}04$	+ 4.9	0
$\bar{8}14$	+ 4.9	5.4
$\bar{8}24$	+ 7.3	8.0
$\bar{8}34$	- 6.2	6.3
$\bar{8}44$	- 6.3	9.5
$\bar{8}54$	+ 4.9	6.9
$\bar{8}64$	+ 0.3	0
$\bar{8}74$	- 2.7	0
$\bar{9}04$	- 3.2	0
$\bar{9}14$	+ 7.8	10.9

TABLE I (Continued)

hkℓ	Calc.	Obs.
$\bar{9}24$	- 3.4	0
$\bar{9}34$	+ 1.1	0
$\bar{9}44$	- 4.7	0
$\bar{9}54$	+ 4.4	5.7
$\overline{10}$,0,4	- 5.5	6.3
$\overline{10}$,1,4	+ 2.3	0
$\overline{10}$,2,4	- 3.4	0
005	+20.9	30.1
015	-14.2	12.6
025	+ 5.5	4.9
035	+10.0	9.2
045	+ 4.5	5.2
055	-10.7	11.5
065	- 6.2	5.2
075		NP
085		NP
095		NP
0,10,5		NP
105	- 5.3	0
115	+ 0.2	0
125	- 3.9	0
135	-14.7	13.2
145	- 3.1	4.6
155	- 0.6	0
165	- 5.1	5.2
175		NP
185		NP
195		NP
1,10,5		NP
$\bar{1}05$	+ 8.9	9.7
$\bar{1}15$	+ 6.4	6.0
$\bar{1}25$	+ 5.1	0
$\bar{1}35$	+10.3	8.3
$\bar{1}45$	+ 4.8	3.7
$\bar{1}55$	+ 6.1	4.6
$\bar{1}65$	+ 5.3	6.0
$\bar{1}75$		NP
$\bar{1}85$		NP
$\bar{1}95$		NP
$\bar{1}$,10,5		NP
205	-16.0	16.3
215	- 4.7	0
225	- 6.8	6.0
235	+ 5.5	0
245	- 2.8	0
255	- 4.5	3.7
265	+ 3.3	0
275		NP
285		NP
295		NP
$\bar{2}05$	- 7.4	11.2
$\bar{2}15$	-13.7	12.6
$\bar{2}25$	-18.0	14.6
$\bar{2}35$	+17.6	13.5
$\bar{2}45$	+ 7.6	4.6
$\bar{2}55$	-11.5	0
$\bar{2}65$	- 2.3	0
$\bar{2}75$		NP
$\bar{2}85$		NP
$\bar{2}95$		NP
$\bar{2}$,10,5		NP
305	- 1.0	0
315	+ 7.6	7.5
325	+ 4.8	7.5
335	+ 4.4	0
345	- 1.0	0
355	+ 6.4	5.7
365	+ 6.1	7.7
375		NP
385		NP
$\bar{3}05$	-12.3	18.1
$\bar{3}15$	- 8.6	6.0
$\bar{3}25$	- 4.8	0
$\bar{3}35$	- 7.4	6.0
$\bar{3}45$	- 6.5	6.0
$\bar{3}55$	- 7.6	0
$\bar{3}65$	- 3.9	0
$\bar{3}75$		NP
$\bar{3}85$		NP
$\bar{3}95$		NP
$\bar{3}$,10,5		NP

TABLE I (Continued)

hkℓ	Calc.	Obs.
405	+ 5.8	0
415	- 1.0	0
425	+10.8	8.3
435	+ 1.2	0
445	- 2.8	0
455	- 0.1	0
465	+ 2.4	0
475		NP
$\bar{4}05$	+15.3	20.6
$\bar{4}15$	-14.1	11.5
$\bar{4}25$	+ 6.4	6.0
$\bar{4}35$	+ 7.3	5.5
$\bar{4}45$	+ 0.4	0
$\bar{4}55$	-11.0	0
$\bar{4}65$	- 5.6	0
$\bar{4}75$		NP
$\bar{4}85$		NP
$\bar{4}95$		NP
$\bar{4}$,10,5		NP
505	- 5.6	9.5
515	- 3.1	0
525	+ 4.1	8.6
535	- 4.9	3.7
545	- 5.0	8.0
555	- 2.9	0
$\bar{5}05$	+ 7.7	0
$\bar{5}15$	0	0
$\bar{5}25$	+ 9.1	6.0
$\bar{5}35$	+12.5	8.6
$\bar{5}45$	+ 2.2	0
$\bar{5}55$	+ 0.5	0
$\bar{5}65$	+ 6.2	0
$\bar{5}75$		NP
$\bar{5}85$		NP
$\bar{5}95$		NP
$\bar{6}05$	-14.3	12.9
$\bar{6}15$	+ 0.3	0
$\bar{6}25$	- 0.7	0
$\bar{6}35$	+ 5.7	4.3
$\bar{6}45$	- 2.6	0
$\bar{6}55$	+ 0.2	0
$\bar{6}65$	+ 7.5	0

hkℓ	Calc.	Obs.
$\bar{7}05$	- 8.0	0
$\bar{7}15$	- 7.1	0
$\bar{7}25$	- 7.1	0
$\bar{7}35$	- 2.3	0
$\bar{7}45$	- 1.8	0
$\bar{7}55$	- 5.6	0
$\bar{7}65$	- 4.3	0
$\bar{8}05$	+ 1.5	0
$\bar{8}15$	+ 0.7	0
$\bar{8}25$	+ 6.8	0
$\bar{8}35$	- 5.5	0
$\bar{8}45$	- 5.2	0
$\bar{8}55$	+ 0.6	0
$\bar{8}65$	- 0.3	0
$\bar{9}05$	+10.5	13.5
$\bar{9}15$	- 0.6	0
$\bar{9}25$	- 0.1	0
$\bar{9}35$	+ 6.3	0
$\bar{9}45$	+ 5.8	0
006	+ 0.7	0
016	+ 7.1	6.9
026	- 5.3	0
036	- 4.1	0
046	- 5.5	0
056	+ 5.6	0
066	-10.3	8.0
076		NP
086		NP
106	+ 5.9	0
116	+ 0.1	0
126	- 2.2	0
136	- 4.2	0
146	+ 3.3	0
156	+ 1.3	0
166	- 3.3	0
176		NP
$\bar{1}06$	- 0.7	0
$\bar{1}16$	+ 3.7	0
$\bar{1}26$	- 5.3	0
$\bar{1}36$	+ 1.8	0
$\bar{1}46$	+ 1.5	0

TABLE I (Continued)

hkℓ	Calc.	Obs.
$\bar{1}56$	+ 1.5	0
$\bar{1}66$	- 2.7	0
$\bar{1}76$		NP
$\bar{1}86$		NP
206	+ 0.8	0
216	+ 9.5	6.6
226	+ 3.1	0
236	-10.9	8.9
246	+ 5.7	4.6
256	+ 8.0	5.5
266	+ 7.7	5.2
$\bar{2}06$	+ 4.0	0
$\bar{2}16$	- 2.9	0
$\bar{2}26$	+ 0.3	0
$\bar{2}36$	+ 0.1	0
$\bar{2}46$	+10.5	8.6
$\bar{2}56$	- 2.7	0
$\bar{2}66$	+ 7.4	0
$\bar{2}76$		NP
$\bar{2}86$		NP
$\bar{2}96$		NP
306	+ 1.2	0
316	+ 0.9	0
326	- 3.1	0
336	+ 2.1	0
346	+ 3.2	3.2
356	+ 0.1	0
$\bar{3}06$	+ 2.1	0
$\bar{3}16$	+ 0.3	0
$\bar{3}26$	+ 5.2	0
$\bar{3}46$	+ 6.0	5.2
$\bar{3}56$	- 0.2	0
$\bar{3}66$	+ 1.6	0
$\bar{3}76$	+ 3.2	0
$\bar{3}86$		NP
$\bar{3}96$		NP
406	- 2.6	0
416	+ 7.4	8.9
426	- 0.7	0
436		NP
$\bar{4}06$	+ 1.3	0
$\bar{4}16$	- 2.5	4.9
$\bar{4}26$	- 4.2	0
$\bar{4}36$	+ 4.6	2.9
$\bar{4}46$	- 5.7	0
$\bar{4}56$	- 1.4	0
$\bar{4}66$	-10.0	5.2
$\bar{4}76$		NP
$\bar{4}86$		NP
$\bar{4}96$		NP
$\bar{5}06$	-12.2	16.6
$\bar{5}16$	+ 5.1	5.5
$\bar{5}26$	+ 4.3	0
$\bar{5}36$	+ 0.6	0
$\bar{5}46$	- 9.3	0
$\bar{5}56$	+ 2.8	0
$\bar{5}66$	+ 3.3	0
$\bar{5}76$		NP
$\bar{5}86$		NP
$\bar{6}06$	+ 0.9	0
$\bar{6}16$	- 0.1	0
$\bar{6}26$	+ 0.4	0
$\bar{6}36$	- 1.5	0
$\bar{6}46$	+ 6.4	3.7
$\bar{6}56$	- 0.7	0
$\bar{6}66$	+ 6.3	0
$\bar{7}06$	- 5.5	0
$\bar{7}16$	+ 3.0	0
$\bar{7}26$	+10.9	4.6
$\bar{7}36$	- 7.3	0
$\bar{7}46$	- 4.5	0
$\bar{7}56$	+ 3.5	0
$\bar{7}66$	+ 8.8	0
$\bar{8}06$	+ 1.2	0
$\bar{8}16$	+ 1.7	0
$\bar{8}26$	- 1.2	0
$\bar{8}36$	- 0.5	0
$\bar{8}46$	- 3.2	0
007	+ 8.6	7.5
017	+ 1.9	0

TABLE I (Continued)

$hk\ell$	Calc.	Obs.	$hk\ell$	Calc.	Obs.
027	+ 6.8	6.0	$\bar{4}07$	+ 7.1	9.5
037	+ 1.5	0	$\bar{4}17$	- 2.5	0
047	- 0.6	0	$\bar{4}27$	+ 9.8	5.4
057	+ 0.1	0	$\bar{4}37$	+ 3.8	0
			$\bar{4}47$	- 2.2	0
107	+ 6.4	9.8	$\bar{4}57$	- 4.0	0
117	- 4.1	0	$\bar{4}67$	+ 1.9	0
127	- 1.5	0			
137	- 4.7	3.7	$\bar{5}07$	+ 2.3	0
147	+ 2.6	0	$\bar{5}17$	- 1.0	0
			$\bar{5}27$	- 1.5	0
$\bar{1}07$	+ 4.3	0	$\bar{5}37$	+10.5	5.7
$\bar{1}17$	- 1.3	0	$\bar{5}47$	+ 2.9	0
$\bar{1}27$	- 7.7	4.3	$\bar{5}57$	- 0.8	0
$\bar{1}37$	+11.0	6.6	$\bar{5}67$	- 2.0	0
$\bar{1}47$	+ 7.3	4.9			
$\bar{1}57$	- 0.7	0	$\bar{6}07$	-10.6	11.2
$\bar{1}67$	- 5.8	0	$\bar{6}17$	- 2.8	0
			$\bar{6}27$	- 4.5	0
207	- 6.5	6.0	$\bar{6}37$	+ 2.3	0
217	- 1.3	0	$\bar{6}47$	- 1.7	0
227	- 5.3	0	$\bar{6}57$	- 0.6	0
$\bar{2}07$	-13.9	19.2	$\bar{7}07$	- 0.3	0
$\bar{2}17$	- 2.4	0	$\bar{7}17$	- 2.7	0
$\bar{2}27$	- 3.9	0	$\bar{7}27$	- 2.0	0
$\bar{2}37$	- 0.2	0	$\bar{7}37$	- 5.2	0
$\bar{2}47$	- 3.5	0			
$\bar{2}57$	- 0.2	0	$\bar{2}08$	+ 0.9	0
$\bar{2}67$	+ 3.1	0			
			$\bar{3}08$	- 3.5	0
$\bar{3}07$	+ 7.9	9.8	$\bar{3}18$	- 2.0	0
$\bar{3}17$	-10.8	9.2			
$\bar{3}27$	- 6.0	0	$\bar{4}08$	- 1.7	0
$\bar{3}37$	+ 0.3	0	$\bar{4}18$		NP
$\bar{3}47$	+ 4.2	0			
$\bar{3}57$	- 9.3	0			
$\bar{3}67$	- 4.4	0			

It is seen that general agreement is very good. Any large discrepancies may arise from poor intensity estimation

and to the use of the isotropic temperature factor. The non-cylindrical cross section of the crystals used for photography increased the difficulty of good cross-calibration of intensities and may account for some errors. For the cut crystals the character of the spots left much to be desired so some deviations are to be expected for this reason. The parameters used for calculation of amplitudes were determined from observed data alone and thus final positions include no corrections for incomplete series. At high values of $(\sin \theta)/\lambda$ very small changes in coordinates have a relatively large effect on Fcalc. and some of the differences may be resolved by better parameter values. The determination of an F calc. synthesis is now in progress but will not be reported here.

A criterion of the quality of a structure determination has been suggested by Smare[18] and Broomhead and Nichol[4] wherein an "index of reliability" is determined as

$$R = \frac{\sum \left| |F_{obs.}| - |F_{calc.}| \right|}{\sum |F_{obs.}|} .$$

Applied to the data herein two values of the index were evaluated. When only reflections for which observed data are available are considered, R = 0.17. If amplitudes, the calculation of which indicates they are too weak to observe (i.e. < 3), are omitted but all others are

and to the use of the isotropic temperature factor. The non-cylindrical cross section of the crystals used for photography increased the difficulty of good cross-calibration of intensities and may account for some errors. For the cut crystals the character of the spots left much to be desired so some deviations are to be expected for this reason. The parameters used for calculation of amplitudes were determined from observed data alone and thus final positions include no corrections for incomplete series. At high values of $(\sin\theta)/\lambda$ very small changes in coordinates have a relatively large effect on Fcalc. Thus some of the differences may be resolved by better parameter values. The determination of an F calc. synthesis is now in progress but will not be reported here.

A criterion of the quality of a structure determination has been suggested by Bunn[12] and Broomhead and Nichol[4] wherein an "index of reliability" is determined as

$$R = \frac{\sum \left|\,|F_{obs.}| - |F_{calc.}|\,\right|}{\sum |F_{obs.}|}.$$

Applied to the data herein two values of the index were evaluated. When only reflections for which observed data are available are considered, R = 0.17. If amplitudes, the calculation of which indicates they are too weak to observe (i.e. < 3), are omitted but all others are

considered, then $R = 0.21$. These values compare favorably with those obtained in other structure determinations by other investigators. More recently it has been suggested that the index is not as good an indication of the quality of a structure as originally supposed.

DISCUSSION OF THE STRUCTURE

As has been stated, there are two strings of molecules, one in the plane $y = 1/4$ and the other in $y = 3/4$ so oriented with respect to each other as to satisfy best packing relations. Distances of close approach in the cell have been calculated and are shown in Figure 9.

To simplify the discussion of the molecular structure the atoms of the molecule have been labelled in Figure 2. Figure 10 is a sketch showing distances and angles between the atoms lying in the symmetry plane. A similar sketch for the atoms occupying fourfold positions is shown in Figure 11. Table II below lists pertinent intramolecular distances and angles together with average values of interest.

TABLE II

(All Distances in Angstroms)

$C_1 - Cl_7$	1.80	$Cl_1 - Cl_4$	2.81
$C_1 - Cl_6$	1.67	$Cl_5 - Cl_8$	2.84
$C_3 - Cl_8$	1.75	$Cl_6 - Cl_7$	2.82
$C_3 - Cl_5$	1.82	Average	2.82
$C_2 - Cl_1$	1.75		
$C_2 - Cl_4$	1.71	$Cl_7 - Cl_8$	4.93
Average	1.75	$Cl_3 - Cl_4$	4.92
		Average	4.92

TABLE II (Continued)

$Cl_5 - Cl_6$	3.36	$Cl_4 - Cl_7$	3.96
$Cl_1 - Cl_2$	3.38	$Cl_4 - Cl_8$	4.00
Average	3.37	Average	3.98
$C_1 - C_3$	2.12	$\angle Cl_1-C_2-C_4$	108° - 20'
$C_2 - C_4$	2.21	$\angle Cl_6-C_1-Cl_7$	108° - 20'
Average	2.16	$\angle Cl_5-C_3-Cl_8$	106°
		Average	107° - 33'
$C_1 - C_2$	1.59		
$C_3 - C_2$	1.55	$\angle C_1-C_2-C_3$	85°
Average	1.57	$\angle C_2-C_1-C_4$	88°
		Average	$86^\circ.5$
$Cl_4 - Cl_6$	3.06		
$Cl_4 - Cl_5$	3.10		
$Cl_1 - Cl_7$	3.11		
$Cl_1 - Cl_8$	3.07		
Average	3.08		

The twofold chlorine atoms form an isosceles trapezoid lying in the symmetry plane and the chlorines occupying fourfold positions form a similar trapezoid essentially of the same dimensions which lies almost in the plane x = 1/4. The two trapezoids are so oriented as to give the idealized molecule the symmetry $\bar{4}m$. From an inspection of the Cl - Cl separations on each side of

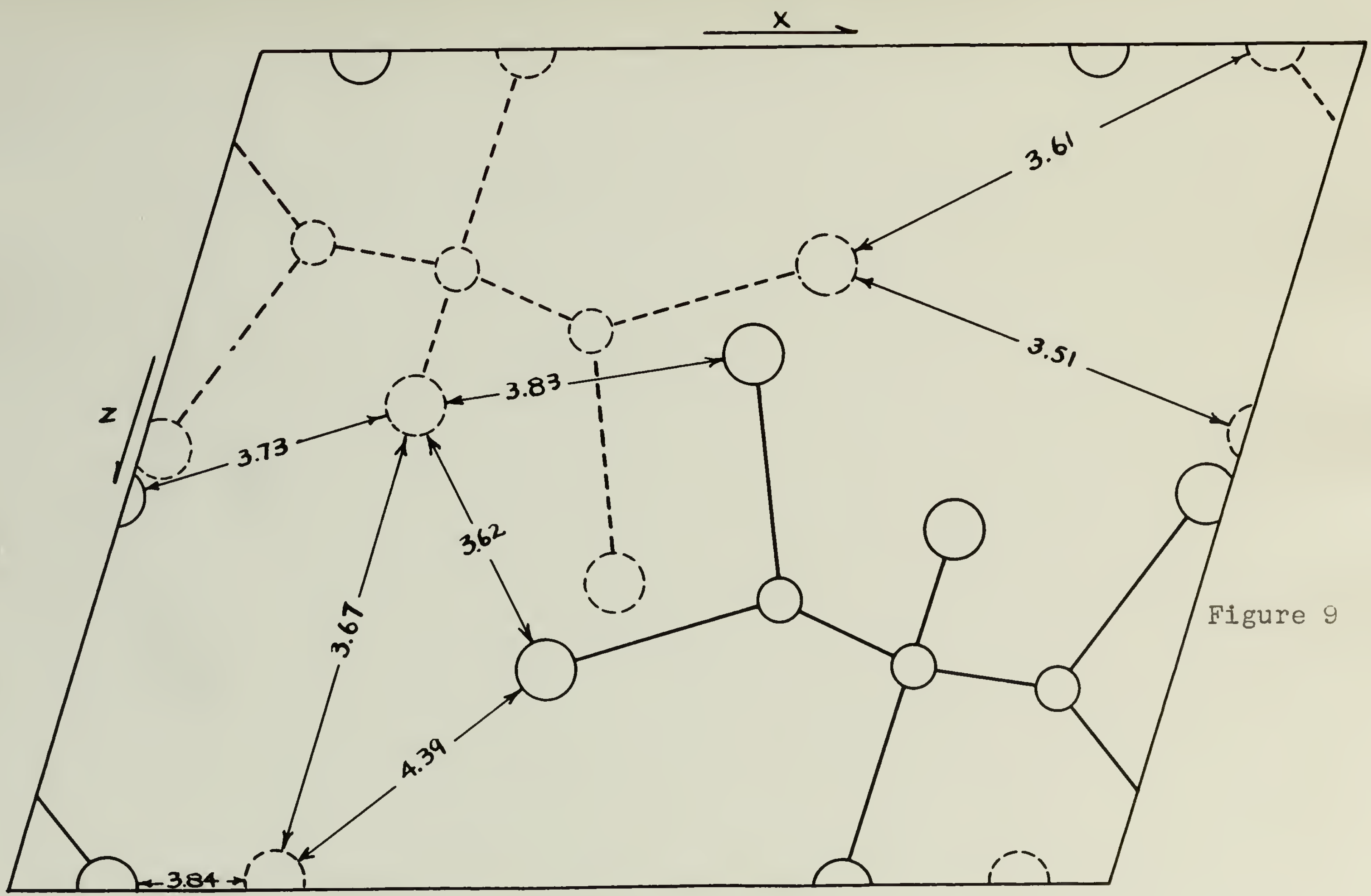

Figure 9

SKETCH SHOWING SOME VAN DER WAAL SEPARATIONS

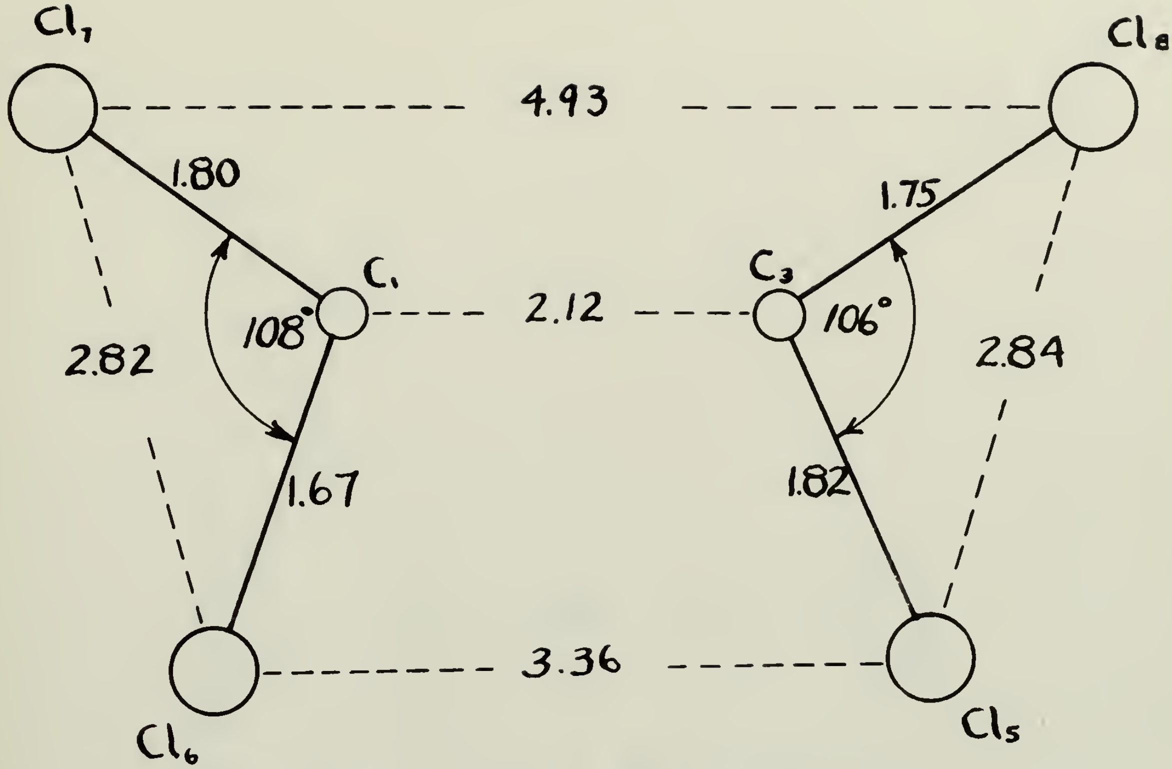

DISTANCES IN PLANE $Y = \frac{1}{4}$

Figure 10

the carbon ring it can be seen that the chlorines have moved so as to equalize Cl - Cl interactions at the expense of deformation of the carbon ring. It is felt that the small amount of energy required for distortion of the ring is more than regained by equalization of the chlorine distances.

The optical behavior of the compound is of interest because the crystals show extinction parallel to the needle axis which the study has shown not to be the unique axis. In the monoclinic case, the orientation of the indicatrix must conform to the crystal symmetry and one axis thereof must coincide with the b axis of the unit cell. Ordinarily this is the only restriction on indicatrix orientation except that its other two axis must obviously lie in the ac plane taking any position in this plane but of course remaining at right angles to each other. For C_4Cl_8 the conclusion is that one of the two indicatrix axes in the ac plane lies parallel to c. This might be expected since the strings of molecules also lie parallel to c as does the fourfold alternating axis of the idealized molecule. The remaining indicatrix axis must then lie normal to c. It is believed that this optical behavior is good evidence in support of the conclusion that the molecular symmetry approximates closely to $\bar{4}m$.

The puckering of the carbon ring is considerable, the dihedral angle being about 16°. From an examination of the literature this appears to be the first direct evidence of a non-planar cyclobutane ring. Edgell[10] from the infra-red and Raman spectra study of C_4F_8 concludes that the ring is planar with a molecular symmetry D_{4h}. Preliminary results of electron diffraction studies of the same molecule by Livingston indicate that the ring is puckered. Spectroscopic studies of C_4H_8 are interpreted by Wilson[20] to show the molecular symmetry is not C_{2v} but rather D_{4h}. Dunitz' X-ray study of tetraphenyl cyclobutane shows the ring carbons to lie in a single plane, a symmetry center for the molecule being required for the space group.

Individual C-Cl distances are erratic because of poor carbon peaks in the Fourier sections. However they average out to 1.75 Å. which is very close to the distance of 1.76 Å. observed by Pauling and Brockway[15] in election diffraction studies of CCl_4. In liquid carbon tetrachloride Bray and Gingrich[3] have observed the corresponding value as 1.74 Å. For chlorines bonded to the same carbon atom an average separation of 2.82 Å. is found in C_4Cl_8. A value of 2.86 Å. is reported by Pauling and Brockway as well as by Cosslett and de Laszlo[7] in independent investigations of gaseous CCl_4.

The puckering of the carbon ring is considerable, the dihedral angle being about 18°. From an examination of the literature this appears to be the first direct evidence of a non-planar cyclobutane ring. Edgell[20] from the infra-red and Raman spectra study of C_4F_8 concludes that the ring is planar with a molecular symmetry D_{4h}. Preliminary results of electron diffraction studies of the same molecule by Livingston indicate that the ring is puckered. Spectroscopic studies of C_4H_8 are interpreted by Wilson[22] to show the molecular symmetry is not C_{2v} but rather D_{4h}. Dunitz' X-ray study of tetraphenyl cyclobutane shows the ring carbons to lie in a single plane, a symmetry center for the molecule being required for the space group.

Individual C-Cl distances are erratic because of poor carbon peaks in the Fourier sections. However they average out to 1.75 Å. which is very close to the distance of 1.76 Å. observed by Pauling and Brockway[15] in electron diffraction studies of CCl_4. In liquid carbon tetrachloride Gray and Gingrich[9] have observed the corresponding value as 1.78 Å. For chlorines bonded to the same carbon atom an average separation of 2.87 Å. is found in C_4Cl_8. A value of 2.86 Å. is reported by Pauling and Brockway as well as by Cosslett and de Laszlo[7] in independent investigations of gaseous CCl_4.

Eisenstein[11] found the separation to be 2.95 Å. at 27°C from X-ray studies for the liquid. The Cl-C-Cl angles observed in C_4Cl_8 were all slightly less than tetrahedral.

Carbon-Carbon bond lengths are not too accurate but the average value is indicative of a departure from the "normal" value of 1.54 Å. The following table summarizes C-C spacings in compounds containing cyclobutane rings. In every case the values are greater than the normal value.

Investigator	Compound	C-C (Å.)
Dunitz	Tetraphenyl-cyclobutane	1.585±0.02, 1.555±0.02 (Avg. 1.57)
Bauer & Beach[1]	Methylene cyclobutane	1.56 ±0.03
Shand, Schomaker, & Fischer[17]	Methylene cyclobutane	1.55 ±0.02
Lipscomb and Schomaker[13]	Dimethyl ketene dimer	1.56 ±0.05
Livingston	Perfluoro-cyclobutane (C_4F_8)	1.60
This investigation	C_4Cl_8	1.59, 1.55 (Avg. 1.57)

Preliminary X-ray analysis of dinaphthylene cyclobutane by Dunitz and Weissman[9] indicate that C-C distances in the central ring may be longer than 1.54 Å. also. They report that the molecule has a center of symmetry which means the ring must be planar.

The average C-C-C angle of 86°.5 is of course only indicative of the puckering of the ring and cannot be taken as a final value since more accurate carbon positions are yet to be obtained.

Giacomello(11) found the separation to be 2.92 Å. at 20°C from X-ray studies for the liquid. The Cl-C-Cl angles observed in C_4Cl_8 were all slightly less than tetrahedral.

Carbon-Carbon bond lengths are not too accurate but the average value is indicative of a departure from the "normal" value of 1.54 Å. The following table summarizes C-C spacings in compounds containing cyclobutane rings. In every case the values are greater than the normal value.

Investigator	Compound	C-C (Å.)
Dunitz	Tetraphenyl-cyclobutane	1.555±0.03 1.585±0.03 Avg.1.57
Bauer & Beach(1) (17)	Methylene cyclobutane	1.56 ±0.03
Shand, Schomaker, & Fischer	Methylene cyclobutane	1.55 ±0.02
Lipscomb and Schomaker(13)	Dimethyl ketene dimer	1.56 ±0.05
Livingston	Perfluoro-cyclobutane (C_4F_8)	1.60
This Investigation	C_4Cl_8	1.56 1.58 Avg. 1.57

Preliminary X-ray analysis of dianisylidene cyclobutane by Dunitz and Weissman(9) indicate that C-C distances in the central ring may be longer than 1.54 Å. also. They report that the molecule has a center of symmetry which means the ring must be planar.

The average C-C-C angle of 89.5° is of course only indicative of the puckering of the ring and cannot be taken as a final value since more accurate carbon positions are yet to be obtained.

SUGGESTIONS FOR FURTHER STUDY

In any refinement procedure one may employ, the atomic coordinates of the chlorine atoms will change little if at all. There does remain the problem of tiling down the positions of the carbon atoms. There are methods that may be used to improve the structure determination.

It has been mentioned previously that many relatively intense reflections were observed at high values of $(\sin \theta)/\lambda$. This indicates that probably there are numerous amplitudes of considerable magnitude beyond the maximum angle observable with Cu $K\alpha$ radiation but which still would contribute substantially to the Fourier summation. The incomplete series gives rise to a rippling effect which results in a displacement of maxima, particularly those of carbon atoms, from their true positions. It is desirable to obtain additional terms in the series to smooth out these ripples. Photographs taken with M_o $K\alpha$ radiation should serve to pick up reflections further out in the reciprocal lattice. Incorporation of those additional amplitudes in the Fourier series should then lead to more accurate positions for carbon atoms.

There is a less desirable procedure that may be

followed but which is considered adequate by many in the field. The parameter values given by the Fourier synthesis of observed amplitudes are used to calculate structure amplitudes for the observed range of $(\sin\theta)/\lambda$. These calculated amplitudes are put through a Fourier synthesis which, since this series also is somewhat incomplete, will not reproduce exactly the peak positions used to obtain the calculated Fourier coefficients. The resulting small shift in position of each peak is applied with reversed sign as a correction to the corresponding atomic positions as given by the experimental Fourier synthesis.

Since carbon maxima may be displaced and ill-defined in the presence of the high chlorine peaks, it would be desirable if the Fourier syntheses could be calculated in such a way that the contributions of the chlorines to the series would not be included. Such a procedure was partially successful in the structure determination of UF_6 in the sense that when uranium peaks were subtracted out, rather well defined peaks for the light fluorine atoms remained. The method of attack was first to determine a scattering factor curve for uranium. Then structure factors were calculated for the U atoms alone and subtracted from the observed values. This left a residue which was taken as the contribution from fluorine atoms.

followed but which is considered adequate by many in the field. The parameter values given by the Fourier synthesis of observed amplitudes are used to calculate structure amplitudes for the observed range of $(\sin\theta)/\lambda$. These calculated amplitudes are put through a Fourier synthesis which, since this series also is somewhat incomplete, will not reproduce exactly the peak positions used to obtain the calculated Fourier coefficients. The resulting small shift in position of each peak is applied with reversed sign as a correction to the corresponding atomic positions as given by the experimental Fourier synthesis.

Since carbon peaks may be displaced and ill-defined in the presence of the high chlorine peaks, it would be desirable if the Fourier syntheses could be calculated in such a way that the contributions of the chlorines to the series would not be included. Such a procedure was partially successful in the structure determination of UF_6 in the sense that when uranium peaks were subtracted out, rather well defined peaks for the light fluorine atoms remained. The method of attack was first to determine a scattering factor curve for uranium. Then structure factors were calculated for the U atoms alone and subtracted from the observed values. This left a residue which was taken as the contribution from fluorine atoms.

Fourier calculations with the residue gave light atom peaks and enabled the investigators to obtain approximate atomic coordinates. This same procedure could probably be carried out for C_4Cl_8 but the determination of the experimental form factor for chlorine is at best a rather uncertain procedure.

PART II

FURTHER STUDY OF THE STRUCTURE OF C_8F_{12}

INTRODUCTION

The first structure work on the dimer of hexafluorobutadiene, C_8F_{12}, was done by Dr. R. W. Broge(21) in this Laboratory. The trial model employed was based on a "chair" configuration of the three cyclobutane rings fused at 120° angles to one another. Reasons for the choice of such a model are reviewed in his work. He found the unit cell to be triclinic and to simplify the problem based his analysis on a face-centered triclinic unit of

$$\underline{a_1}' = 9.95 \text{ Å.} \qquad \alpha' = 86.2^\circ$$
$$\underline{a_2}' = 7.39 \text{ Å.} \qquad \beta' = 84.8^\circ$$
$$\underline{a_3}' = 13.20 \text{ Å.} \qquad \gamma' = 86.8^\circ$$

containing one molecule per lattice point. Since no positive pyroelectric effect was observed the molecule was believed to have a center of symmetry. Using zero-layer a' - axis data with the centrosymmetric model he determined a set of atomic parameters which, however, led to erratic C-C and C-F bond lengths and to poor agreement between calculated and observed amplitudes. It was clear that the structure problem required further study.

Since for triclinic lattices the choice of a

structural unit is not indicated by symmetry, Buerger has recommended that such lattices be reported in terms of what he calls the "reduced primitive cell." This is a unit the edges of which have the three shortest translations in the lattice and the axes of which are, labelled such that $\underline{a}_1 < \underline{a}_2 < \underline{a}_3$. An additional requirement is that the interaxial angles α, β, and γ are all obtuse. It was thought that if all reflections that might be observed were indexed on the basis of this unit the problem might be clarified and some progress might be made toward the final solution.

Figure 12 shows the face centered unit used by Broge together with the primitive reduced cell employed in the present study. It is seen that $\underline{a}_1$ = BD , $\underline{a}_2$ = DE , and $\underline{a}_3$ = AB. The transformation from the compound to the primitive unit is:

$$\underline{a}_1 = \frac{-\underline{a}_2' + \underline{a}_1'}{2}$$

$$\underline{a}_2 = \frac{-\underline{a}'_1 - \underline{a}'_2}{2}$$

$$\underline{a}_3 = \frac{-\underline{a}'_3 + \underline{a}'_2}{2} .$$

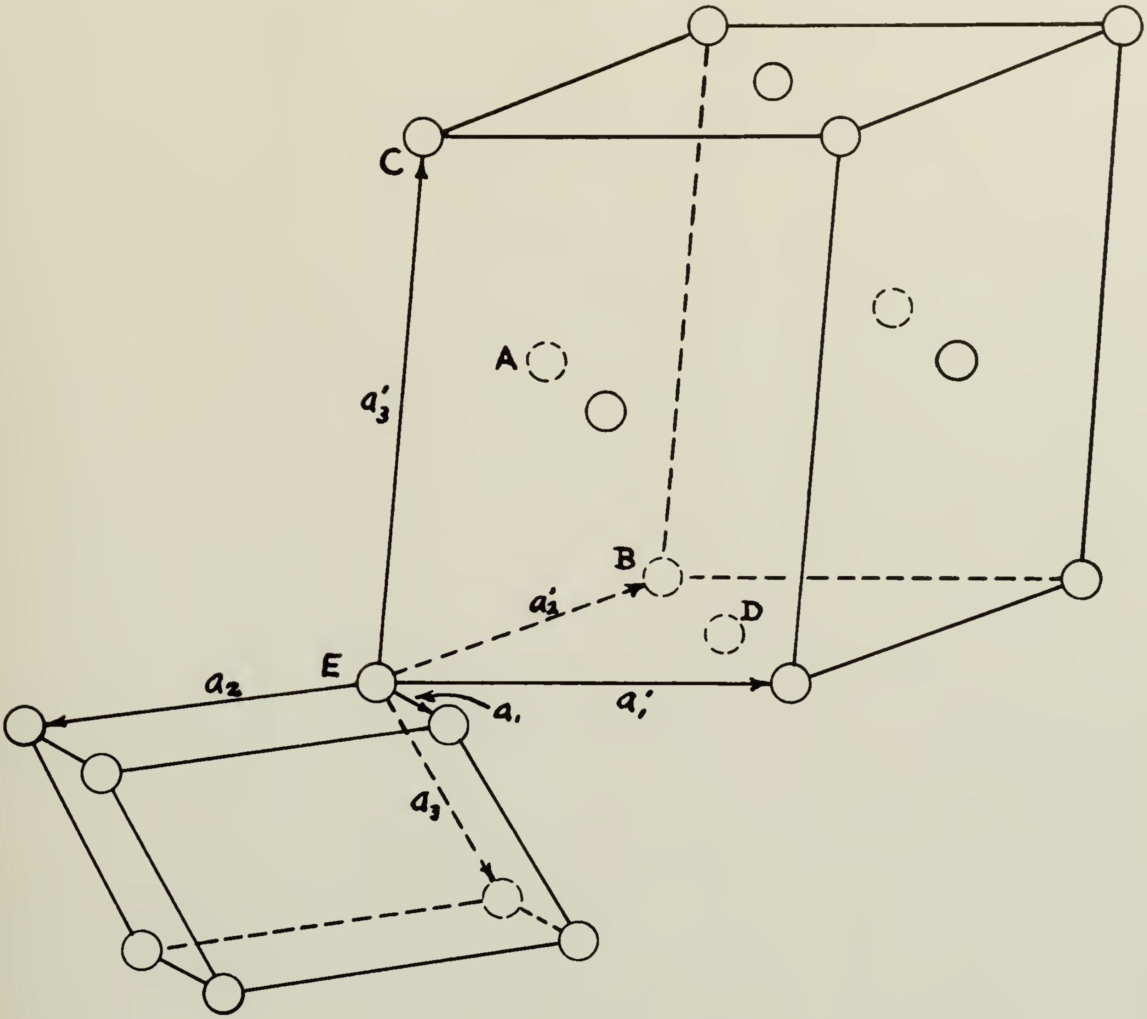

CENTERED CELL
AND
REDUCED PRIMITIVE CELL

Figure 12

The present work was based on the centrosymmetric model. Although practically complete data for the primitive cell were obtained, no new atomic coordinates have been assigned and the structure still awaits solution. It is to be understood that the work reported herein was done prior to the investigation of the structure of octochlorocyclobutane. In view of the fact that the carbon ring is puckered in C_4Cl_8, it may be that the rings in C_8F_{12} are not planar. If this be true a new trial model having no center of symmetry must be considered.

EXPERIMENTAL PROCEDURE

Single crystals of the compound were grown under vacuum by sublimation in thin-walled glass capillaries. The procedure is described by Broge and is a standard procedure in this Laboratory for crystals having high vapor pressures. In this study the capillaries were about 1 mm. in diameter and wall thickness averaged 0.01 mm. as measured under a microscope fitted with a micrometer eyepiece.

The crystals were mounted on the goniometer head such that the face of growth in the capillary was perpendicular to the rotation axis. Oscillation photographs were used to locate rational directions and to align the crystals for Weissenberg photography. Since the various repeat distances for rational directions could be calculated from Broge's work it was a simple matter to identify these directions on the photographs. Four crystals were photographed and the rational directions found may be described as follows:

Crystal number	Repeat distance (Å.)	Description
1	6.3	$\underline{a}_2$ of reduced unit
2	6.0	$\underline{a}_1$ of reduced unit
3	6.3	$\underline{a}_2$ of reduced unit
4	7.4	$\underline{a}_2$, of centered cell.

EXPERIMENTAL PROCEDURE

Single crystals of the compound were grown under vacuum by sublimation in thin-walled glass capillaries. The procedure is described by Kruge and is a standard procedure in this laboratory for crystals having high vapor pressures. In this study the capillaries were about 1 mm. in diameter and wall thickness averaged 0.01 mm. as measured under a microscope fitted with a micrometer eyepiece.

The crystals were mounted on the goniometer head such that the face of growth in the capillary was perpendicular to the rotation axis. Oscillation photographs were used to locate rational directions and to align the crystals for Weissenberg photography. Since the various repeat distances for rational directions could be calculated from Kruge's work it was a simple matter to identify these directions on the photographs. Four crystals were photographed and the rational directions found may be described as follows:

Crystal number	Repeat distance (Å.)	Description
1	6.3	a_2 of reduced unit
2	6.0	a_1 of reduced unit
3	6.3	a_3 of reduced unit
4	7.4	a_4 of centered cell.

Crystal #1 was cracked and gave separation of spots; it was discarded after #3 was obtained.

Complete zero and higher layer equi-inclination Weissenberg photographs of all samples were taken with Cu $K\alpha$ radiation using the triple-film technique. The films were given exposure times of thirty minutes and four hours for each layer in order to be able to read spots over a wide range of intensity. Zero-layer NaCl reflections were superimposed on separate zero-layer photographs of C_8F_{12} for good lattice constant measurement.

Indexing the Reflections.

The problem was simplified in that the reciprocal lattice of the primitive cell was known. In that lattice it was thus possible to calculate distances and angles which served to identify unequivocally the reflections on the films. Reflections from crystals 1, 2, and 3 were easily indexed. For crystal #4 it was necessary to choose an appropriate reciprocal lattice and the corresponding direct cell for use in indexing reflections and then transform indices so that they would refer to the reduced unit. The cell chosen was:

$$\underline{a_1}'' = 6.03\ \text{Å}. \qquad \alpha'' = 57^\circ$$

$$\underline{a_2}'' = 7.39 \qquad \beta'' = 74^\circ$$

$$\underline{a_3}'' = 7.76 \qquad \gamma'' = 55.5^\circ.$$

The transformation to the primitive cell is:

$$\underline{a_1} = \underline{a_1}''$$

$$\underline{a_2} = \underline{a_2}'' - \underline{a_1}''$$

$$\underline{a_3} = \underline{a_3}'' - \underline{a_2}'' .$$

Determination of the Lattice constants.

Using the cell constants determined by Broge for the centered unit the reciprocal lattice for the reduced cell has

$$\underline{a_1}^* = 0.1891 \text{ Å}^{-1} \qquad \alpha^* = 70.8^\circ$$

$$\underline{a_2}^* = 0.1742 \qquad \beta^* = 66.3^\circ$$

$$\underline{a_3}^* = 0.1525 \qquad \gamma^* = 68.0^\circ$$

However measurements on zero-layer Weissenberg photographs taken in the present study lead to

$$\underline{a_1}^* = 0.1890 \pm 0.0002 \text{ Å.}^{-1} \qquad \alpha^* = 69.3^\circ$$

$$\underline{a_2}^* = 0.1772 \pm 0.0002 \qquad \beta^* = 66.3^\circ$$

$$\underline{a_3}^* = 0.1545 \pm 0.0002$$

The spacing of $\underline{a_2}$ was measured from an oscillation photograph upon which NaCl reflections had been superimposed and was found to be 6.29 Å. Using this value with appropriate formulae the reciprocal lattice angle γ^*

was determined to be 67.4°. Direct cell constants are then

$$\underline{a_1} = 6.02 \text{ Å} \quad \alpha = 103.6°$$

$$\underline{a_2} = 6.29 \quad \beta = 107.9°$$

$$\underline{a_3} = 7.27 \quad \gamma = 106.4°$$

for the primitive reduced unit. These values lead to a unit cell volume of 235.2 $Å^3$ and an X-ray density of 2.29 gm./cc. Broge lists 240.7 $Å^3$ and 2.23 gm./cc. as a result of his study. It is to be noted that he had to employ the method of angular lag to determine angles in reciprocal space.

Intensity Measurement.

The relative intensities were determined by visual comparison of the reflections with the intensity scale described in Part I. Values of $(\sin\theta)/\lambda$ were computed graphically rather than from film measurements. The Lorentz and Polarization and the Tunell factor where applicable were applied to the intensities to obtain relative F^2 values. By careful cross-calibration all data were reduced to the four hour zero layer a_1 axis photograph. Excellent checks were obtained for reflections common to two or more films. The relative F^2 values are listed in Table III.

TABLE III

$hk\ell$	$\frac{\sin\theta}{\lambda}$	Rel. $\lvert F_{hk\ell}\rvert^2$
010	0.089	950
020	0.178	800
030	0.255	660
040	0.355	24
050	0.443	176
060	0.533	2.4
070	0.620	0
100	0.084	1600
110	0.156	370
120	0.234	40
130	0.311	72
140	0.402	100
150	0.486	33
160	0.578	-
$\bar{1}10$	0.097	2000
$\bar{1}20$	0.162	100
$\bar{1}30$	0.240	1000
$\bar{1}40$	0.331	1750
$\bar{1}50$	0.415	3.6
$\bar{1}60$	0.565	35
$\bar{1}70$	0.636	1.2
001	0.077	660
011	0.136	625
021	0.218	140
031	0.300	145
041	0.388	14
051	0.475	12
061	0.564	2
$01\bar{1}$	0.094	2300
$02\bar{1}$	0.166	350
$03\bar{1}$	0.248	60
$04\bar{1}$	0.334	16
$05\bar{1}$	0.422	62
$06\bar{1}$	0.511	2.7
$07\bar{1}$	0.597	6.7
101	0.143	860

$hk\ell$	$\frac{\sin\theta}{\lambda}$	Rel. $\lvert F_{hk\ell}\rvert^2$
111	0.201	280
121	0.272	1.8
131	0.357	1750
141	0.435	13
151	0.526	0
161	0.610	-
$10\bar{1}$	0.084	1300
$11\bar{1}$	0.136	150
$12\bar{1}$	0.208	5800
$13\bar{1}$	0.292	52
$14\bar{1}$	0.376	110
$15\bar{1}$	0.467	111
$16\bar{1}$	0.551	0
$17\bar{1}$	0.636	0
$\bar{1}11$	0.123	85
$\bar{1}21$	0.188	94
$\bar{1}31$	0.272	630
$\bar{1}41$	0.357	5
$\bar{1}51$	0.441	159
$\bar{1}61$	0.532	110
$\bar{1}1\bar{1}$	0.130	62
$\bar{1}2\bar{1}$	0.149	980
$\bar{1}3\bar{1}$	0.234	610
$\bar{1}4\bar{1}$	0.318	230
$\bar{1}5\bar{1}$	0.396	410
$\bar{1}6\bar{1}$	0.480	195
$\bar{1}7\bar{1}$	0.571	3
002	0.154	337
012	0.204	5595
022	0.274	580
032	0.351	22
042	0.434	64
052	0.518	37
062	0.604	6
$01\bar{2}$	0.147	155
$02\bar{2}$	0.139	900

TABLE III (Continued)

$hk\ell$	$\frac{\sin\theta}{\lambda}$	Rel. $\lvert F_{hk\ell}\rvert^2$
$03\bar{2}$	0.254	15
$04\bar{2}$	0.332	613
$05\bar{2}$	0.414	14.7
$06\bar{2}$	0.495	39
$07\bar{2}$	0.584	22
102	0.208	430
112	0.259	1000
122	0.331	6
132	0.402	2
142	0.486	47
152	0.571	0
$10\bar{2}$	0.149	330
$11\bar{2}$	0.162	7.5
$12\bar{2}$	0.214	5
$13\bar{2}$	0.285	600
$14\bar{2}$	0.370	270
$15\bar{2}$	0.454	0
$16\bar{2}$	0.538	-
$17\bar{2}$	0.623	-
$\bar{1}12$	0.175	190
$\bar{1}22$	0.240	57
$\bar{1}32$	0.318	19
$\bar{1}42$	0.396	85
$\bar{1}52$	0.480	218
$\bar{1}62$	0.565	37
$\bar{1}1\bar{2}$	0.188	510
$\bar{1}2\bar{2}$	0.208	900
$\bar{1}3\bar{2}$	0.252	2200
$\bar{1}4\bar{2}$	0.324	2.9
$\bar{1}5\bar{2}$	0.396	17
$\bar{1}6\bar{2}$	0.473	112
$\bar{1}7\bar{2}$	0.519	6.4
003	0.230	590
013	0.275	760
023	0.338	72
033	0.407	10.8

$hk\ell$	$\frac{\sin\theta}{\lambda}$	Rel. $\lvert F_{hk\ell}\rvert^2$
043	0.485	37
053	0.565	0
063	0.645	0
$01\bar{3}$	0.214	370
$02\bar{3}$	0.235	8
$03\bar{3}$	0.282	19
$04\bar{3}$	0.347	340
$05\bar{3}$	0.421	96
$06\bar{3}$	0.498	40
$07\bar{3}$	0.580	0
103	0.379	22
113	0.321	25
123	0.389	10
133	0.461	52
143	0.538	75
153	0.545	0
$10\bar{3}$	0.214	108
$11\bar{3}$	0.214	6970
$12\bar{3}$	0.246	53
$13\bar{3}$	0.305	360
$14\bar{3}$	0.376	370
$15\bar{3}$	0.454	26
$16\bar{3}$	0.538	-
$17\bar{3}$	0.590	-
$\bar{1}13$	0.246	210
$\bar{1}23$	0.305	70
$\bar{1}33$	0.370	50
$\bar{1}43$	0.447	80
$\bar{1}53$	0.532	13
$\bar{1}63$	0.610	15
$\bar{1}1\bar{3}$	0.253	960
$\bar{1}2\bar{3}$	0.260	1100
$\bar{1}3\bar{3}$	0.292	180
$\bar{1}4\bar{3}$	0.344	180
$\bar{1}5\bar{3}$	0.409	285
$\bar{1}6\bar{3}$	0.480	16

TABLE III (Continued)

$hk\ell$	$\frac{\sin\theta}{\lambda}$	Rel. $\lvert F_{hk\ell}\rvert^2$	$hk\ell$	$\frac{\sin\theta}{\lambda}$	Rel. $\lvert F_{hk\ell}\rvert^2$
$\bar{1}7\bar{3}$	0.558	2.5	$\bar{1}4\bar{4}$	0.383	120
			$\bar{1}5\bar{4}$	0.435	640
004	0.307	25	$\bar{1}6\bar{4}$	0.499	16
014	0.350	24	$\bar{1}7\bar{4}$	0.571	0
024	0.405	620			
034	0.472	0	005	0.384	5.4
044	0.540	0	015	0.423	0
054	0.622	0	025	0.477	0
			035	0.533	6.4
$01\bar{4}$	0.287	610	045	0.607	0
$02\bar{4}$	0.296	48			
$03\bar{4}$	0.327	800	$01\bar{5}$	0.363	86
$04\bar{4}$	0.377	430	$02\bar{5}$	0.361	0
$05\bar{4}$	0.441	43	$03\bar{5}$	0.381	67
$06\bar{4}$	0.513	175	$04\bar{5}$	0.420	110
$07\bar{4}$	0.587	0	$05\bar{5}$	0.473	6
			$06\bar{5}$	0.535	0
104	0.357	8	$07\bar{5}$	0.604	14.5
114	0.402	15			
124	0.461	7	105	0.428	139
134	0.532	0	115	0.474	24
144	0.596	5	125	0.499	5
			135	0.590	10
$10\bar{4}$	0.285	240			
$11\bar{4}$	0.279	24	$10\bar{5}$	0.357	2300
$12\bar{4}$	0.298	900	$11\bar{5}$	0.344	2.2
$13\bar{4}$	0.337	415	$12\bar{5}$	0.331	200
$14\bar{4}$	0.396	18	$13\bar{5}$	0.382	370
$15\bar{4}$	0.461	88	$14\bar{5}$	0.428	4.6
$16\bar{4}$	0.538	-	$15\bar{5}$	0.486	0
$17\bar{4}$	0.616	-	$16\bar{5}$	0.558	-
			$17\bar{5}$	0.629	-
$\bar{1}14$	0.318	3			
$\bar{1}24$	0.369	21	$\bar{1}15$	0.389	3.5
$\bar{1}34$	0.434	63	$\bar{1}25$	0.441	33
$\bar{1}44$	0.506	0	$\bar{1}35$	0.499	6
$\bar{1}54$	0.584	0	$\bar{1}45$	0.571	19
			$\bar{1}55$	0.636	6.4
$\bar{1}1\bar{4}$	0.331	73			
$\bar{1}2\bar{4}$	0.324	1200	$\bar{1}1\bar{5}$	0.402	185
$\bar{1}3\bar{4}$	0.344	10	$\bar{1}2\bar{5}$	0.389	8

TABLE III (Continued)

$hk\ell$	$\frac{\sin\theta}{\lambda}$	Rel. $\lvert F_{hk\ell}\rvert^2$
$\bar{1}3\bar{5}$	0.402	300
$\bar{1}4\bar{5}$	0.428	3.1
$\bar{1}5\bar{5}$	0.474	20
$\bar{1}6\bar{5}$	0.526	3
$\bar{1}7\bar{5}$	0.590	0
006	0.462	110
016	0.500	3
026	0.549	0
036	0.608	30
$01\bar{6}$	0.438	7.3
$02\bar{6}$	0.432	260
$03\bar{6}$	0.443	180
$04\bar{6}$	0.472	7.5
$05\bar{6}$	0.516	193
$06\bar{6}$	0.569	0
$07\bar{6}$	0.630	0
106	0.506	5
116	0.552	0
126	0.603	8.5
$10\bar{6}$	0.434	14
$11\bar{6}$	0.415	270
$12\bar{6}$	0.422	40
$13\bar{6}$	0.441	0
$14\bar{6}$	0.474	80
$15\bar{6}$	0.525	9
$16\bar{6}$	0.590	-
$\bar{1}16$	0.467	125
$\bar{1}26$	0.519	4
$\bar{1}36$	0.571	1.6
$\bar{1}46$	0.640	3
$\bar{1}1\bar{6}$	0.480	140
$\bar{1}2\bar{6}$	0.467	18.5
$\bar{1}3\bar{6}$	0.467	140
$\bar{1}4\bar{6}$	0.486	180
$\bar{1}5\bar{6}$	0.519	0

$hk\ell$	$\frac{\sin\theta}{\lambda}$	Rel. $\lvert F_{hk\ell}\rvert^2$
$\bar{1}6\bar{6}$	0.571	0
$\bar{1}7\bar{6}$	0.623	0
007	0.539	14
017	0.570	11
027	0.623	0
$01\bar{7}$	0.514	0
$02\bar{7}$	0.504	6
$03\bar{7}$	0.510	0
$04\bar{7}$	0.530	0
$05\bar{7}$	0.563	0
$06\bar{7}$	0.608	10.8
107	0.584	4
117	0.623	0
$10\bar{7}$	0.513	10
$11\bar{7}$	0.493	40
$12\bar{7}$	0.487	115
$13\bar{7}$	0.499	0
$14\bar{7}$	0.526	0
$15\bar{7}$	0.571	5.3
$16\bar{7}$	0.623	-
$\bar{1}17$	0.545	105
$\bar{1}27$	0.590	6
$\bar{1}37$	0.643	1.1
$\bar{1}1\bar{7}$	0.558	12
$\bar{1}2\bar{7}$	0.538	110
$\bar{1}3\bar{7}$	0.538	0
$\bar{1}4\bar{7}$	0.551	0
$\bar{1}5\bar{7}$	0.577	0
$\bar{1}6\bar{7}$	0.616	0
008	0.616	0
$01\bar{8}$	0.591	4
$02\bar{8}$	0.578	0
$03\bar{8}$	0.578	5.3

TABLE III (Continued)

$hk\ell$	$\frac{\sin\theta}{\lambda}$	Rel. $\lvert F_{hk\ell}\rvert^2$
$04\bar{8}$	0.592	50
$05\bar{8}$	0.620	0
$10\bar{8}$	0.597	14
$11\bar{8}$	0.571	0
$12\bar{8}$	0.564	1.6
$13\bar{8}$	0.564	10.4
$14\bar{8}$	0.584	0
$15\bar{8}$	0.622	0
$\bar{1}18$	0.624	4
$\bar{1}1\bar{8}$	0.629	6.1
$\bar{1}2\bar{8}$	0.616	0
$\bar{1}3\bar{8}$	0.603	2.6
$\bar{1}4\bar{8}$	0.616	0
$\bar{1}5\bar{8}$	0.636	0
$02\bar{9}$	0.647	-
$03\bar{9}$	0.645	0
$11\bar{9}$	0.640	14.7
$12\bar{9}$	0.624	-
$13\bar{9}$	0.624	-
$14\bar{9}$	0.635	-
200	0.188	600
210	0.240	1180
220	0.305	200
230	0.383	300
240	0.467	0
250	0.545	0
260	0.636	0
$\bar{2}10$	0.175	27.5
$\bar{2}20$	0.194	25.
$\bar{2}30$	0.259	500
$\bar{2}40$	0.324	130
$\bar{2}50$	0.402	15
$\bar{2}60$	0.487	120
$\bar{2}70$	0.571	1.8

$hk\ell$	$\frac{\sin\theta}{\lambda}$	Rel. $\lvert F_{hk\ell}\rvert^2$
201	0.227	400
211	0.285	485
221	0.350	42
231	0.422	95
241	0.499	17
251	0.583	0
$20\bar{1}$	0.175	880
$21\bar{1}$	0.214	14
$22\bar{1}$	0.278	200
$23\bar{1}$	0.357	120
$24\bar{1}$	0.441	0
$25\bar{1}$	0.519	0
$26\bar{1}$	0.603	-
$\bar{2}11$	0.169	314
$\bar{2}21$	0.208	6550
$\bar{2}31$	0.272	108
$\bar{2}41$	0.350	17
$\bar{2}51$	0.428	290
$\bar{2}61$	0.512	1.7
$\bar{2}71$	0.585	0
$\bar{2}1\bar{1}$	0.208	4100
$\bar{2}2\bar{1}$	0.214	80
$\bar{2}3\bar{1}$	0.259	70
$\bar{2}4\bar{1}$	0.324	700
$\bar{2}5\bar{1}$	0.396	0
$\bar{2}6\bar{1}$	0.473	160
$\bar{2}7\bar{1}$	0.558	20
202	0.285	167
212	0.337	13
222	0.402	71
232	0.473	52
242	0.551	17
252	0.629	0
$20\bar{2}$	0.188	800
$21\bar{2}$	0.214	230
$22\bar{2}$	0.272	840

TABLE III (Continued)

$hk\ell$	$\frac{\sin\theta}{\lambda}$	Rel. $\lvert F_{hk\ell}\rvert^2$	$hk\ell$	$\frac{\sin\theta}{\lambda}$	Rel. $\lvert F_{hk\ell}\rvert^2$
$23\bar{2}$	0.344	6	$\bar{2}53$	0.506	0
$24\bar{2}$	0.422	260	$\bar{2}63$	0.583	6.6
$25\bar{2}$	0.506	35			
$26\bar{2}$	0.584	-	$\bar{2}1\bar{3}$	0.318	6.5
			$\bar{2}2\bar{3}$	0.311	9
$\bar{2}12$	0.201	470	$\bar{2}3\bar{3}$	0.331	420
$\bar{2}22$	0.246	15	$\bar{2}4\bar{3}$	0.369	100
$\bar{2}32$	0.305	170	$\bar{2}5\bar{3}$	0.421	500
$\bar{2}42$	0.383	125	$\bar{2}6\bar{3}$	0.487	60
$\bar{2}52$	0.461	61	$\bar{2}7\bar{3}$	0.558	1.4
$\bar{2}62$	0.543	20	$\bar{2}8\bar{3}$	0.630	63
$\bar{2}72$	0.618	0			
			204	0.422	0
$\bar{2}1\bar{2}$	0.260	11	214	0.467	80
$\bar{2}2\bar{2}$	0.260	490	224	0.499	0
$\bar{2}3\bar{2}$	0.292	150	234	0.590	8.8
$\bar{2}4\bar{2}$	0.337	1.4			
$\bar{2}5\bar{2}$	0.402	85	$20\bar{4}$	0.292	145
$\bar{2}6\bar{2}$	0.474	0	$21\bar{4}$	0.298	400
$\bar{2}7\bar{2}$	0.551	0	$22\bar{4}$	0.324	5.3
$\bar{2}8\bar{2}$	0.630	5.5	$23\bar{4}$	0.369	900
			$24\bar{4}$	0.434	180
203	0.350	1500	$25\bar{4}$	0.506	0
213	0.402	16	$26\bar{4}$	0.577	26.6
223	0.461	80			
233	0.532	5	$\bar{2}14$	0.311	90
243	0.603	13	$\bar{2}24$	0.357	1.4
			$\bar{2}34$	0.415	10
$20\bar{3}$	0.235	200	$\bar{2}44$	0.486	70
$21\bar{3}$	0.246	74	$\bar{2}54$	0.558	15
$22\bar{3}$	0.292	300	$\bar{2}64$	0.630	5
$23\bar{3}$	0.344	13			
$24\bar{3}$	0.422	1.9	$\bar{2}1\bar{4}$	0.389	110
$25\bar{3}$	0.499	177	$\bar{2}2\bar{4}$	0.376	2.3
$26\bar{3}$	0.577	0	$\bar{2}3\bar{4}$	0.389	190
			$\bar{2}4\bar{4}$	0.415	2.8
$\bar{2}13$	0.253	1100	$\bar{2}5\bar{4}$	0.454	113
$\bar{2}23$	0.298	240	$\bar{2}6\bar{4}$	0.512	36
$\bar{2}33$	0.357	1900	$\bar{2}7\bar{4}$	0.572	21
$\bar{2}43$	0.428	34			

TABLE III (Continued

$hk\ell$	$\frac{\sin\theta}{\lambda}$	Rel. $\lvert F_{hk\ell}\rvert^2$	$hk\ell$	$\frac{\sin\theta}{\lambda}$	Rel. $\lvert F_{hk\ell}\rvert^2$
205	0.493	27	$\bar{2}1\bar{6}$	0.545	16
215	0.538	51	$\bar{2}2\bar{6}$	0.512	94
225	0.596	2	$\bar{2}3\bar{6}$	0.506	9.2
			$\bar{2}4\bar{6}$	0.525	100
$20\bar{5}$	0.357	2.4	$\bar{2}5\bar{6}$	0.551	1.4
$21\bar{5}$	0.350	184	$\bar{2}6\bar{6}$	0.584	17
$22\bar{5}$	0.369	120	$\bar{2}7\bar{6}$	0.635	4.6
$23\bar{5}$	0.408	50			
$24\bar{5}$	0.461	630	207	0.635	0
$25\bar{5}$	0.519	0			
$26\bar{5}$	0.590	12.6	$20\bar{7}$	0.499	26
			$21\bar{7}$	0.486	68
$\bar{2}15$	0.383	18	$22\bar{7}$	0.486	40
$\bar{2}25$	0.428	115	$23\bar{7}$	0.506	245
$\bar{2}35$	0.480	74	$24\bar{7}$	0.538	0
$\bar{2}45$	0.545	100	$25\bar{7}$	0.583	6.4
$\bar{2}55$	0.616	3	$26\bar{7}$	0.636	-
$\bar{2}1\bar{5}$	0.461	0	$\bar{2}17$	0.525	14.6
$\bar{2}2\bar{5}$	0.447	150	$\bar{2}27$	0.564	0
$\bar{2}3\bar{5}$	0.447	72	$\bar{2}37$	0.617	0
$\bar{2}4\bar{5}$	0.467	118			
$\bar{2}5\bar{5}$	0.499	2.7	$\bar{2}1\bar{7}$	0.610	10
$\bar{2}6\bar{5}$	0.545	0	$\bar{2}2\bar{7}$	0.590	0
$\bar{2}7\bar{5}$	0.596	64	$\bar{2}3\bar{7}$	0.584	0
			$\bar{2}4\bar{7}$	0.584	12
206	0.564	7	$\bar{2}5\bar{7}$	0.603	0
216	0.609	2.9	$\bar{2}6\bar{7}$	0.636	12
$20\bar{6}$	0.428	29	$20\bar{8}$	0.571	0
$21\bar{6}$	0.415	0	$21\bar{8}$	0.558	47
$22\bar{6}$	0.428	450	$22\bar{8}$	0.558	0
$23\bar{6}$	0.454	53	$23\bar{8}$	0.571	1.8
$24\bar{6}$	0.499	9.1	$24\bar{8}$	0.590	9.0
$25\bar{6}$	0.551	8.4	$25\bar{8}$	0.629	7.6
$26\bar{6}$	0.610	-			
			$\bar{2}18$	0.617	25.6
$\bar{2}16$	0.454	8	$\bar{2}28$	0.636	0
$\bar{2}26$	0.493	0			
$\bar{2}36$	0.538	1.6	$20\bar{9}$	0.649	2.5
$\bar{2}46$	0.610	4	$21\bar{9}$	0.630	0

TABLE III (Continued)

$hk\ell$	$\frac{\sin\theta}{\lambda}$	Rel. $\lvert F_{hk\ell}\rvert^2$
$22\bar{9}$	0.621	21
$23\bar{9}$	0.629	0
$24\bar{9}$	0.637	-
300	0.279	169
310	0.331	860
320	0.389	13
330	0.461	98
340	0.538	0
350	0.616	-
$\bar{3}10$	0.259	235
$\bar{3}20$	0.266	162
$\bar{3}30$	0.298	26
$\bar{3}40$	0.356	580
$\bar{3}50$	0.422	30
$\bar{3}60$	0.493	65
$\bar{3}70$	0.571	35
$\bar{3}80$	0.643	-
301	0.318	11
311	0.370	9
321	0.435	85
331	0.499	0
341	0.570	3.4
$30\bar{1}$	0.266	350
$31\bar{1}$	0.305	230
$32\bar{1}$	0.363	3
$33\bar{1}$	0.435	152
$34\bar{1}$	0.506	13
$35\bar{1}$	0.584	28
$\bar{3}11$	0.247	37
$\bar{3}21$	0.266	38
$\bar{3}31$	0.305	480
$\bar{3}41$	0.370	120
$\bar{3}51$	0.441	120
$\bar{3}61$	0.512	7.5
$\bar{3}71$	0.596	20

$hk\ell$	$\frac{\sin\theta}{\lambda}$	Rel. $\lvert F_{hk\ell}\rvert^2$
$\bar{3}1\bar{1}$	0.292	98
$\bar{3}2\bar{1}$	0.292	800
$\bar{3}3\bar{1}$	0.311	230
$\bar{3}4\bar{1}$	0.357	380
$\bar{3}5\bar{1}$	0.422	80
$\bar{3}6\bar{1}$	0.486	70
$\bar{3}7\bar{1}$	0.565	0
$\bar{3}8\bar{1}$	0.630	2
302	0.369	110
312	0.422	53
322	0.480	97
332	0.545	4.6
342	0.617	3.4
$30\bar{2}$	0.266	1600
$31\bar{2}$	0.292	200
$32\bar{2}$	0.350	540
$33\bar{2}$	0.415	24
$34\bar{2}$	0.486	64
$35\bar{2}$	0.564	0
$36\bar{2}$	0.636	-
$\bar{3}12$	0.259	52
$\bar{3}22$	0.285	150
$\bar{3}32$	0.331	120
$\bar{3}42$	0.389	0
$\bar{3}52$	0.467	130
$\bar{3}62$	0.545	0
$\bar{3}72$	0.609	0
$\bar{3}1\bar{2}$	0.337	114
$\bar{3}2\bar{2}$	0.331	17.5
$\bar{3}3\bar{2}$	0.344	460
$\bar{3}4\bar{2}$	0.383	270
$\bar{3}5\bar{2}$	0.435	90
$\bar{3}6\bar{2}$	0.493	160
$\bar{3}7\bar{2}$	0.558	4
$\bar{3}8\bar{2}$	0.630	14

TABLE III (Continued)

$hk\ell$	$\frac{\sin\theta}{\lambda}$	Rel. $\lvert F_{hk\ell}\rvert^2$
303	0.428	34
313	0.473	4.5
323	0.538	4.5
333	0.597	2.7
$30\bar{3}$	0.285	150
$31\bar{3}$	0.311	45
$32\bar{3}$	0.350	640
$33\bar{3}$	0.415	30
$34\bar{3}$	0.487	228
$35\bar{3}$	0.558	26
$36\bar{3}$	0.629	-
$\bar{3}13$	0.292	530
$\bar{3}23$	0.324	15
$\bar{3}33$	0.370	21
$\bar{3}43$	0.435	48
$\bar{3}53$	0.506	33
$\bar{3}63$	0.577	0
$\bar{3}73$	0.654	0
$\bar{3}1\bar{3}$	0.396	334
$\bar{3}2\bar{3}$	0.383	60
$\bar{3}3\bar{3}$	0.389	130
$\bar{3}4\bar{3}$	0.415	45
$\bar{3}5\bar{3}$	0.454	0
$\bar{3}6\bar{3}$	0.512	40
$\bar{3}7\bar{3}$	0.571	0
$\bar{3}8\bar{3}$	0.637	-
304	0.493	36
314	0.538	12
324	0.597	2
$30\bar{4}$	0.331	200
$31\bar{4}$	0.337	800
$32\bar{4}$	0.376	128
$33\bar{4}$	0.428	135
$34\bar{4}$	0.486	16
$35\bar{4}$	0.558	0
$36\bar{4}$	0.629	-
$\bar{3}14$	0.337	1525
$\bar{3}24$	0.370	4
$\bar{3}34$	0.421	10
$\bar{3}44$	0.480	30
$\bar{3}54$	0.551	1.5
$\bar{3}64$	0.623	8
$\bar{3}1\bar{4}$	0.461	3.2
$\bar{3}2\bar{4}$	0.441	125
$\bar{3}3\bar{4}$	0.441	130
$\bar{3}4\bar{4}$	0.461	0
$\bar{3}5\bar{4}$	0.493	140
$\bar{3}6\bar{4}$	0.538	0
$\bar{3}7\bar{4}$	0.591	11
305	0.558	26
315	0.603	8
$30\bar{5}$	0.383	10
$31\bar{5}$	0.389	300
$32\bar{5}$	0.409	36
$33\bar{5}$	0.454	558
$34\bar{5}$	0.506	114
$35\bar{5}$	0.571	0
$36\bar{5}$	0.636	-
$\bar{3}15$	0.395	2.9
$\bar{3}25$	0.435	170
$\bar{3}35$	0.480	0
$\bar{3}45$	0.538	0
$\bar{3}55$	0.598	2.3
$\bar{3}1\bar{5}$	0.532	3.9
$\bar{3}2\bar{5}$	0.513	12
$\bar{3}3\bar{5}$	0.506	0
$\bar{3}4\bar{5}$	0.513	14
$\bar{3}5\bar{5}$	0.538	0

TABLE III (Continued)

$hk\ell$	$\frac{\sin\theta}{\lambda}$	Rel. $\lvert F_{hk\ell}\rvert^2$
$\bar{3}6\bar{5}$	0.577	0
$\bar{3}7\bar{5}$	0.623	1.8
306	0.629	0
$30\bar{6}$	0.441	320
$31\bar{6}$	0.441	45
$32\bar{6}$	0.454	51
$33\bar{6}$	0.486	24
$34\bar{6}$	0.532	20
$35\bar{6}$	0.590	9.5
$36\bar{6}$	0.648	-
$\bar{3}16$	0.461	115
$\bar{3}26$	0.493	280
$\bar{3}36$	0.538	14.5
$\bar{3}46$	0.597	0
$\bar{3}56$	0.650	0.1
$\bar{3}1\bar{6}$	0.597	6.2
$\bar{3}2\bar{6}$	0.571	2.8
$\bar{3}3\bar{6}$	0.564	9.4
$\bar{3}4\bar{6}$	0.571	17
$\bar{3}5\bar{6}$	0.591	0
$\bar{3}6\bar{6}$	0.616	10
$30\bar{7}$	0.506	45
$31\bar{7}$	0.499	17.5
$32\bar{7}$	0.512	145
$33\bar{7}$	0.532	21.8
$34\bar{7}$	0.571	6.1
$35\bar{7}$	0.616	14.8
$\bar{3}17$	0.525	32
$\bar{3}27$	0.558	16
$\bar{3}37$	0.610	9.5
$\bar{3}2\bar{7}$	0.642	-
$\bar{3}3\bar{7}$	0.629	-
$\bar{3}4\bar{7}$	0.629	-
$\bar{3}5\bar{7}$	0.642	-
$30\bar{8}$	0.577	0
$31\bar{8}$	0.571	2.4
$32\bar{8}$	0.571	2.4
$33\bar{8}$	0.584	0
$34\bar{8}$	0.616	0
$\bar{3}18$	0.596	5.4
$\bar{3}28$	0.630	6.8
$30\bar{9}$	0.641	1.3
$31\bar{9}$	0.630	4.1
$32\bar{9}$	0.630	1.3
$33\bar{9}$	0.641	14
400	0.376	130
410	0.422	13
420	0.473	90
430	0.538	0
440	0.610	1.1
$\bar{4}10$	0.350	300
$\bar{4}20$	0.350	210
$\bar{4}30$	0.363	400
$\bar{4}40$	0.402	90
$\bar{4}50$	0.454	25
$\bar{4}60$	0.512	0
$\bar{4}70$	0.577	0
401	0.408	75
411	0.454	84
421	0.519	77
431	0.577	0
$40\bar{1}$	0.357	80
$41\bar{1}$	0.389	310
$42\bar{1}$	0.447	90
$43\bar{1}$	0.512	0
$44\bar{1}$	0.578	4.1
$\bar{4}11$	0.337	80
$\bar{4}21$	0.337	500

TABLE III (Continued)

$hk\ell$	$\frac{\sin\theta}{\lambda}$	Rel. $\lvert F_{hk\ell}\rvert^2$	$hk\ell$	$\frac{\sin\theta}{\lambda}$	Rel. $\lvert F_{hk\ell}\rvert^2$
$\bar{4}31$	0.383	34	$\bar{4}8\bar{2}$	0.648	-
$\bar{4}41$	0.402	15			
$\bar{4}51$	0.461	130	403	0.512	9.1
$\bar{4}61$	0.525	0	413	0.558	0
$\bar{4}71$	0.596	15	423	0.596	8.9
$\bar{4}1\bar{1}$	0.383	115	$40\bar{3}$	0.357	48
$\bar{4}2\bar{1}$	0.376	90	$41\bar{3}$	0.383	160
$\bar{4}3\bar{1}$	0.383	6	$42\bar{3}$	0.428	123
$\bar{4}4\bar{1}$	0.408	190	$43\bar{3}$	0.486	19
$\bar{4}5\bar{1}$	0.454	10	$44\bar{3}$	0.551	0
$\bar{4}6\bar{1}$	0.512	70	$45\bar{3}$	0.623	-
$\bar{4}7\bar{1}$	0.577	0			
			$\bar{4}13$	0.357	185
402	0.461	86	$\bar{4}23$	0.369	160
412	0.506	42	$\bar{4}33$	0.402	125
422	0.564	20	$\bar{4}43$	0.454	0
432	0.623	7	$\bar{4}53$	0.512	18
			$\bar{4}63$	0.577	18
$40\bar{2}$	0.350	34	$\bar{4}73$	0.647	-
$4\bar{1}\bar{2}$	0.382	76			
$42\bar{2}$	0.435	12	$\bar{4}1\bar{3}$	0.480	38
$43\bar{2}$	0.493	27	$\bar{4}2\bar{3}$	0.461	2.5
$44\bar{2}$	0.558	12.3	$\bar{4}3\bar{3}$	0.461	65
$45\bar{2}$	0.636	-	$\bar{4}4\bar{3}$	0.473	20
			$\bar{4}5\bar{3}$	0.499	50
$\bar{4}12$	0.337	6.5	$\bar{4}6\bar{3}$	0.545	0
$\bar{4}22$	0.344	600	$\bar{4}7\bar{3}$	0.597	7.5
$\bar{4}32$	0.376	260			
$\bar{4}42$	0.422	400	404	0.571	0
$\bar{4}52$	0.480	80	414	0.616	5
$\bar{4}62$	0.545	4.5			
$\bar{4}72$	0.592	0	$40\bar{4}$	0.383	115
			$41\bar{4}$	0.402	305
$\bar{4}1\bar{2}$	0.428	26	$42\bar{4}$	0.441	14.5
$\bar{4}2\bar{2}$	0.408	170	$43\bar{4}$	0.487	86
$\bar{4}3\bar{2}$	0.415	3	$44\bar{4}$	0.551	18
$\bar{4}4\bar{2}$	0.434	22	$45\bar{4}$	0.616	-
$\bar{4}5\bar{2}$	0.473	0			
$\bar{4}6\bar{2}$	0.525	10.8	$\bar{4}14$	0.383	58
$\bar{4}7\bar{2}$	0.584	13.3	$\bar{4}24$	0.402	20

TABLE III (Continued)

$hk\ell$	$\frac{\sin\theta}{\lambda}$	Rel. $\lvert F_{hk\ell}\rvert^2$	$hk\ell$	$\frac{\sin\theta}{\lambda}$	Rel. $\lvert F_{hk\ell}\rvert^2$
$\bar{4}34$	0.441	283	$\bar{4}16$	0.479	135
$\bar{4}44$	0.493	63	$\bar{4}26$	0.506	0
$\bar{4}54$	0.551	55	$\bar{4}36$	0.545	29
$\bar{4}64$	0.596	8.1	$\bar{4}46$	0.596	7.8
$\bar{4}1\bar{4}$	0.538	12.5	$\bar{4}2\bar{6}$	0.636	-
$\bar{4}2\bar{4}$	0.519	6.7	$\bar{4}3\bar{6}$	0.630	-
$\bar{4}3\bar{4}$	0.506	0	$\bar{4}4\bar{6}$	0.623	2.1
$\bar{4}4\bar{4}$	0.519	2.3	$\bar{4}5\bar{6}$	0.636	0
$\bar{4}5\bar{4}$	0.538	0			
$\bar{4}6\bar{4}$	0.577	0	$40\bar{7}$	0.525	21
$\bar{4}7\bar{4}$	0.623	0	$41\bar{7}$	0.525	0
			$42\bar{7}$	0.538	8.3
405	0.636	3	$43\bar{7}$	0.571	17
			$44\bar{7}$	0.609	6
$40\bar{5}$	0.422	4.5			
$41\bar{5}$	0.434	190	$\bar{4}17$	0.538	7.5
$42\bar{5}$	0.461	4	$\bar{4}27$	0.564	42
$43\bar{5}$	0.506	0	$\bar{4}37$	0.603	1.6
$44\bar{5}$	0.558	10			
$45\bar{5}$	0.623	-	$40\bar{8}$	0.584	9
			$41\bar{8}$	0.584	32
$\bar{4}15$	0.428	53	$42\bar{8}$	0.590	3.2
$\bar{4}25$	0.448	160	$43\bar{8}$	0.616	15.5
$\bar{4}35$	0.493	39	$44\bar{8}$	0.649	3.2
$\bar{4}45$	0.545	2.5			
$\bar{4}55$	0.598	-	$\bar{4}18$	0.591	0
			$\bar{4}28$	0.630	1.5
$\bar{4}1\bar{5}$	0.597	0			
$\bar{4}2\bar{5}$	0.577	10	$40\bar{9}$	0.592	0
$\bar{4}3\bar{5}$	0.564	11	$41\bar{9}$	0.649	2.3
$\bar{4}4\bar{5}$	0.571	35	$42\bar{9}$	0.636	-
$\bar{4}5\bar{5}$	0.584	0	$43\bar{9}$	0.649	-
$\bar{4}6\bar{5}$	0.616	0			
			$\bar{4}19$	0.649	0.6
$40\bar{6}$	0.467	130			
$41\bar{6}$	0.473	21	500	0.472	90
$42\bar{6}$	0.499	109	510	0.514	53.3
$43\bar{6}$	0.532	11.5	520	0.565	0
$44\bar{6}$	0.577	0	530	0.623	0
$45\bar{6}$	0.636	-			

TABLE III (Continued)

hkℓ	$\frac{\sin\theta}{\lambda}$	Rel. $\lvert F_{hk\ell}\rvert^2$	hkℓ	$\frac{\sin\theta}{\lambda}$	Rel. $\lvert F_{hk\ell}\rvert^2$
$\bar{5}10$	0.448	4.5	$\bar{5}12$	0.416	174
$\bar{5}20$	0.435	7.1	$\bar{5}22$	0.416	120
$\bar{5}30$	0.435	160	$\bar{5}32$	0.435	19
$\bar{5}40$	0.467	634	$\bar{5}42$	0.474	50
$\bar{5}50$	0.505	14.9	$\bar{5}52$	0.518	276
$\bar{5}60$	0.552	31.4	$\bar{5}62$	0.578	7
$\bar{5}70$	0.611	3.1	$\bar{5}72$	0.637	0
501	0.506	0	$\bar{5}1\bar{2}$	0.520	0
511	0.552	0	$\bar{5}2\bar{2}$	0.500	41
521	0.611	0	$\bar{5}3\bar{2}$	0.493	240
			$\bar{5}4\bar{2}$	0.506	0
$50\bar{1}$	0.447	4	$\bar{5}5\bar{2}$	0.537	4.1
$51\bar{1}$	0.487	184	$\bar{5}6\bar{2}$	0.572	0
$52\bar{1}$	0.539	3	$\bar{5}7\bar{2}$	0.624	-
$53\bar{1}$	0.598	11.2			
			503	0.601	2
$\bar{5}11$	0.422	90	513	0.643	0
$\bar{5}21$	0.416	16			
$\bar{5}31$	0.429	195	$50\bar{3}$	0.443	563
$\bar{5}41$	0.461	49	$51\bar{3}$	0.461	8.1
$\bar{5}51$	0.505	26.6	$52\bar{3}$	0.507	72.9
$\bar{5}61$	0.559	10.1	$53\bar{3}$	0.559	0
$\bar{5}71$	0.617	0	$54\bar{3}$	0.623	0
$\bar{5}1\bar{1}$	0.474	28	$\bar{5}13$	0.422	278
$\bar{5}2\bar{1}$	0.461	54	$\bar{5}23$	0.429	123
$\bar{5}3\bar{1}$	0.461	16	$\bar{5}33$	0.455	21
$\bar{5}4\bar{1}$	0.481	72	$\bar{5}43$	0.493	40
$\bar{5}5\bar{1}$	0.516	0	$\bar{5}53$	0.542	19
$\bar{5}6\bar{1}$	0.559	16.7	$\bar{5}63$	0.598	6.8
$\bar{5}7\bar{1}$	0.611	38.1			
			$\bar{5}1\bar{3}$	0.565	7.7
502	0.550	0	$\bar{5}2\bar{3}$	0.546	0
512	0.598	0	$\bar{5}3\bar{3}$	0.533	25
			$\bar{5}4\bar{3}$	0.539	0
$50\bar{2}$	0.433	18	$\bar{5}5\bar{3}$	0.571	18.8
$51\bar{2}$	0.467	31	$\bar{5}6\bar{3}$	0.598	-
$52\bar{2}$	0.520	33	$\bar{5}7\bar{3}$	0.640	-
$53\bar{2}$	0.572	16			
542	0.637	-	534	0.559	0

TABLE III (Continued)

$hk\ell$	$\frac{\sin\theta}{\lambda}$	Rel. $\lvert F_{hk\ell}\rvert^2$
$50\bar{4}$	0.447	380
$51\bar{4}$	0.474	103
$52\bar{4}$	0.510	165
$53\bar{4}$	0.559	0
$54\bar{4}$	0.617	0
$\bar{5}14$	0.442	6
$\bar{5}24$	0.455	2.5
$\bar{5}34$	0.481	60
$\bar{5}44$	0.520	3
$\bar{5}54$	0.575	6
$\bar{5}64$	0.637	0
$\bar{5}1\bar{4}$	0.618	3
$\bar{5}2\bar{4}$	0.580	44
$\bar{5}3\bar{4}$	0.624	0.8
$\bar{5}4\bar{4}$	0.580	0
$\bar{5}5\bar{4}$	0.609	0
$\bar{5}6\bar{4}$	0.630	-
$50\bar{5}$	0.473	21
$51\bar{5}$	0.494	16.5
$\bar{5}2\bar{5}$	0.525	0
$53\bar{5}$	0.565	-
$54\bar{5}$	0.617	8.7
$\bar{5}15$	0.474	95
$\bar{5}25$	0.490	148
$\bar{5}35$	0.520	18
$\bar{5}45$	0.565	16
$\bar{5}55$	0.613	3.5
$\bar{5}3\bar{5}$	0.636	4
$\bar{5}4\bar{5}$	0.636	3.6
$50\bar{6}$	0.508	1
$51\bar{6}$	0.520	200
$52\bar{6}$	0.545	0
$53\bar{6}$	0.585	-
$54\bar{6}$	0.630	-

$hk\ell$	$\frac{\sin\theta}{\lambda}$	Rel. $\lvert F_{hk\ell}\rvert^2$
$\bar{5}16$	0.513	130
$\bar{5}26$	0.533	21
$\bar{5}36$	0.565	8
$\bar{5}46$	0.611	0
$50\bar{7}$	0.551	0
$51\bar{7}$	0.558	0
$52\bar{7}$	0.584	-
$53\bar{7}$	0.611	-
$\bar{5}17$	0.558	0
$\bar{5}27$	0.585	7.5
$\bar{5}37$	0.617	2.2
$50\bar{8}$	0.601	14
$51\bar{8}$	0.603	-
$52\bar{8}$	0.624	0
$53\bar{8}$	0.646	-
$\bar{5}18$	0.617	0
$\bar{5}28$	0.643	0
600	0.565	6.3
610	0.604	3.6
$\bar{6}10$	0.539	0
$\bar{6}20$	0.519	3.2
$\bar{6}30$	0.520	0
$\bar{6}40$	0.533	0
$\bar{6}50$	0.572	4.5
$\bar{6}60$	0.607	7.6
601	0.600	6.3
611	0.643	0
$60\bar{1}$	0.540	9.3
$61\bar{1}$	0.578	10.9
$62\bar{1}$	0.630	-
$\bar{6}11$	0.513	60
$\bar{6}21$	0.506	152

TABLE III (Continued)

hkℓ	$\frac{\sin\theta}{\lambda}$	Rel. $\lvert F_{hk\ell}\rvert^2$
$\bar{6}31$	0.506	0
$\bar{6}41$	0.526	0
$\bar{6}51$	0.565	12
$\bar{6}61$	0.603	0
$\bar{6}1\bar{1}$	0.565	40
$\bar{6}2\bar{1}$	0.552	0
$\bar{6}3\bar{1}$	0.552	1.7
$\bar{6}4\bar{1}$	0.552	2.5
$\bar{6}5\bar{1}$	0.585	8
$\bar{6}6\bar{1}$	0.615	5
602	0.640	0
$60\bar{2}$	0.524	0
$61\bar{2}$	0.558	0
$62\bar{2}$	0.611	0
$\bar{6}12$	0.500	90
$\bar{6}22$	0.500	0
$\bar{6}32$	0.506	0
$\bar{6}42$	0.529	0
$\bar{6}52$	0.572	8.9
$\bar{6}62$	0.613	0
$\bar{6}1\bar{2}$	0.604	2.4
$\bar{6}2\bar{2}$	0.592	-
$\bar{6}3\bar{2}$	0.578	-
$\bar{6}4\bar{2}$	0.581	2.6
$\bar{6}5\bar{2}$	0.591	0
$\bar{6}6\bar{2}$	0.635	0
$60\bar{3}$	0.518	4.9
$61\bar{3}$	0.552	0
$62\bar{3}$	0.598	0
633	0.643	-
$\bar{6}13$	0.500	50
$\bar{6}23$	0.500	20
$\bar{6}33$	0.513	138
$\bar{6}43$	0.546	10

hkℓ	$\frac{\sin\theta}{\lambda}$	Rel. $\lvert F_{hk\ell}\rvert^2$
$\bar{6}53$	0.591	7
$\bar{6}3\bar{3}$	0.615	5
$\bar{6}5\bar{3}$	0.600	3
$\bar{6}6\bar{3}$	0.633	17
$60\bar{4}$	0.524	2.8
$61\bar{4}$	0.552	0
$62\bar{4}$	0.592	-
$63\bar{4}$	0.636	12
$\bar{6}14$	0.513	6.5
$\bar{6}24$	0.519	102
$\bar{6}34$	0.532	3.5
$\bar{6}44$	0.565	0
$\bar{6}54$	0.611	0
$60\bar{5}$	0.540	0
$61\bar{5}$	0.565	0
$62\bar{5}$	0.598	-
$63\bar{5}$	0.636	-
$\bar{6}15$	0.532	0
$\bar{6}25$	0.546	8.6
$\bar{6}35$	0.565	2.5
$\bar{6}45$	0.597	15
$60\bar{6}$	0.566	1
$61\bar{6}$	0.585	0
$62\bar{6}$	0.617	-
$63\bar{6}$	0.649	-
$\bar{6}16$	0.565	5
$\bar{6}26$	0.578	0
$\bar{6}36$	0.604	9
$\bar{6}46$	0.640	0
$60\bar{7}$	0.601	2.6
$61\bar{7}$	0.617	-
$62\bar{7}$	0.647	-

TABLE III (Continued)

$hk\ell$	$\frac{\sin\theta}{\lambda}$	Rel. $\lvert F_{hk\ell}\rvert^2$
$\bar{6}17$	0.604	0
$\bar{6}27$	0.624	6.3
$\bar{6}37$	0.646	-
$60\bar{8}$	0.641	0
$\bar{6}18$	0.649	-
750	0.636	24.8
$\bar{7}30$	0.610	15
$70\bar{1}$	0.634	0
$\bar{7}11$	0.604	0
$\bar{7}21$	0.598	5
$\bar{7}31$	0.591	7
$\bar{7}41$	0.604	0
$\bar{7}51$	0.622	14
$\bar{7}3\bar{1}$	0.630	0
$70\bar{2}$	0.615	13.3
$\bar{7}12$	0.591	0
$\bar{7}22$	0.585	0
$\bar{7}32$	0.585	0
$\bar{7}42$	0.597	0

$hk\ell$	$\frac{\sin\theta}{\lambda}$	Rel. $\lvert F_{hk\ell}\rvert^2$
$70\bar{3}$	0.606	6.5
$71\bar{3}$	0.637	52.6
$74\bar{3}$	0.618	17
$\bar{7}13$	0.618	17
$\bar{7}23$	0.585	0
$\bar{7}33$	0.585	14
$\bar{7}43$	0.585	3.2
$\bar{7}53$	0.604	12
$70\bar{4}$	0.606	19
$71\bar{4}$	0.633	-
$\bar{7}14$	0.591	18.9
$\bar{7}24$	0.591	4
$\bar{7}34$	0.604	10
$70\bar{5}$	0.615	48.7
$75\bar{1}$	0.640	-
$\bar{7}15$	0.604	10.6
$\bar{7}25$	0.610	0
$\bar{7}35$	0.623	0
$\bar{7}45$	0.649	0
$70\bar{6}$	0.633	2.9
$\bar{7}16$	0.627	38.4
$\bar{7}26$	0.637	25.0

The factors by which relative F^2 values of a given film were multiplied to reach the common level are:

Axis	Layer	Factor	Axis	Layer	Factor
a_1	1	1.20	a_3''	0	2.05
	2	0.99		1	2.35
	3	1.05		2	2.56
	4	1.46		3	2.78
a_2	0	o.56		4	2.55
	1	0.91		5	3.04
	2	1.29			
	3	1.32			
	4	1.62			

Absorption effects were calculated to be negligible.

The atomic parameters listed by Broge for the compound cell were converted by graphical means to the coordinates in the primitive unit as follows:

	x	y	z
C_1	-0.139	+0.044	-0.057
C_2	-0.198	-0.024	-0.259
C_3	-0.224	-0.266	-0.204
C_4	-0.133	-0.170	0.000
F_1	+0.220	-0.229	0.000
F_2	-0.116	+0.115	-0.454
F_3	-0.487	+0.030	-0.364
F_4	-0.083	-0.415	-0.354
F_5	-0.374	-0.479	-0.268
F_6	-0.244	-0.354	+0.180

Figures 13 and 14 show projections on (010) and (100) of the reduced cell that would be obtained using the above. The centrosymmetric model is clearly outlined.

Amplitudes calculated from these positions however failed to agree with observed values. This indicated that the proposed structure was not close to the true one and that the experimental data should be used systematically in a search for the correct structure.

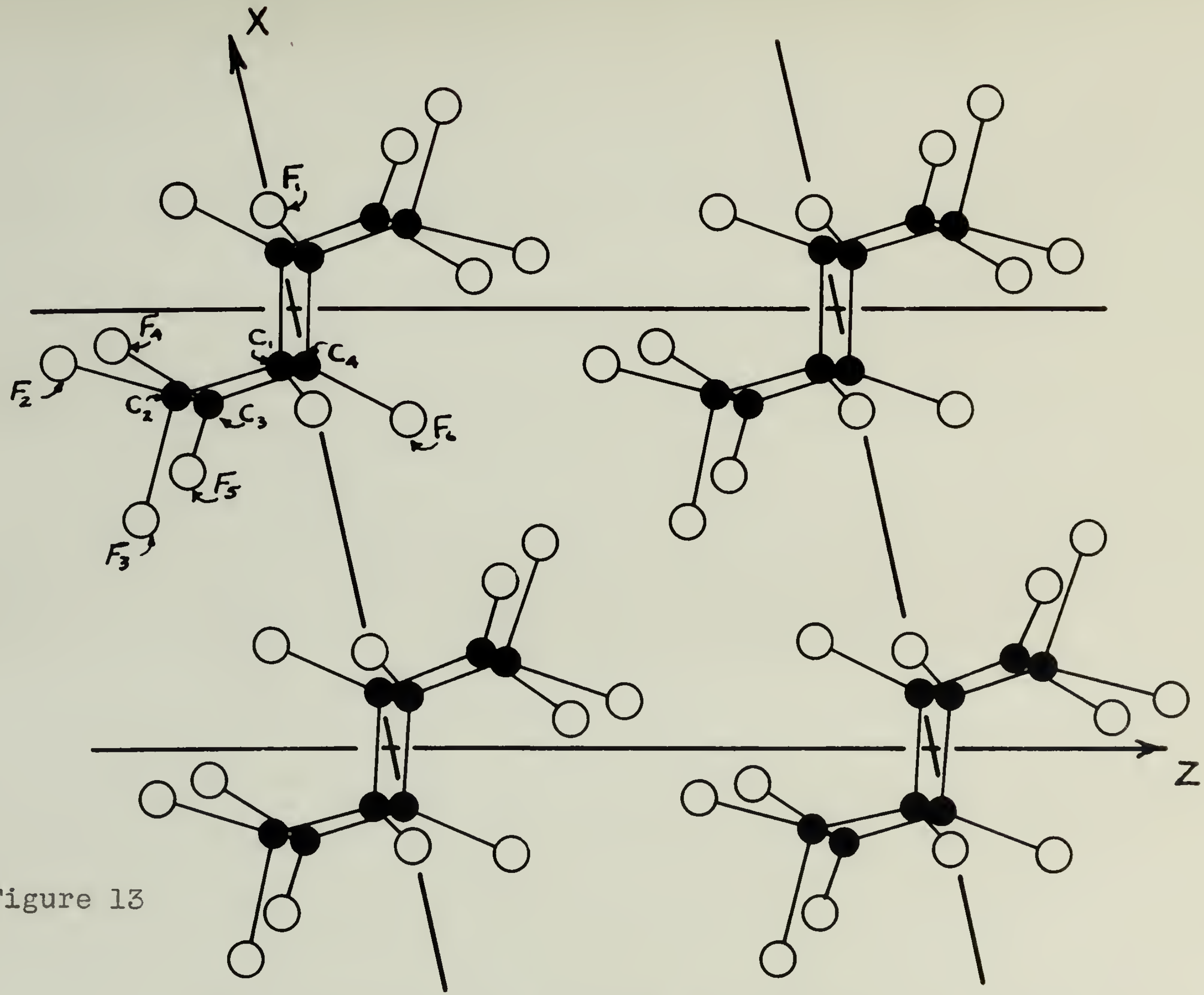

Figure 13

PROJECTION ON (010) FROM DATA OF BROGE

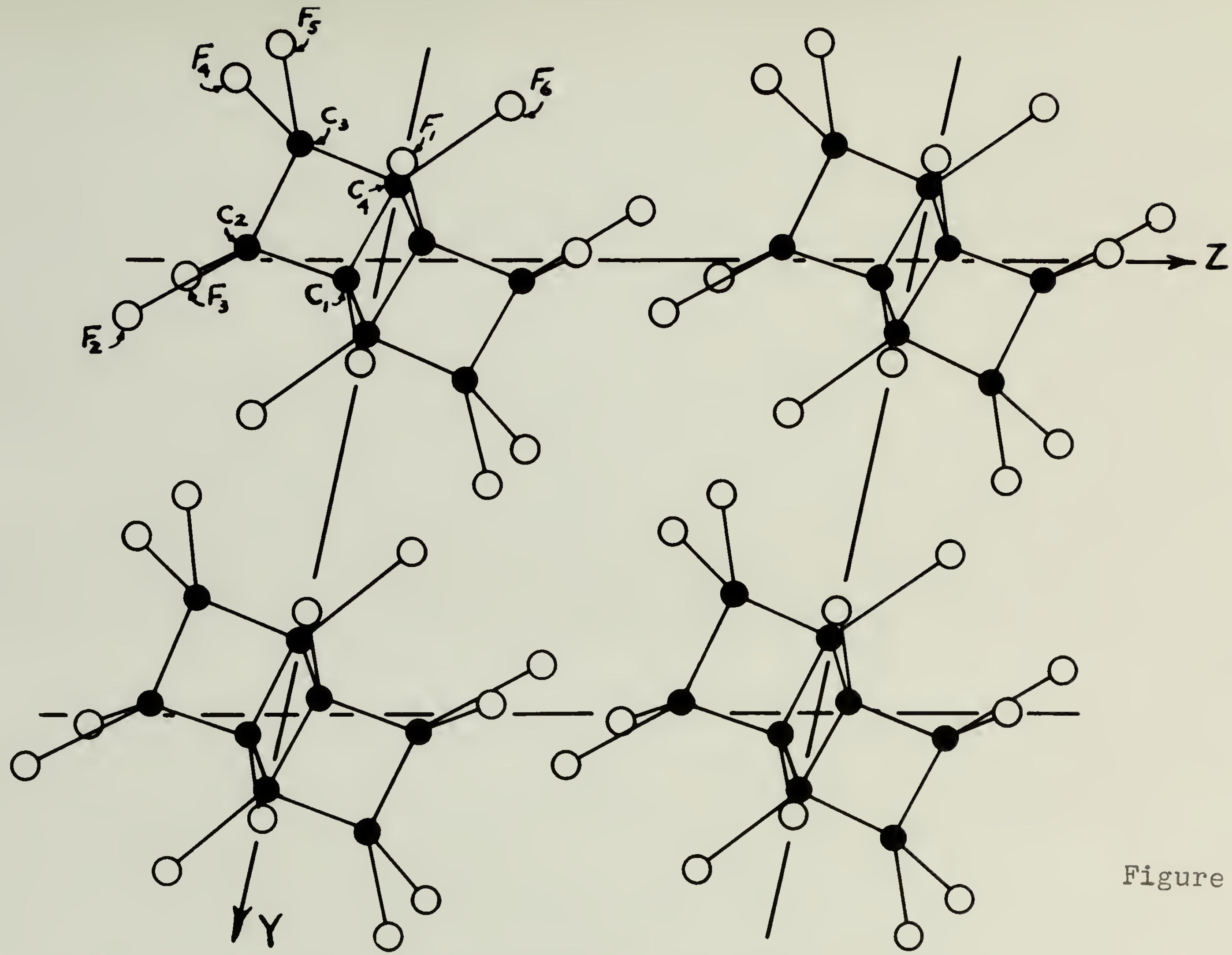

Figure 14

PROJECTION ON (100) FROM DATA OF BROGE

Patterson Projection, $P(Y,Z)$.

Since the first data were observed for rotation about $\underline{a_1}$ the Patterson projection on (100) was computed. It can be shown that

$$KP(Y,Z) = \sum_{k=0}^{\infty} \sum_{\ell=0}^{\infty} \left[|F_{0k\ell}|^2 + |F_{0\bar{k}\ell}|^2 \right] \cos 2\pi k Y \cos 2\pi \ell Z$$

$$- \sum_{k=1}^{\infty} \sum_{\ell=1}^{\infty} \left[|F_{0k\ell}|^2 - |F_{0\bar{k}\ell}|^2 \right] \sin 2\pi k Y \sin 2\pi \ell Z$$

(neglecting constant additive terms).

The projection is shown in Figure 15. Contours start at 0 and are drawn at intervals of 50 in relative Patterson density. Aside from the identity peak at the origin, a single solid ridge is seen extending from $Y=0, Z=0$ to $Y=1, Z=-1/2$ with peaks at intervals along the entire length. This would lead one to believe that the long axis of the molecule lay parallel to the ridge. Further evidence lies in the fact that the (012) reflection is indicative of strong temperature diffuse scattering. The significance of such reflections is discussed by Lonsdale.[22] Trial parameters assigned to the atoms on the basis of such an orientation failed to give a satisfactory comparison of calculated and observed amplitudes for $F_{(00\ell)}$ and $F_{(0k0)}$.

Patterson Projection, $P(Y,Z)$.

Since the first data were observed for rotation about $\underline{a_1}$ the Patterson projection on (100) was computed. It can be shown that

$$P(Y,Z) = \sum_{k=0}^{\infty}\sum_{\ell=0}^{\infty}\left[|F_{0k\ell}|^2 + |F_{0\bar{k}\ell}|^2\right]\cos 2\pi kY \cos 2\pi \ell Z$$

$$- \sum_{k=1}^{\infty}\sum_{\ell=1}^{\infty}\left[|F_{0k\ell}|^2 - |F_{0\bar{k}\ell}|^2\right]\sin 2\pi kY \sin 2\pi \ell Z$$

(neglecting constant additive terms).

The projection is shown in Figure 10. Contours start at 0 and are drawn at intervals of 30 in relative Patterson density. Aside from the identity peak at the origin, a single solid ridge is seen extending from $Y=0, Z=0$ to $Y=1, Z=-1/2$ with peaks at intervals along the entire length. This would lead one to believe that the long axis of the molecule lay parallel to the ridge. Further evidence lies in the fact that the (012) reflection is indicative of strong temperature diffuse scattering. The significance of such reflections is discussed by Lonsdale.(22) Trial parameters assigned to the atoms on the basis of such an orientation failed to give a satisfactory comparison of calculated and observed amplitudes for $F(00\ell)$ and $F(0k0)$.

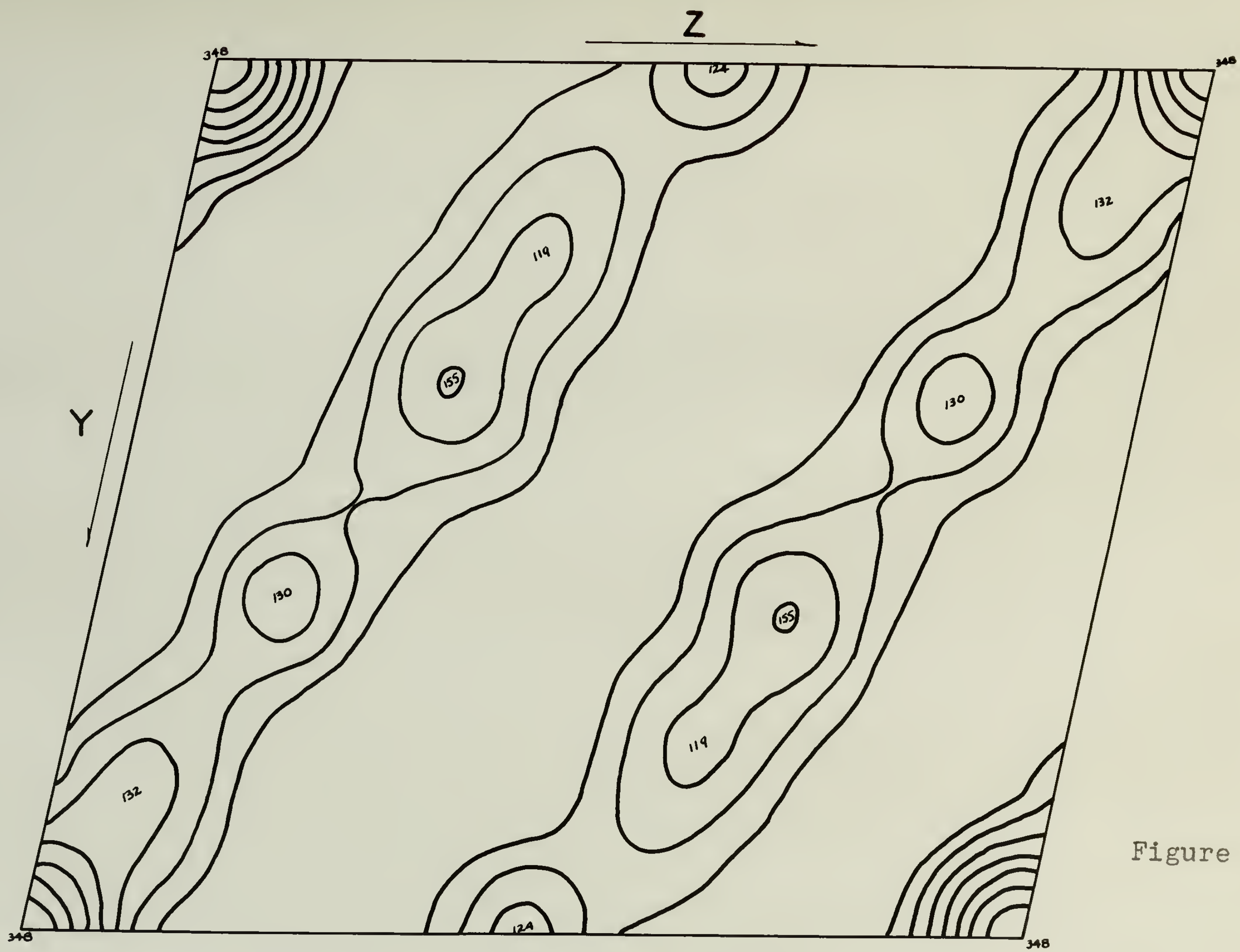

PATTERSON PROJECTION P(Y,Z)

Figure 15

Patterson Projection, $P(X,Z)$.

The function, apart from constant additive terms, may be expressed as:

$$KP(X,Z) = \sum_{h=0}^{\infty} \sum_{\ell=0}^{\infty} \left[|F_{h0\ell}|^2 + |F_{\bar{h}0\ell}|^2 \right] \cos 2\pi hX \cos 2\pi \ell Z$$

$$- \sum_{h=1}^{\infty} \sum_{\ell=1}^{\infty} \left[|F_{h0\ell}|^2 - |F_{\bar{h}0\ell}|^2 \right] \sin 2\pi hX \sin 2\pi \ell Z.$$

The projection on (010) of the primitive reduced cell is shown in Figure 16. Contours are drawn as before. Several isolated peaks appear and may be grouped along straight lines with striking regularity. Several orientations based on features of this projection were tried but failed to give satisfactory agreement of observed and calculated amplitudes.

Peaks arising from vectors between equivalent atoms will appear on $P(X,Z)$ at $X=2x, Z=2z$. A scaled model of the unit cell was made so that trial structures could be set up with cork balls to represent appropriate atoms. Even with the model it was not possible to determine which of the peaks appeared because of equivalent atoms. The parameters obtained from Broge's analysis were used to plot peaks at $2x, 2z$ on an overlay of the Patterson projection. The coordinates were adjusted to agree with the peaks on the projection and structure amplitudes

Patterson Projection, P(X,Z).

The function, apart from constant additive terms, may be expressed as:

$$KP(X,Z) = \sum_{h=0}^{\infty}\sum_{l=0}^{\infty}\left[|F_{h0l}|^2 + |F_{h0\bar{l}}|^2\right] \cos 2\pi hX \cos 2\pi l Z$$

$$- \sum_{h=1}^{\infty}\sum_{l=1}^{\infty}\left[|F_{h0l}|^2 - |F_{h0\bar{l}}|^2\right] \sin 2\pi hX \sin 2\pi l Z.$$

The projection on (010) of the primitive reduced cell is shown in Figure 16. Contours are drawn as before. Several isolated peaks appear and may be grouped along straight lines with striking regularity. Several orientations based on features of this projection were tried but failed to give satisfactory agreement of observed and calculated amplitudes.

Peaks arising from vectors between equivalent atoms will appear on P(X,Z) at X=2x, Z=2z. A scaled model of the unit cell was made so that trial structures could be set up with cork balls to represent appropriate atoms. Even with the model it was not possible to determine which of the peaks appeared because of equivalent atoms. The parameters obtained from Kropp's analysis were used to plot peaks at 2x, 2z on an overlay of the Patterson projection. The coordinates were adjusted to agree with the peaks on the projection and structure amplitudes

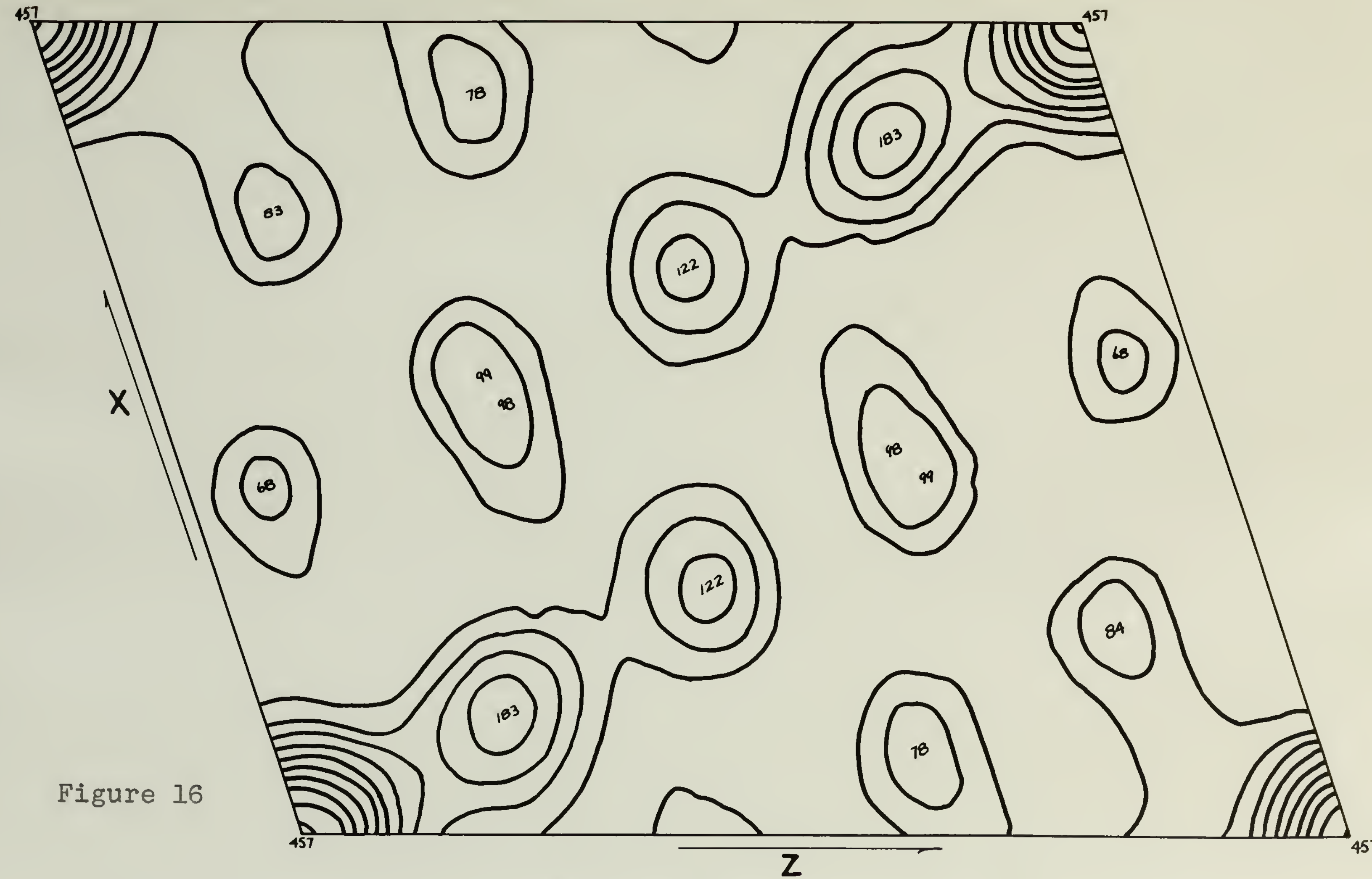

Figure 16

PATTERSON PROJECTION P(X,Z)

computed. Again there was no agreement.

Since the ($\bar{2}21$) reflection was so very strong it was suspected that a large amount of scattering material was located in the corresponding plane. The Patterson density from $P(X,Z)$ was plotted on a properly drawn grid of the ($\bar{2}21$) plane. Any vectors between atoms lying in this plane would appear in their true length in the preceding plot. The scaled molecular model was placed in several orientations such that many of the fluorines lay in the plane. No vectors could be recognized however.

Patterson Projection, $P(X',Z')$.

The projection on the $a_1'' \; a_3''$ face of the unit cell of crystal #4 was calculated. This corresponds to ($01\bar{1}$) of the reduced unit. It is shown in Figure 17. Contours start at 0 and are drawn at intervals of 20 in arbitrary relative Patterson density. Here again there is a long ridge extending from $X'=0, Z'=0$ to $X'=1/2, Z'=1$ with poorly defined peaks all along the ridge. The plane of projection was properly fitted into the primitive reduced cell to see if three coordinates could be assigned to any one vector peak. This procedure failed to clarify the situation however.

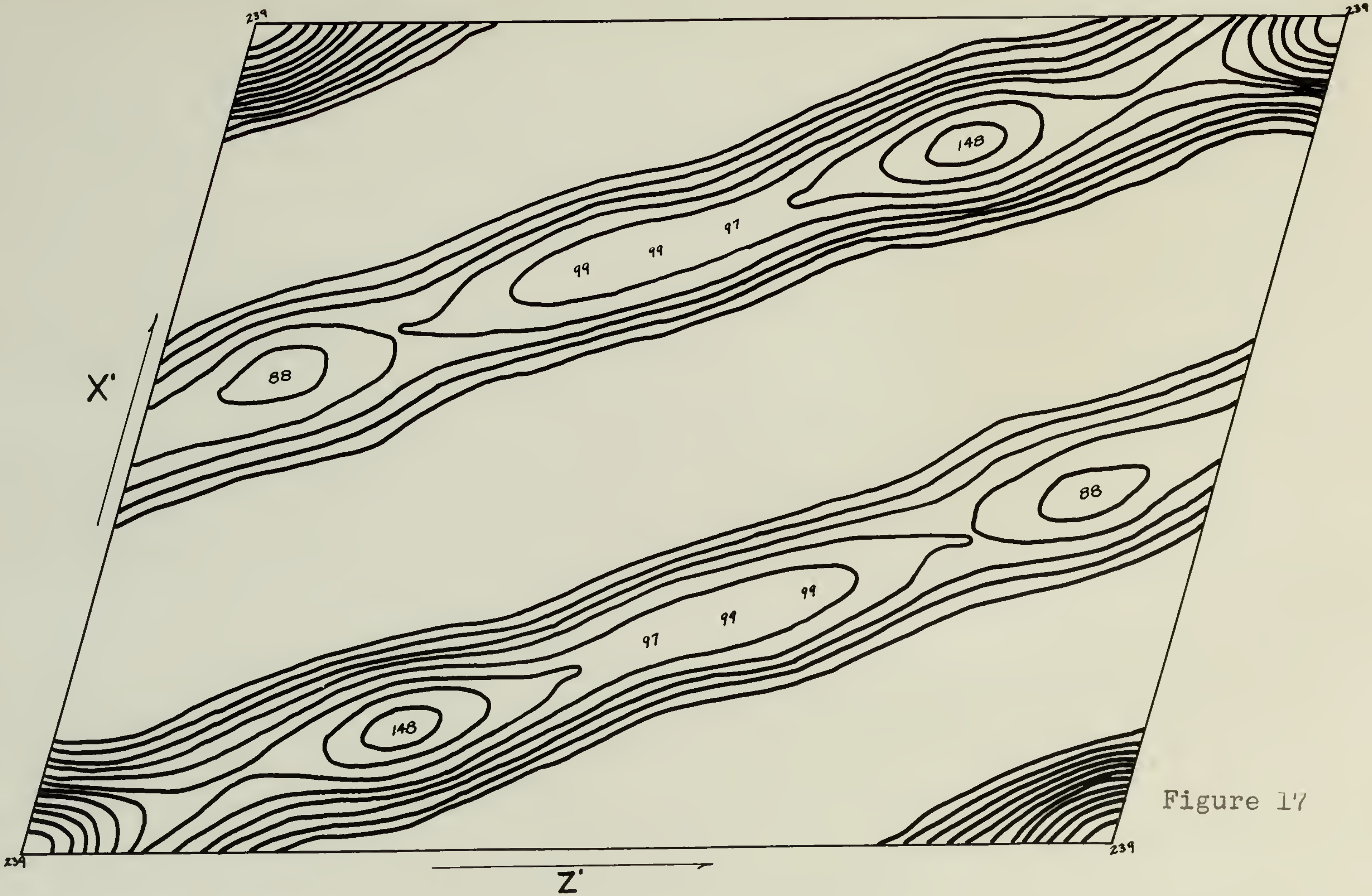

PATTERSON PROJECTION P(X',Z')

Figure 17

Phase Inequalities and Unitary Structure Amplitudes.

Since none of the projections were successfully interpreted, the possibility of phase determination by the recently proposed inequality procedure was explored. Unitary amplitudes are required in the inequality method and were, therefore, calculated for (0kℓ) and (h0ℓ) data.

It was soon clear that only a few F's were greater than 0.5 and that there were certainly not enough of sufficiently high magnitude to determine more than a few phases. If the assumed model were correct, the method might be further exploited. However, if the center of symmetry is lost, the procedure no longer is applicable.

Temporary Conclusion of the Work

Thus far, all attempts at parameter determination had failed. It was at this point that C_4Cl_8 became available for study. It was decided that more would be accomplished in the long run if the C_8F_{12} problem were dropped at this time in order to determine the structure of the octachlorocyclobutane. Any knowledge gained concerning the configuration of the carbon ring in the latter compound might then lead to reconsideration of the proper model to use in work on the former.

Recently Professor Miller made available for study the compound $C_8Cl_4F_8$ analagous to C_8F_{12} wherein the

phase inequalities and Unitary structure amplitudes.

Since none of the projections were successfully interpreted, the possibility of phase determination by the recently proposed inequality procedure was explored. Unitary amplitudes are required in the inequality method and were, therefore, calculated for (0kl) and (h0l) data.

It was soon clear that only a few F's were greater than 0.5 and that there were certainly not enough of sufficiently high magnitude to determine more than a few phases. If the assumed model were correct, the method might be further exploited. However, if the center of symmetry is lost, the procedure no longer is applicable.

Temporary Conclusion of the Work

Thus far, all attempts at parameter determination had failed. It was at this point that C_4Cl_8 became available for study. It was decided that more would be accomplished in the long run if the C_8F_{12} problem were dropped at this time in order to determine the structure of the octachlorocyclobutane. Any knowledge gained concerning the configuration of the carbon ring in the latter compound might then lead to reconsideration of the proper model to use in work on the former.

Recently Professor Miller made available for study the compound $C_6Cl_4F_8$ analogous to C_8F_{12} wherein the

fluorines attached to the central carbon ring have been replaced by chlorine atoms. It was at first believed that structure studies of this material might help in the solution of the hexafluorobutadiene dimer. Preliminary work has shown that crystals of the new compound have cubic symmetry and thus are not isomorphous with C_8F_{12}. There is, however, evidence of molecular rotation at room temperatures so further work at lower temperatures may give more information.

SUGGESTIONS FOR FURTHER STUDY

In view of the evidence of the non-planar carbon ring in C_4Cl_8 it may be possible that the rings in C_8F_{12} are puckered with a resulting loss of a center of symmetry for the molecule. If this be true, the structure problem will be extremely difficult but not impossible.

Nearly complete $(hk\ell)$ data have been obtained for the primitive reduced cell. It is thus possible to calculate a series of three-dimensional Patterson sections for small increments along a chosen axis, probably $\underline{a}_2$. From these sections enough vectors might be resolved to lead to a satisfactory structure determination.

BIBLIOGRAPHY

1. Bauer, S. H. & Beach, J. Y.
   J. Amer. Chem. Soc. 64 1142 (1942).

2. Beevers, C. A. & Lipson, H.
   Proc. Phys. Soc. London 48 772 (1936).

3. Bray, E. E. & Gingrich, N. S.
   J. Chem. Phys. 11 351 (1943).

4. Broomhead, J. M. & Nichol, A. D. I.
   Acta Cryst. 1 88 (1948).

5. Buerger, M. J.
   X-ray Crystallography. New York: Wiley.

6. Bunn, C. W.
   Chemical Crystallography. London: Oxford.

7. Cosslett, V. E. & de Laszlo, H. G.
   Nature 134 63 (1934).

8. Dunitz, J. D.
   Acta Cryst. 2 1 (1949).

9. Dunitz, J. D. & Weissman, L.
   Acta Cryst. 2 62 (1949).

10. Edgell, W. F.
    J. Amer. Chem. Soc. 69 660 (1947).

11. Eisenstein, A.
    Phys. Rev. 63 304 (1943).

12. Hendershot, O. P.
    Rev. Sci. Instrum. 8 436 (1936).

13. Lipscomb, W. N. & Schomaker, V.
    J. Chem. Phys. 14 475 (1946).

14. Livingston, R. L.
    Private Communication to J. L. Hoard.

15. Pauling, L. & Brockway, L. O.
    J. Amer. Chem. Soc. 57 2684 (1935).

16. Prober, M. & Miller, W. T.
J. Amer. Chem. Soc. 71 598 (1949).

17. Shand, W., Schomaker, V., & Fischer, J. R.
J. Amer. Chem. Soc. 66 636 (1944).

18. Smare, D. L.
Acta Cryst. 1 150 (1948).

19. Tunell, G.
Amer. Min. 24 448 (1939).

20. Wilson, T. P.
J. Chem. Phys. 11 369 (1943).

21. Broge, R. W.
Ph. D. Thesis, Cornell University. 1948.

22. Lonsdale, K.
Crystals and X-rays London: Bell & Son 1948.

16. Probst, W., & Müller, W. T.
J. Amer. Chem. Soc. 71 598 (1949).

17. Shand, W., Schomaker, V., & Fischer, J. R.
J. Amer. Chem. Soc. 66 [illegible] (1944).

18. [illegible], H. C.
Acta Cryst. 1 [illegible] (1948).

19. Tunell, G.
Amer. Min. 24 448 (1939).

20. [illegible], T. F.
J. Chem. Phys. 11 [illegible] (1943).

21. [illegible], H. F.
Ph. D. Thesis, Cornell University. 1949.

22. Lonsdale, K.
Crystals and X-rays London: Bell & Son 1948.

Thesis 12786
O95 Owen
I. The structure of octachlorocyclobutane, C4Cl8. II. Further study of the structure of C8F12.